STUDIES ON THE INTERACTION OF MIXED MERCURY (II) HALIDES WITH COPPER (I) AND SILVER (I) HALIDES IN SOLID STATE

SUMMARY

THESIS

SUBMITTED FOR THE AWARD OF THE DEGREE OF

Doctor of Philosophy

IN

CHEMISTRY

BY

SABA BEG

DEPARTMENT OF CHEMISTRY
ALIGARH MUSLIM UNIVERSITY
ALIGARH (INDIA)

1991

This thesis entitled, "Studies on the interaction of Mixed Mercury Halides with Copper (I) and Silver (I) halides in Solid State" deals with the study of the following five reactions in solid state.

1. Mercuric chlorobromide - Copper (I) iodide
2. Mercuric chlorobromide - Silver (I) iodide
3. Mercuric chloroiodide - Copper (I) iodide
4. Mercuric chloroiodide - Silver (I) iodide
5. Mercuric chloroiodide - Copper (I) tetra iodo mercurate

All these reactions were studied by reflectance and resistivity measurements, chemical and x-ray diffraction analysis. Kinetics of the reactions were studied by visual technique.

Kinetic Studies

Kinetics of the reactions were studied by placing mixed mercury halide over copper (I) iodide, silver (I) iodide and copper (I) tetra iodo mercurate in separate glass tubes of 0.5 cm internal diameter. The glass tube was kept in an air thermostat controlled to $\pm$ 0.5 ^{o}C. The progress of the reaction was followed by measuring the total thickness of the product layer formed at the interface by a travelling microscope (least count 0.001cm), having a calibrated scale in its eyepiece.

X-ray Studies

The reactants were mixed thoroughly in an agate mortar in different molar ratios and heated in an air thermostat at 100°C for three days. X-ray diffractograms of the reaction mixtures were recorded by Norelco Geiger Counter X-ray diffractometer (PW 1010 Philips) using CuK_{α} radiation and Ni-filter applying 32Kv at 12 mA. The compounds were identified by calculating the d values and comparing them with the standard values of the expected compounds.

Resitivity Measurements

The reactants were thoroughly mixed with each other in different molar ratios separately and pressed into a disc. The disc was then fixed between platinum electrodes and the resistance was measured at 80°C at different times by LCR Bridge (Gen. Rad. 1659 Digibridge) at constant frequency (10×10^3 Hz).

Reflectance Spectra

The reflectance measurements for the different molar ratio mixtures of the reactants, heated at 100°C for three days, was made with PYE UNICAM PU 8800 UV/VIS Spectrophotometer (Philips), using white standard as a reference material.

Chemical Analysis

Reaction tubes having distinct product layers were broken carefully and the different layers were collected separately. Products were identified by chemical analysis and X-ray diffraction analysis.

1. HgClBr - CuI Reaction

Compounds identified, in different molar mixtures of the reactants, by X-ray analysis are given in table I.

The reaction occured stoichiometrcally in 1:4 molar ratio. Electrical resistivity measurements show a sharp decrease followed by a continous rise in the resistivity leading to a constant value. This indicates the presence of the intermediate, HgI_2. HgI_2 so formed is immediately consumed by the unreacted CuI present in the reaction mixture to form low resistance Cu_2HgI_4. The overall reaction can be represented as :

$$HgClBr + 2CuI \text{ -------} > CuCl + CuBr + HgI_2$$

$$HgI_2 + 2CuI \text{ -------} > Cu_2HgI_4$$

$$HgClBr + 4CuI \text{ ------} > Cu_2HgI_4 + CuCl + CuBr$$

TABLE I

Molar ratios of HgClBr : CuI	Compounds identified on heating the mixtures at 100°C for 3 days
1 : 4	Cu_2HgI_4, CuCl and CuBr
1 : 3	Cu_2HgI_4, CuCl, CuBr and HgI_2
1 : 2	Cu_2HgI_4, CuCl, CuBr and HgI_2
1 : 1	CuCl, CuBr, HgI_2 + $HgCl_2$ and HgBrI
2 : 1	Cu_2HgI_4, CuCl, CuBr and HgI_2

The lateral diffusion data best fit the rate equation

$$X^n = kt$$

where X is the total thickness (cm) of the product layers at time t (hrs), and k and n are the constants. The rate constant k follows the Arrhenius equation

$$k = A \exp(-E/RT)$$

The activation energy evaluated from Arrhenius plot was found to be 43.3 kJ/mole. It was found that the reaction is diffusion controlled taking place via vapour phase diffusion.

2. HgClBr - AgI Reaction

Compounds identified in different molar mixtures of reactants are given in table II.

TABLE II

Molar ratios of HgClBr : AgI	Compounds identified in mixtures heated at 100° for 3 days
1 : 4	Ag_2HgI_4, AgCl and AgBr
1 : 3	Ag_2HgI_4, AgCl, AgBr and HgI_2
1 : 2	AgCl, AgBr and HgI_2
1 : 1	AgCl, AgBr, $HgCl_2$, HgI_2 and HgBrI
2 : 1	AgCl, AgBr, HgClI, HgBrI and HgClBr

The reaction occured stoichiometrically in 1:4 molar ratio. When the reactants were mixed red colour product was obtained which gradually changed to yellow. This suggests, that the reaction proceeds through the formation of the intermediate HgI_2. Stoichiometcally the proposed mechanism is :

$$HgClBr + 2AgI \longrightarrow AgCl + AgBr + HgI_2 \quad \ldots (1a)$$

$$HgI_2 + 2AgI \longrightarrow Ag_2HgI_4 \quad \ldots (1b)$$

$$HgClBr + 4AgI \longrightarrow Ag_2HgI_4 + AgCl + AgBr$$

Resitivity measurements show only one inflection and thus provide no evidence for multistep reaction.

The kinetic data for lateral diffusion best fit the rate equation,

$$X^n = kt$$

The activation energy calculated from Arrhenius plot is 57.35 kJ/mole. When the rate was measured by keeping an air-gap of different lengths between the two reactants, it was observed that the reaction rate decreased with the increase in the lengths of air-gap. Hence, it was concluded , that the reaction is controlled by vapour phase.

3. HgClI - CuI Reaction

Compounds identified in different molar ratic mixtures of the reactants are given in table III.

TABLE III

Molar ratio of HgClI : CuI	Compounds identified in mixtures heated at 100°C for 3 days
1 : 4	CuCl and β- Cu_2HgI_4
1 : 3	CuCl and β- Cu_2HgI_4
1 : 2	CuCl, HgI_2 and β-Cu_2HgI_4
1 : 1	CuCl, HgI_2 and β- Cu_2HgI_2
2 : 1	CuCl, HgI_2, $HgCl_2$ and β- Cu_2HgI_2

X-ray diffraction analysis of reaction carried out with different molar ratios suggest that the reaction takes place in 1:3 molar ratio. The mechanism proposed on the basis of X-ray analysis and resistivity measurements is

$$HgClI + 3CuI \longrightarrow Cu_2HgI_4 + CuCl \qquad \ldots (1)$$

However, above temperatures 70°C, the reaction mass turned from red to chocolate colour showing the transition to be taking place in Cu_2HgI_4. Even at higher temperature, a red colour was observed to be present. It was concluded that this red colour is due to the formation of HgI_2 as an intermediate.

$$HgClI + CuI \longrightarrow CuCl + HgI_2 \quad \ldots (1a)$$

$$HgI_2 + 2CuI \longrightarrow Cu_2HgI_4 \quad \ldots (1b)$$

As the step (1b) is very fast, the evidence for the fist step was not detected during the resistivity measurements.

The kinetic data for lateral diffusion best fit the rate equation

$$X^n = kt$$

The activation energy calculated from the Arrhenius plot is 56.43 kJ/mole. When the rate was measured by keeping an air-gap of different lengths between the two reactants, it was observed that the reaction rate decreased with the increase in the length of air-gap. Hence, it was concluded, that the reaction is diffusion controlled taking place via vapour phase diffusion.

4. HgClI - AgI Reaction

Compounds identified in different molar ratio mixtures of the reactants are given in table IV.

TABLE IV

Molar ratio of HgClI : AgI	Compounds identified in mixtures heated at 100°C for 3 days
1 : 3	AgCl and Ag_2HgI_4
1 : 2	AgCl, HgI_2, $HgCl_2$ and Ag_2HgI_4
1 : 1	AgCl, HgI_2, $HgCl_2$ and Ag_2HgI_4
2 : 1	AgCl, HgI_2, $HgCl_2$ and Ag_2HgI_4

It is evident from the table IV that HgClI and AgI react by the same mechanism in different molar mixtures. It was observed that when the reactants were mixed at room temperature, a red colour was formed that gradually changed to yellow. The red colour is due to the formation of HgI_2 which immediately reacted with AgI to give the addition product Ag_2HgI_4. Hence, the overall mechanism can be given as

$$HgClI + AgI \longrightarrow AgCl + HgI_2 \quad \ldots (1a)$$

$$HgI_2 + 2AgI \longrightarrow Ag_2HgI_4 \quad \ldots (1b)$$

$$HgClI + 3AgI \longrightarrow AgCl + Ag_2HgI_4$$

The resistivity measurements show only one inflection.

The resistivity curves for 1:2, 1:1 and 2:1 molar ratio mixtures follow the same pattern as that of 1:3. So we can say that the reaction with mixtures in these molar ratios follow the same chemical interaction as that for 1:3 molar mixture. The presence of $HgCl_2$ and HgI_2 in the mixture is due to the presence of excess HgClI which,being not very stable,decomposes into its components $HgCl_2$ and HgI_2.

The kinetic data for lateral diffusion best fit the rate equation

$$X^n = kt$$

The activation energy calculated from the Arrhenius plot is 111.84kJ/mole. It was also found that the reaction is diffusion controlled taking place via vapour diffusion.

5. <u>HgClI - Cu_2HgI_4 Reaction</u>

Compounds identified in different molar mixtures of reactants are given in table V.

for 1:2 molar mixture of HgClI and Cu_2HgI_4 the resistivity measurements suggest the reaction to be a multistep one. Therefore, the mechanism proposed for this reaction is

$HgClI + Cu_2HgI_4 \longrightarrow CuI + CuCl + 2HgI_2$ ... (1a)

$2CuCl + HgI_2 \longrightarrow 2CuI + HgCl_2$ ... (1b)

$Cu_2HgI_4 + HgCl_2 \longrightarrow 2CuCl + 2HgI_2$ ... (1c)

$HgClI + 2Cu_2HgI_4 \longrightarrow CuI + CuCl + 3HgI_2$

TABLE V

Molar ratio of $HgClI : Cu_2HgI_4$	Compounds identified in mixture heated at 100°C for 3 days
1 : 3	β- Cu_2HgI_4, CuCl, CuI and HgI_2
1 : 2	CuI, CuCl and HgI_2
1 : 1	CuCl, HgI_2 and β- Cu_2HgI_4
2 : 1	CuCl and HgI_2
3 : 1	CuCl and HgI_2

The resistance first decreases, then a slight increase and finally it becomes constant. This shows that initially more conducting products (CuCl and CuI) are formed. Rise in resistivity is due to step (1c). The lines of Cu_2HgI_4 present in the mixture may be due to the unreacted Cu_2HgI_4 present in excess.

The resistivity curve for 1:3 molar mixture follows the same pattern as that of 1:2. Therefore, this molar mixture follows the same mechanism as proposed above. The analysis of the end products of this mixture showed the presence of Cu_2HgI_4 because it is present in greater amount than is required by the proposed mechanism.

For 1:1, 2:1 and 3:1 molar mixture, the resistance first shows an increase and then becomes constant. The first step must therefore suggests the formation of non-conducting products. The mechanism proposed is

$$2HgClI + Cu_2HgI_4 \text{ -----> } 2CuI + HgCl_2 \quad \ldots (2a)$$

$$2CuI + HgI_2 \text{ ------> } Cu_2HgI_4 \quad \ldots (2b)$$

$$Cu_2HgI_4 + HgCl_2 \text{ -----> } 2CuCl + 2HgI_2 \quad \ldots (2c)$$

$$2HgClI + Cu_2HgI_4 \text{ ----> } 2CuCl + 3HgI_2$$

There is no decrease in the resistance due to the formation of Cu_2HgI_4 (2b) because it is being consumed as soon as it is formed.

It seems from this discussion, that when Cu_2HgI_4 is in excess than HgClI, one type of mechanism is followed in which case the stoichiometry of the reaction is 1:2 of HgClI and

Cu_2HgI_4. When HgClI is in excess, stoichiometry of the reaction is 2:1 of HgClI and Cu_2HgI_4.

The reflectance studies also reveal that the pattern followed in 1:2 and 1:3 molar mixtures and Cu_2HgI_4 are similar and that followed in 1:1, 2:1 and 3:1 are similar.

The kinetic data for lateral diffusion best fit the rate equation

$$X^n = kt$$

The activation energy calculated from the Arrhenius plot is 43.382 kJ/mole. It was also found that the reaction is diffusion controlled taking place via vapour phase diffusion.

STUDIES ON THE INTERACTION OF MIXED MERCURY (II) HALIDES WITH COPPER (I) AND SILVER (I) HALIDES IN SOLID STATE

THESIS

SUBMITTED FOR THE AWARD OF THE DEGREE OF

Doctor of Philosophy

IN

CHEMISTRY

BY

SABA BEG

DEPARTMENT OF CHEMISTRY
ALIGARH MUSLIM UNIVERSITY
ALIGARH (INDIA)

1991

PHONE : 25515

DEPARTMENT OF CHEMISTRY
ALIGARH MUSLIM UNIVERSITY
ALIGARH—202 002

December 25,1991.

This is to certify that the thesis entitled "Studies on the Interaction of Mixed /Mercury(II) halides with Copper(I) and Silver(I) halides in Solid State submitted to the Aligarh Muslim University describes the original work of Ms. Saba Beg carried out under my supervision and is suitable for the award of Ph.D. Degree in Chemistry.

Afaq Ahmad

(Dr.Afaq Ahmad)

AKNOWLEDGEMENT

I feel privileged to express my deep sense of gratitude towards Dr. Afaq Ahmad for his constant encouragement and inspiring guidance in carrying out this work.

I am very greatful to Dr. Safia Mehdi, Head, Inorganic and Physical Chemistry Division, Indian Institute of Chemical Technology, Hyderabad, for providing facilities for X-ray measurements.

I am also thankful to the Chairman, Department of Chemistry, for providing the research facilities.

In the last, but not the least, I would like to thank Dr. Anees Ahmad for the help in computation on VAX-II.

Saba Beg

(Saba Beg)

CONTENTS

The growing application of solid state devices and the emergence of materials like superconducting ceramics, conducting polymers and the use of solid fuels in rockets and spacecrafts, and requirements of better refractory materials has stimulated interest in the search of newer solids exhibiting the projected properties and the study of solid state reactions.

Despite the natural abundance of solids, reactions in the solid state remained unrecognised for a long time. Though some systematic study of reactions between solids was done in the nineteenth century [1], it was only in 1920, that Hedvall [2,3] observed the first evidence that reactions may be carried out by the motion of lattice elements. Wagner [4] expressed the formal rate expression in terms of the gradient of chemical potential, mobility of lattice particles in solids and of the lattice disorder models as postulated by Frenkel and by Schottky.

A solid state reaction, in the classical sense, occurs when local transport of matter takes place in crystalline phases. Therefore, the general problem of the solid state reaction is two fold. Firstly, the experimental determination of reaction rate and morphology as a function of all independent variables. Secondly, the calculation of the morphology under a given set of independent variables in terms of known thermodynamic and

transport properties of the system under consideration. These require the knowledge of the atomistic mechanism of the fundamental steps such as nucleation, phase boundary reaction, sintering and diffusion. Theoretical models are in general not adequate for interpretation of real cases. Real systems are usually in a state of considerable imperfections. Enhanced and desirable activity and lattice reactivity are often obtained by producing a solid in the form of imperfect crystal. All the elementary steps in a solid state reaction are influenced by lattice imperfections. Lattice imperfections often constitute preferred sites for the reaction and nucleation and make solid state diffusion possible by enabling the reactants to reach each other.

For a quantitative treatment of the reaction kinetics, one has to assume, the local thermodynamic equilibrium in the solid phases taking part in the reaction and a thermodynamically well defined system in which the proper number of independent thermodynamic variables are predetermined. Knowledge of point defect thermodynamics, thermodynamic properties of the systems and that of Fick's Law are sufficient to treat the problem quantitatively.

The gradient of chemical potential is the local driving force

for the fluxes of the components. There are other solid state reactions in heterogeneous systems which proceed under the action of other kinds of driving forces such as relative temperature gradients [5] and those driven by phase boundary free energies called as the Ostwald ripening process [6,7].

The reaction between heterogeneous solid phases, where phase boundary controls the overall rate, are very important and have been studied in a number of solid gas reactions where a linear rate law indicates that diffusion control does not play the predominent role. Although it has been found in a number of solid state reactions in ionic systems that the linear rate law is the initial rate determining step, the atomistic reaction mechanisms are not yet understood. This is due to the fact that in contrast to gas solid reactions, it is extremely difficult to study the linear reaction rate as a function of the component activities at solid - solid interfaces. But a knowledge of the reaction rate as a function of the independent variables is a pre-requisite for a correct analysis of the atomistic reaction steps of a phase boundary reaction.

The process associated with the solid state reactions are fundamentally more complicated than those involved in gas phase or liquid phase processes. In the latter, mixing occurs at molecular level so the rate can be expressed as a function of

concentrations of reactants. In solid state reactions, at least one reactant diffuses into the other in order that the reaction may be initiated and propagated. Thus, the main point on which chemical reactions with solids distinguish themselves from those ocurring in liquid or gaseous phase is the effect of lattice structure [8,9] and diffusion mechanism. Furthermore, as the solid state processes involve movement of the interphase boundary, the mathematical formulation of the rate processes must be expressed in terms of space and time coordinates.

Five reaction types have been distinguished in the solid state reactions namely: solid state decomposition, dimerization etc., reaction between a solid and a gas, another solid or a liquid and reactions at the surface of a solid which does not enter into the overall reaction equation. Mechanismwise, solid state reactions are roughly classified as under.

1. Diffusion controlled reactions in which atomic motions are largely uncorrelated.
2. Diffusionless phase transformations which involve co-operative motion of lattice elements.
3. Reactions that involve extended defects and that combine features of the first two classes.

There are, however, alternative schemes for classifying

solid state reactions in which the product structure bears a definite relationship with that of the reactants. The reference has been made to the phenomenon of topotaxy [10] and to such processes as topotactic reaction [11,12]. Topotaxy thus describes the mechanism of reactions which involve structural relation between reactant and product. Likewise, epitaxy is a two dimensional correlation between the reactant and the product, but having no correlation in the third dimension.

The properties of solids may be divided into two groups, structure insensitive and structure sensitive. Structure insensitive properties are well defined under given external conditions and are independent of the history of the specimen and of its dimensions like chemical formula, lattice dimension, density, etc. Structure sensitive properties on the other hand, are directly affected by factors like the mode of preparation of the specimen, the particle size and shape for instance, electrical conductivity and absorption spectra of real crystals. The chemical reactivity is usually structure sensitive as is evidenced by the fact that the catalytic activity of solids and the ability to luminence and fluorescence may vary with the mode of preparation.

In a solid - solid reaction, different steps, such as

nucleation, transfer of matter across phase boundaries and diffusion in reaction product occur. Therefore, besides defect thermodynamics, the diffusion theory is the basis for the explaination of solid - solid reactions.

Lattice Imperfections and their role in Solid State Reactions

For understanding the reactivity of solids, a classification of crystal defects is essential. Point defects are atomic in nature whose effect is limited only to their immediate surroundings like interstitial atoms or vacancies in the regular lattice. Example of one dimensional defect is dislocation. Grain boundaries, phase boundaries, stacking faults and surfaces are two dimensional defects. Finally, pores and macroscopic inclusions are three dimensional defects.

The simple lattice defects, vacancies and interstitial atoms, take part in variety of processes leading to phase changes, precipitation, order - disorder transformation and chemical reactions in solids.

Frenkel in 1926 and Schottky in 1935 developed theories regarding the presence of interstitials and vacancy defects in crystals. The two most important type of native lattice defects are vacant lattice sites or vacancies and interstitials, which

are atoms or ions introduced into the normally unoccupied spaces between regular lattice sites. When regular lattice sites are occupied by foreign particles then the disorder is substi tutional. In a pure stoichiometric crystal two types of natural disorders often occur. First the Schottky disorder where an equal amount of anion and cation vacancies exists. Secondly, the Frenkel disorder where equal concentrations of ion vacancies and interstitials of the same type occur :

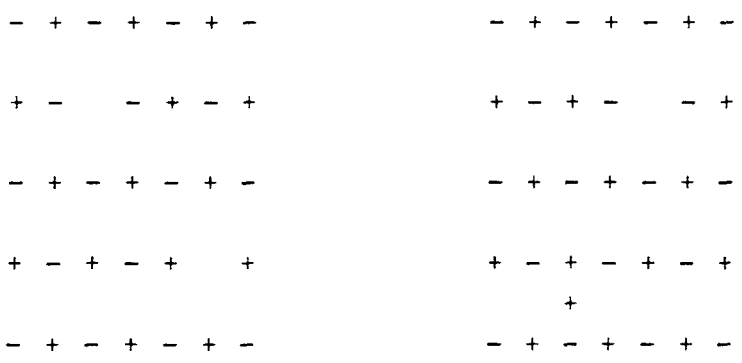

(a) Schottky defect (b) Frenkel defect

The concept of dislocation was first developed by Taylor and Orowan. Dislocations are one dimensional defect and are largely responsible for the plastic behaviour of solids. They can serve as sites of repeatable growth within crystal and also as fast diffusion paths. They also act as preferential nucleation sites for the formation of new phases.

Lattice defects [13] play a crucial role in solid state

reactions because diffusion processes in solids are controlled by the concentration and mobility of such defects. In most mettallic systems the vacancy is the most important defect since it is responsible for the interchange of atoms. Experimental evidence for vacancy diffusion is provided by Kirkendall effect.

In high temperature chemical processes, role played by point imperfections predominates over that played by line imperfection and therefore the mechanism of diffusion is in favour of migration via point defects. This is the basis of Wagner Theory [14] of the high temperature oxidation which has been applied to describe the high temperature oxidation of metals. Thus we can say that the reactivity of solids is a structure sensitive property.

Point defects predominate in high temperature ranges, whereas dislocations may be more important in the low temperature ranges.

Diffusion

Diffusion is a transport process of matter in matter, due to thermally activated motion of ions, atoms or molecules. Depending on the mode of migration of the atoms, ions, etc. we have bulk diffusion, surface diffusion and diffusion along crystal faces, the former of which has been a subject of thorough study.

Elucidation of diffusion mechanisms is often very difficult

and is quite complex. It was not clear in early stages whether solid state reactions go through diffusion in solid state or via vapour phase [15 - 17]. The first idea of difffusion mechanism seems to have been given by Havesy. Joffe [18] in 1923 suggested other ideas on the mechanism of mass transfer in crystalline lattice which was the basis of the quantitative treatment of the diffusion theories of Frenkel and later Wagner and Schottky [19].

In a solid - solid reaction, two solids react to form a product which separates them. Furthermore reaction progresses through three steps in series: self diffusion of the reactant species, its diffusion through the product layer and finally its diffusion and reaction in the other reactant. Thus three different diffusivities are involved.

To decide which of the mechanism will be operational in a particular case, the following considerations are outlined.

1. Diffusion takes place by defect mechanism if the activation energy is much higher than the heat of sublimation, while vapour phase mechanism occurs when activation energy is equal to that of sublimation energy. Low value of activation energy would indicate either surface migration or grain boundary diffusion.
2. If the initial rate of reaction is directly proportional to

the dissociation pressure of the species, the reaction should proceed via the vapour phase diffusion.

3. Kinetic studies, when reactants are separated by an air-gap and when in contact, may be helpful for distinguishing whether surface diffusion or vapour phase diffusion takes place. If the reaction rate is the same in the two cases, it indicates that reaction proceeds via vapour phase diffusion. On the other hand, if reaction ceases when the reactants are separated by an air gap, diffusion is not via vapour phase. This simple experiment has been used in determining the course of certain solid-state reactions.

Sintering

Sintering is one of the most important phenomenon which occur when a metal or a ceramic powder is transformed into a dense, solid product of greater strength or the phenomenon by which useful solid products are formed from metallic or non-metallic inorganic powders on heating. It can affect both the rate of reaction between solid substances and also the properties of the resulting products. Therefore, the role of sintering in the study of solid state reactions is of prime importance.

Several stages are involved in the sintering process. First,

the surface roughness is destroyed, that is, surface becomes smooth. This is followed by the welding of the particles at the contact site and finally there is the so called densification phenomenon, where much of the void volume which resulted from the initial misfit of the powder particles is eliminated. The area of the entire surface of the particle decreases and the surface of the contact increases. During sintering there is also an increase in the number of non-equilibrium grains, a decrease in the lattice defects and removal of existing stresses in the contact area of the material. Earlier, it was thought that liquid phase has to be present but now it has been proved that particles which are solids at all times can be joined by sintering. Though the technological process has been known for many centuries, the explaination, which depends upon solid state diffusion and defects in solids, has developed only within the last decade or so.

Nucleation

In solid-state reactions, initially surface diffusion rapidly coats the surface of the reacting particles with a continuous product layer and the rate of reaction is taken to be the rate diffusional growth of the product blanket. However, this is not always the case, especially in phase transformation and

decomposition reactions or new crystalline phase formation from supersaturated solutions. Phase transformations take place more rapidly than is expected from the reaction rate theory [20].

However, the rate of transformation is determined by two distinct processes, nucleation and growth, each having characteristic activation energies that are usually different.

Nucleation is the process whereby particles of more stable phases are formed which are large enough to be thermodynamically stable. Nucleation can occur in a crystal in two ways. A local imperfection in the crystal, produces strains in its vicinity so that the total energy required for the transition to a new configuration is lowered by the strain energy at the site of the imperfection. The reduction in the activation energy means that such sites may become preferred nucleation centres and so called heterogeneous nucleation takes place.Nucleation that takes place uniformly throughout the parent phase, is called homogeneous.

Homogeneous Nucleation

In homogeneous nucleation the probability of nucleation occuring at any given site is identical to that of any other site within the volume of the parent phase. In this type of nucleation, spontaneous fluctuations of atomic configurations

serve to form nuclei. When a small region of the second more stable phase is formed, there is a lowering of the volume free energy. However, there is also a surface free energy for the nuclei and there may be an elastic energy associated with strains in the lattice to accommodate the nuclei and both of these oppose the change. Therefore the change in the free energy when a nucleus is formed is

$$\Delta G = -\Delta G_v + \Delta G_s + \Delta G_e \qquad \ldots (1)$$

where V, s and e denote the free energy changes due to the volume chemical change, the formation of a new surface and elastic strain. ΔG_v is negative because the transformation proceeds from less stable to a more stable state.

To a first approximation we can ignore the last term. ΔG_v is proportional to the volume of the nuclei, whereas ΔG_s is the free energy change accompanying the formulation of a spherical new phase particles, we can write,

$$\Delta G = 4\, r^2 \Delta g_s + \frac{4\, r^3 \Delta g_v}{3} \qquad \ldots (2)$$

where Δg_s is the surface free energy per unit area, r is the radius of the nucleus, Δg_v is the change in free energy (negative) resulting from the transformation for unit volume and

the term due to elastic strain is assumed to be negligible. Upto a certain critical size r*, any enlargement of the nucleus requires an increase in free energy, because the r^2 dependence of ΔG_s dominates, but beyond the critical size the decrease in free energy due to chemical change, with it r^3 dependence, outweighs the increase in free energy required to produce new surface. Hence, fluctuations may produce small nuclei and they may get the critical size and grow, as further increase in their size results in a decrease of the total free energy for the system.

The number of nuclei, N, formed per unit volume of solid is givem by

$$N = N_o e^{-\Delta g^*/Kt} \qquad \ldots (3)$$

where N_o is the total number of particles in the new phase and Δg^* is the increase in the free energy for a nucleus of critical size. The critical size of the nuclei can be determined by differentiating eq (2) with respect to r and setting this derivative equal to zero, $(d\Delta g/dr) = 0$ with the result,

$$r^* = \frac{-2\Delta g_s}{\Delta g_v} \qquad \ldots (4)$$

and the corresponding critical free energy is

$$\Delta g^* = \frac{16 \pi (g_s)^3}{3(\Delta g_v)^2} \qquad \ldots (5)$$

The rate of nucleation depends on the critical free energy as well as on the frequency with which the atoms jump across the interface from the parent phase to a daughter phase. According to Volmer and Weber, the frequencies of such jumps in a condensed systems are given by,

$$f = S^* \nu_o e^{(-\Delta G_a/KT)} \qquad \ldots (6)$$

where as ΔG_a is the free energy of activation of a single atomic jump to the embryo surface , S* is the number of atoms adjacent to the embryo surface when this is of critical size, $\nu \simeq 10^{13}$ sec^{-1} is the vibration of the atoms and K is the Boltzmann's constant.

Heterogeneous Nucleation

When nucleation is occuring at certain preferred sites the process is called heterogeneous nucleation. In a solid - solid transformation foreign inclusions, grain boundaries, interfaces, stacking faults and dislocations can provide sites for preferred nucleation. The formation of nuclei is influenced by the relative interfacial tentions between the nucleus and the imperfection

σ_{ni} and between the parent phase and imperfection σ_{pi}

$$\Delta G_i = \sigma_{ni} - \sigma_{pi} \qquad \ldots (7)$$

where ΔG_i is the change in the free energy due to the formation of a unit area of interface between the nucleus and the imperfection. According to this equation the free energy decreases (change is negative) when $\sigma_{pi} > \sigma_{ni}$.

Analysis of the rate expression for nucleus formation in heterogeneous system shows that the rate of nucleation is proportional to

$$\exp(-\Delta f_{\ddagger}/RT) \qquad \ldots (8)$$

where $\Delta f_{\ddagger}$ is the free energy of formation for the critically sized nucleus and is inversely dependent upon the square of the free energy difference between the free phases, Δf_s. For a spherical nucleus,

$$F_{\ddagger} = \frac{16\, y^3 (V_m)^2}{(\Delta F_s)^2} \qquad \ldots (9)$$

where y is the strain energy per unit interfacial area between phases and V_m is the molecular volume of the nucleating phase. ΔF_s can be expressed in terms of the reaction pressure, P, and the pressure P_e for the univarient equilibrium at the reaction

temperature.

$$\Delta F_s = (-RT \ln P/P_e)^2 \quad \ldots (10)$$

By substituting equation (9) and (10) into equation (8) the relation between the nucleation rate and the reaction pressure becomes,

$$\log N = C_1 (-RT \ln p/P_e)^{-2} + C_2 \quad \ldots (11)$$

where C_1 and C_2 are constants.

Grain boundaries and dislocations provide important sites for heterogeneous nucleation in solid state transformation. The grain boundary energy decreases the free energy of nucleation because stresses producing during nucleation are more readily relieved at grain boundaries. The theory of nucleation at various kinds of grain boundary sites has been given by Gibbs [21]. Cahn [22] has given theory explaining the formation of nucleus at dislocation sites and calculations of rate of heterogeneous nucleation have been performed successfully for various types of transformation [22]. Growth is the increase in size of product particle after it has nucleated. Therefore, it is obvious that nucleation and the growth are complimentary and take place almost simultaneously.

Kinetic Models

Three kinetic models based on the following rate controlling mechanism of solid state reactions are discussed

1. Product growth controlled by diffusion of reactants through a continuous product layer.
2. Product growth controlled by nuclei growth.
3. Product growth controlled by phase boundary reactions.

Diffusion Models

There are two fundamental processes involved in a solid state reaction :

1. Phase boundary processes such as chemical reaction itself, formation of nuclei and growth of the reaction products.
2. The transport of matter to the reaction zone, i.e. diffusion through the reaction products for a unidirectional diffusion with constant diffusion coefficient across the product layer the rate of growth of the product layer is given by,

$$\frac{dy}{dt} = \frac{DK}{y}$$

where y is the thickness of the product layer, t is the reaction time, D is the diffusion coefficient of the migrating

species and K is a proportionlity constant. If the diffusion is independent of time and the area of contact remains constant, integration yields,

$$y^2 = 2KDt + c$$

choosing the boundary condition, y = 0 when t = 0, gives

$$y^2 = 2KDt = K_p t \qquad \ldots (12)$$

This is the well known parabolic rate law, where K_p is the parabolic rate constant.

In 1927, Jander applied the parobolic rate law, developed for planar interface reactions, to powdered compacts. Jander's model is based on on the following assumptions :

1. The reaction under consideration can be classified as an additive reaction.
2. Nucleation which is followed by surface diffusion, occurs at a temperature below that needed for bulk diffusion so that a coherent product layer is present when bulk diffusion does occur.
3. The chemical reaction at the boundary is considerably faster than the transport process and thus, the solid state reaction

is bulk diffusion controlled.

4. The surface of the component on which reaction takes place is completely and continously covered with particles of the other component, as though the former particles were immersed in a melt of the latter. This assumption is approximately true when the ratio of (r_A/r_B) is very large and the amount of (B) is greatly in excess compared with that of component (A).
5. Bulk diffusion is unidirectional.
6. The product phase is not miscible with any of the reactant phase.
7. The reacting particles are all spheres of uniform radii.
8. The increase in the thickness of the product layer follows the parabolic rate law.
9. The diffusion coefficient of the species being transported is not a function of time.
10. The activity of the reactants remain constant on both sides of the reactant interface.

He derived the following expression for the fractional conversion x :

$$K_J t = [1 - (1 - x)^{1/3}]^2 \qquad \ldots (13)$$

Equation (13) is the well known Jander equation relating the

fraction of reaction completed to time, K_J is the rate constant. Practical evidence have not been able to satisfy equation (13).

Kroger and Ziegler assumed that the rate of change of product layer thickness is inversely proportional to time, which is the basis of Tamman Theory,

$$y^2 = 2K \ln t$$

This equation combined together with the Jander equation gives rise to the Kroger - Ziegler equation

$$K_{k-z} \ln t = [1 - (1-x)^{1/3}]^2 \quad \ldots (14)$$

Zhuravlev, Lesokhin and Templeman [23] assumed that the activity of the reacting substance was proportional to the fraction of unreacted material (1-x).

$$K_{Z-L-T} t = [(1/1-x)^{1/3} -1]^2 \quad \ldots (15)$$

Ginstling and Brounshtein [24] suggested a model using Barrer's growth of the product layer equation for steady state heat transfer through a spherical shell. They gave the equation

$$K_{G-B} t = 1 - (2/3)x - (1-x)^{2/3} \quad \ldots (16)$$

Carter [25] took into account the difference in the volume of the product layer with respect to that of volume of reactant

consumed. He introduced " Z " for the volume of the reaction product formed per unit volume of reactant consumed and gave the equation,

$$K_{C-V}\, t = \frac{Z-(Z-1)(1-x)^{2/3}-[1+(Z-1)x]^{2/3}}{Z-1} \qquad \ldots (17)$$

Valensi developed the same solid state reaction model mathematically from a different starting point. Thus equation (17) is referred to as the Valensi - Carter equation.

Dunwald-Wagner derived an equation for solid state reactions using the Fick's second law for diffusion into or out of sphere. The equation is

$$K_{D-W}\, t = \ln\ 6/\ (1-x) \qquad \ldots (18)$$

All the models discussed here have the drawback that they are based on the reaction of spherical particles of uniform radius. However they are able to explain many solid state reactions in a satisfactory way. There are many other models which take into account the particle size gradation. These have been developed by Miyagi [26], Sasaki [27] and Gallagher [28].

Nuclei growth model

The theory of nucleation and growth of the product phase initially formulated for the kinetics of phase change processes, has been successfully employed to decomposition reactions [29]. This theory considers two steps : (1) Formation of the nuclei and (2) the growth of these nuclei. The general form of the expression for conversion time relationship,

$$\ln(1-x) = -(kt)^m \qquad \ldots (19)$$

The parameter m accounts for the reaction mechanism nucleation rate and geometry of the nuclei. If a reaction is represented by this model, a plot of ln(ln 1/1-x) vs ln t should give a straight line with slope m and intercept m ln K.

Application of nuclei growth model to solid - solid reactions are rare. Hubert and Klawitter [29] applied it to the reaction between zinc oxide and barium carbonate.

Phase boundary models

When the diffusion of the reactant species through the product layer is fast compared to reaction, the kinetics is controlled by phase boundary reactions. Models have been developed for different geometries and corresponding boundary conditions. Thus, for a sphere reacting from the surface inwards, the fractional reaction completed x and time t are related by

$$Kt = 1 - [1-x]^{1/3} \qquad \ldots (20)$$

For a circular disc reacting from the edge inwards, or for a cylinder, the relation is

$$Kt = 1 - [1-x]^{1/2} \qquad \ldots (21)$$

and for a contracting cube,

$$x = 8K^3t^3 - 12\,K^2t^2 + 6Kt \qquad \ldots (22)$$

Several empirical rate laws have been proposed to describe the course of different solid state diffusion controlled reactions.

(i) $Y^2 = Kt$

(ii) $Y^3 = Kt$

(iii) $Y^2 + Yb = Kt$

(iv) $Y = Kt$

(v) $Y = K \log t$

(vi) $Y^2 = 2Kt \exp[-PY]$

Generalized equations $Y=Kt^n$ and $Y^n = Kt$ have also been used by

Rastogi [30] and Beg [31], respectively. In these equations Y is the thickness of product layer, t is the time, K, b, n and P are constants.

Factors affecting Reactivity of solids

The factors that influence the reactivity in the solid state are particle size and contact area, strain, temperature and additives.

Particle size and contact area

Particle size distribution affects the course of a solid state reaction to a great extent. The smaller particle in the ensemble will be consumed in a shorter period of time as compared to the bigger particles. Hence, the reaction rate per unit volume, which is based on the radius of an individual particle, will be affected. Particle size distribution will also have an effect on voidage and hence on the effective contact area, since smaller particles can go into the interstitial spaces formed by bigger particles. According to Montierth, Gordon and Cutler the greater the contact area the more enhanced is the reaction. Kutty and Murthy [32] observed that the reaction obeys a first order equation, when both the reactants are fine and a parabolic rate

law, when the reactants are coarse.

Strain

Strain is a measure of the time independent displacement of the atoms from their mean positions to some other nearby positions. Lattice strain may arise from external pressure, from imperfections or from the existence of impurity atoms of such a nature as to disturb the regularity of the lattice. It has an important effect on rate of reactions. Such strain may act as a source of energy, and so may increase the ease with which imperfections are formed and hence increase the rate of diffusion.

Temperature

It is a well established fact, that velocity of a chemical reaction increases with rise in temperature. Increase in temperature provides extra energy to the reactants and enable them to overcome the barrier of interaction and thus leads to a tremendous increase in reaction velocity and hence in rate constants.

Additives

In a solid - state mixed powder system both catalytic and

inhibitory effects are exhibited by the additives. Thus, they may affect the crystal structure of a solid by increasing or decreasing the number of defects in the lattice, thereby creating or diminishing vacancy concentration. Such effects are well known in solid state chemistry, particularly in connection with the semiconducting properties of a solid. In fact, doping is a very important technique in semiconductor technology. By the addition of the dopants the conductivity of a sample can be increased or decreased.

References

1. Robert - Austen: Proc. Roy. Soc. (London) 59, 283 (1896).
2. Hedvall, J.A.: Anorg. Chem., 86, 201, 296 (1914).
3. Hedvall, J.A.: ibid, 93, 313 (1915).
4. Wagner, C. and Schottky, W.: Z. Physik chem. B11, 163 (1930).
5. Wagner, C.: Progress in Solid State Chemistry, eds. Reiss, H. and Mclaldin, J.O. Vol 7 pp.1 (Pergamon, Oxford), 1972.
6. Wagner, C.: Ber. Bunsenges : Physik Chem. 65, 581 (1961).
7. Lifshilz, I.M. and Slazov. V.V : Soviet phys. - JETP, 35,331 (1959).
8. Bernal, J.D.: Trans. Farad. Soc. 34, 834 (1938).
9. De Boer, J.H.: Discuss. Farad. Soc. 23, 171 (1957).
10. Lotgering, F.K.: J. Inorg. Nucl. Chem. 9, 113 (1959).
11. Bernal, J.D., Dasgupta, D.R. and Mackay A.L.: Clay Minerals Bulletin, 4, 15 (1959).
12. Mackay, A.L.: Min. Mag. 32,545 (1960).
13. Schwab, G.M.: Reactivity of solids (Amsterdam - London. New York) (1965)
14. Wagner,C., Grunwald, K., Z. Phys. Chem., B40, 455 (1938)
15. Tammann, G. and Balarew, D. :Z. anorg. allg. Chem, 160, 92 (1927).
16. Ginstling, A.M. :Zhur. Prikl. Kim. Leningr, 24, 267 (1951).

17. Ginstling, A.M. and Fradkina, T.R. : J. Appl. Chem. U.S.S.R, 25, 1199, 1325 (1952).

18. Joffe, A.E., Ann. d. Phys. Chem, 72, 261 (1923).

19. Wagner, C. and Koch E : Z.Phys. Chem. B 38, 295 (1937).

20. Bradley, R.S. : J. Phys. Chem., 60, 1347 (1956)

21. Gibbs, J.W. : Scientific Papers, Dover, New York, Vol 1 (1961).

22. Cahn, J.W. : Acta Met., 5, 169 (1957).

23. Zhuravlev, V.F., Lesokhin, I.G. and Templeman, R.G. : J. Appl. Chem. USSR, 21,887 (1948).

24. Ginstling, A.M. and Brounshtein, B.I. : J. Appl. Chem. USSR (English Translation), 23, 1327 (1950).

25. Carter, R.E. : J. Chem. Phys., 34, 2010 (1961).

26. Miyagi, S. : J. Jap. Cer. Soc., 59, 132 (1951).

27. Sasaki, H. : J. Am. Cer. Soc., 47, 512 (1964).

28. Gallagher, K.J. : Reactivity of Solids, ed. by Schwab, G.M. 192 - 203 (1965).

29. Hulbert, S.F. and Klawitter, J.J. : J. Am. Ceram. Soc., 50, 484 (1967).

30. Rastogi, R.P. and Singh, N.B. : Indian J. Chem., 15A, 941 (1977).

31. Beg, M.A. and Ansari, S.M. : J. Solid State Chem, 20,103 (1977).

CHAPTER-II

Chemistry of Copper (I), Silver and Mercury (II) Halides

Copper is the only element in the first row transition elements which in its first valence state shows the typical class behaviour. The chemistry of copper (I) occurs in a number of accounts [1 - 5] which describe the chemistry of simple compounds of copper (I) with less emphasis on the co-ordination compounds of copper (I) [2,3,6]. During the last two decades, the realisation of copper (I) species to be involved in as the precursor of the silent partner in the complexes of copper (III) with proteins [7,8] has resulted in the study of coordination compounds of copper (I) compounds [2,3,9]. Such a great importance of copper (I) compound is of special interest in the study of the compounds since beginning and till to date with the possible exception of copper (I) fluoride, all the monohalides of copper are known.

Ryss showed that copper (I) fluoride is thermodynamically unstable and Wartenberg had earlier suggested that CuF_2 dissociates at higher temperatures into copper (I) fluoride and fluorine gas. Therefore copper (I) fluoride can be preffered as a metastable entity at low temperatures in the absence of catalysts. CuF is white with rutile crystal structure.

Copper (I) chloride crystals are cubic and white in colour. Wyckoff and Posnjak [10] found that x - radiograms correspond with the double centered cubic lattice of zinc blende. Similar

structures have been reported for copper (I) bromide and copper (I) iodide crystals. However, the copper (I) iodide crystal does not retain its zinc blende structure above 300 °c but has a disordered distribution of copper (I) ions. Above 400 °c, copper (I) iodide belongs to hexagonal system. The vapour density at 1700 °c indicates that copper (I) exists almost entirely as dimer. Even at high temperatures, substantial amounts of cyclic

TABLE I

Physical properties of copper (I) halides

Properties	CuCl	CuBr	CuI	Ref
Melting point	430 °c	483 °c	588 °c	11
Boiling point	1359 °c	1345 °c	1293 °c	12
Colour	White	White	White	11
Solubility in water in mg/l at 25 °c	110	29	0.42	11
$-\Delta H_{298}$ in cal/mole	32.2	24.9	16.2	11
$-\Delta S_{298}$ in cal/mole	20.8	23.0	23.1	11
$-\Delta G_{300}$ in cal/mole	28.0	24.2	19.0	11
CuCl radius in Cu_3Cl_3	1.17	-	-	13

Cu_3X_3 are present. Nevertheless the structures of copper (I) halides, but for copper (I) fluoride, are polymerized cubic. Some of the physical properties of cuprous halides are given in Table I.

The addition of halide ions greatly increases the solubilities of copper (I) halides due to the formation of halocuprate (I) anions [14 - 16] of the type $[CuX_2]^-$ and $[CuX_3]^{--}$.

Complexes of copper (I) halides are formed by all the halogens except fluorine and contain 2, 3 or 4 atoms. Remy and Laves Found that the number belonging to various types of copper (I) chloride complex with chloride, like $[CuCl_2]^-$, $[CuCl_3]^{2-}$ and $[CuCl_4]^{3-}$ are roughly in the ratio 10 : 15 : 1. In fact complexes such as $(NH_4)_4CuCl_2$ and potassium dichlorocuprate (I) $KCuCl_2$, have been prepared [17]. Similarly, sodium dichloro cuprite and potassium trichlorocuprite have also been prepared. The stepwise formation of chlorocomplexes in KCl solution with increasing CuCl/KCl ratio may be represented as

$$CuCl + 2Cl^- = [CuCl_3]^{2-} \quad K = 1.45 \times 10^{-6} \text{ at } 23\ ^\circ c$$

$$CuCl + Cl^- = [CuCl_2]^{2-} \quad K = 11.4 \times 10^{-6} \text{ at } 25\ ^\circ c$$

$$CuCl + [CuCl_2]^{-2} = [CuCl_3]^{2-}$$

The most common coordination number adopted by copper (I) is four, the metal atom being tetrahedrally surrounded by the four ligands. Coordination number of two or three are also known, but

are less common [18, 19]. Many of the compounds having a composition LCuX, where L = ligand and X = halogen, might be expected to contain two co-ordination number. Indeed x-ray studies show them to be tetrameric, having tetrahedral cluster of copper atoms. Non linear trimers of CuCl with two co-ordination number occur in the gas phase. There are only few compounds of copper with co-ordination number four.

The di-iodo cuprate (I) ion is also known, but is considerably less stable than the corresponding chloro and bromo complexes. $[CuBr_2]^-$, $[CuBr_3]^{2-}$ and $[CuBr_4]^{3-}$. Complexes of Copper (I) are known, as also that of $[CuI_2]^-$, $[CuI_3]^{2-}$ and $[CuI_4]^{3-}$. Several copper (I) halide - ammonia complexes have been prepared by the reaction of Cux with NH_3. The compound $Cu(NH_3)_4$ $[CuI_2]$ contains a distorted tetrahedral arrangement of iodine atoms about the copper (I) atom [20].

K. Monkemeyer obtained a series of mixed crystals between copper (I) bromide and copper (I) iodide, between copper (I) chloride and copper (I) bromide, and copper (I) chloride and copper (I) iodide. Batronov and Co-workers oxidised copper (I) chloride with bromine and iodine to obtain CuClBr and CuClI. X-ray examination of these products showed that they were merely mixtures of copper dihalides but no information on the chemical

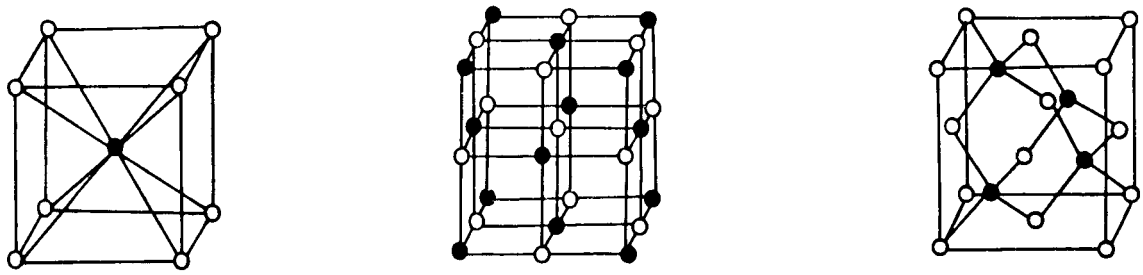

FIG.1. UNIT CUBES OF THE B_2 , B_1 AND B_3 STRUCTURE

properties of the compounds is available.

Recently, halocomplexes of copper (I) such as $[Cu_2I_6]^{4-}$, $[Cu_2Br_5]^{3-}$ and $[Cu_2Br_6]^{4-}$ have been reported by Ahrland and Togession [21].

Silver halide structures are interesting as they involve several different types of structures and the chief attractive forces are coulombic, hence these can be regarded as examples of ionic crystals. But in iodide at least there are considerable contributions of electron pair bond forces. The silver ions are free to move within the structure in silver iodide at high temperature. The photo sensitive properties of these crystals which are of great interest and importance appear to be due to defect lattices. Conventional photographic emulsion contain face -centered AgBr and AgCl and may contain upto 10 wt % hexagonal AgI. The primary sensitivity to light which is in the order AgBr > AgCl > AgI is magnified up to 10^{11} times when the emulsions are developed.

Various types of structures, which have been found for silver halide crystals are listed in Table II. The designation of the structure types as B_1, B_2 etc. (fig. 1) is from Strukturbericht. He also listed the interatomic distances, except that for AgI in the B_1 structure, which is from Jacobs [22] work.

TABLE II

Observed structures types, coordination numbers and shortest interatomic distances.

structure type	B_1	B_2	B_3	B_4
M , M'	6, 12	8,6	4,12	4,12
AgF	2.46	-	-	-
AgCl	2.77	-	-	-
AgBr	2.88	-	-	-
AgI	3.04	-	2.80	2.81

M = The number of closest neighbours of opposite charge.

M'= The number of closest neighbours of like charge.

The B_4 structure has hexagonal symmetry, where each atom has four close neighbours of the other kind tetrahedrally surrounding it as in the B_3 structure. The arrangement of atomic centre in the B_3 and B_4 structure types are such as to permit electron pair bonding throughout, each silver ion being bonded by the four neighbouring halide ions and vice versa. Born and Mayer [23], Huggins and Mayer [24], Huggins [25] and Pauling calculated the lattice energies and interatomic distances for silver halides. Huggins [26] studied the stability of structures at different

temperature and pressure and the presence of interstitial ions and electrons.

Due to rise in temperature the transition in the structure falls in the order

$$B_2 \text{ ----> } B_1 \text{ -----> } B_4 \text{ -----> } B_3,$$

while increasing pressure transition favour the order

$$(B_3 \text{ or } B_4) \text{ -----> } B_1 \text{ -----> } B_2$$

The presence of extra electrons and of extra (not-too-large) ions favour the B_3 arrangement over B_1. The transition from B_1 to B_3 or vice versa, can occur easily as a result of slight shifts of the silver ions only, provided that the dimensions of the two structures are sufficiently similar. The similarity in structures can for example be attained as a consequence of presence of extra ions.

At high temperatures the silver ions in AgI are extremely mobile, giving this solid substance high electrical conductance. At the melting point, its conductance is higher than its melt. Van Klooster [27] reported the heat of formation of silver halides and their thermodynamic properties have been studied by Kubaschewski and Evans [28]. Melting and boiling points are available on Sidgwick [29] and NBS (National Bureau of Standard) [30]

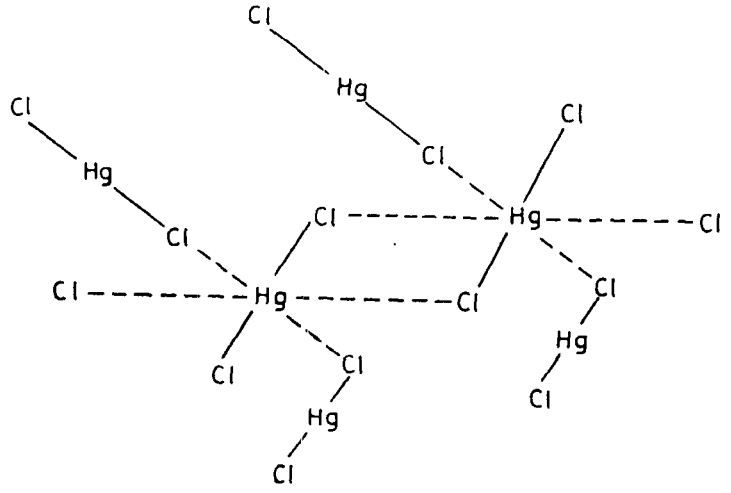

(a)

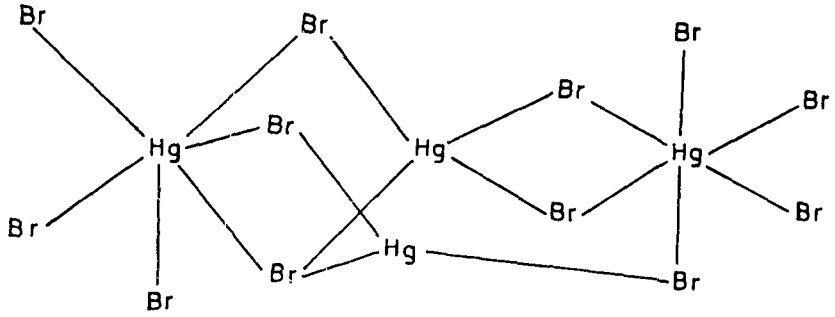

(b)

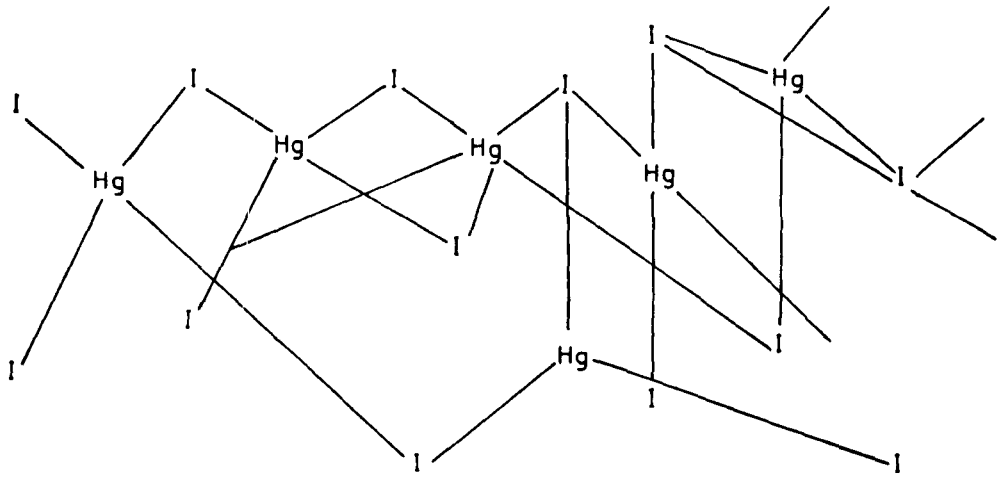

(c)

FIG. 2. ENVIRONMENT OF MERCURY IN THE CRYSTAL STRUCTURE OF (a) $HgCl_2$ (b) $HgBr_2$ AND (c) HgI_2.

A series of mixed crystals of AgBr and AgI of varying composition are known. The variation in crystal lattice as a function of composition has been studied by x-ray and by determination of specific mass. The effect of temperature and pressure on the saturated crystals of silver halides show a remarkable change in the lattice arrangement. Chateau studied the thermodynamic properties of mixed crystals of silver halides.

Mercury fluoride, HgF_2, is obtained by fluorination of metallic mercury or $HgCl_2$. It is a white crystalline solid which darkens in colour on exposure to air due to hydrolysis. HgF_2 possesses the fluorite structure. It is one of the few mercury (II) compounds in which the bonding is believed to be mainly ionic. The other three mercury (II) halides, HgX_2 (X = Cl, Br, I) are simply obtained from the reaction of the elements. In the lattices of $HgCl_2$, $HgBr_2$ and the high temperature form of HgI_2 (stable above 120 °c) "molecules" of the halides are present. In each of these four halogen atoms from neighbouring "molecules" approach the mercury atom at relatively long distances.

In mercuric chloride, mercury has distorted octahedral stereochemistry Fig. 2, the structure is essentially molecular having discrete linear Cl - Hg - Cl molecules.

TABLE III
MERCURY (II) HALIDES

Compounds	Structure (pm; °)		Ref.
HgF_2	CaF_2 type	8 x Hg - F = 246	
$HgCl_2$	Distorted octahedral,	2 x Hg - Cl = 225	32, 33
	Pnma, Z = 4	2 x Hg - Cl = 334	
		2 x Hg - Cl = 363	
		Cl - Hg - Cl = 177.8	
$HgBr_2$	Brucite type, Cmc 21, Z = 4	2 x Hg - Br = 248	34
		4 x Hg - Br = 323	
		Br - Hg - Br = 180	
HgI_2 (yellow)	Brucite type, Cmc 21, Z = 4	Hg - I = 261.5 (6)	31
		Hg - I = 262.0 (6)	
		I - Hg - I = 178.3 (3)	
HgI_2 (red)	Distorted tetrahedral	4 x Hg - I = 278.3 (3)	31
	$P4_2/nmc$, Z = 2	2 x Hg - I = 350.7 (6)	
		2 x Hg - I = 351.0 (6)	
		I - Hg - I = 112.72; (103.14)	

$HgBr_2$ and yellow HgI_2 are isostructural, having a distorted brucite structure. The six Hg - Br distances being less than R

(Hg) + R (Br). Thus the effective coordination is octahedral.

The red form of HgI_2, which is stable at room temperature, consists of corner linked HgI_4 tetrahedra, [31]. Structural data are listed in Table III.

Besides the high temperature form of HgI_2 there is a high pressure form, HgI_2. Compression of the red form above 10 kbar induces a change to a phase which appears yellow under the microscope [35]. The far - IR and Raman spectra of HgI_2 (h.t.) and HgI_2 (h.p.) are significantly different from each other and suggest that the two yellow materials have different structures.

Mercury (II) bromide exists in four polymorphic modifications, which have been studied by IR and Raman spectroscopy [35, 36]. Bridgman found that $HgCl_2$ shows only one phase. A recent Nuclear Quadrupole Resonance study has revealed that $HgCl_2$ shows two phase transition and all three phases have been investigated by IR and Raman Spectroscopy [37]. Some of the physical properties of mercury halides are tabulated in Table IV.

Numerous mixed halides have been characterized by x-ray powder patterns. Rastogi et.al [38-40] studied HgClI, HgBrI, HgFI and HgClBr by x-ray powder patterns in order to rule out the possibility that these products are of the corresponding

TABLE IV

Property	HgF_2	$HgCl_2$	$HgBr_2$	HgI_2
ΔH_{fusion} (K cal/mole)	-	-4.64	-4.28	-4.43
ΔS_{fusion} (cal/deg/mole)	-	7.50	7.70	8.60
ΔH_{subl} (K cal/mole)	-	18.50	18.80	19.90
ΔS_{subl} (cal/deg/mole)	-	33.60	36.60	37.50
ΔH_{vap} (K cal/mole)	22.00	14.08	14.15	14.14
ΔS_{vap} (K cal/mole)	-	24.40	23.80	22.70
Melting point (°c)	-	277.00	241.00	257.00
Boiling point (°c)	-	304.00	319.00	354.00
Transition Temperature(°c)	-	-	-	127.00
Resistivity(ohm cm x 10^{-3})	-	1.22 at 294 °c	6.9 at 243 °c	6 x 10^{-3} at 260 °c
Solubility (g/100g water)	-	6.6 at 20 °c	0.62 at 25 °c	0.12 at 25 °c
d(Hg - X) A^0	2.46	2.23, 2.27	2.48	(i) 2.78 (ii) 2.62 (iii) 3.51
Colour	White	White	White	(1) Red(∝) (2) Yellow (β) (3) Orange
Molecular Structure	-	Linear	Linear	Linear
Crystal Structure	Cubic CaF_2 structure	Ortho-rhombic molecular	Ortho-rhombic molecular	(1) ∝, red Tetragonal (2) β, yellow ortho-rhombic (3) Orange tetragonal

TABLE V

Lattice parameters of mixed mercury halides

Compound	Crystal type	a(Å)	b(Å)	c(Å)	Z
HgBrI	Orthorhombic	7.26	14.60	4.80	4
HgFBr	Orthorhombic	16.56	6.56	8.08	12
HgFI	Orthorhombic	13.03	6.28	5.49	6
HgClBr	Orthorhombic	11.24	7.45	13.42	12

symmetrical mercury (II) halides. The lattice parameters of the mixed mercury halides reported by Rastogi and Dubey are listed in Table V.

The structures of the mixed fluorohalides HgXF (X = Cl, Br, I) have been established by vibrational spectrometry [41].

$$HgCl_2 + Br_2 \text{ -------> } \underset{\alpha\text{ - form}}{2HgClBr} \quad \ldots (1)$$

$$HgCl_2 + HgBr_2 \text{ -----> } \underset{\beta\text{ - form}}{2HgClBr} \quad \ldots (2)$$

The reaction (1) and (2) yield two forces of the mixed halide HgClBr [42]. The cell parameters of two are as follows

	a(A)	b(A)	c(A)	Z	ρ(gm/cm^3)
α- HgClBr	6.196	13.120	4.37	4	5.91
β - HgClBr	6.78	13.175	4.17	4	5.40

The powder pattern and all parameters of the α - HgClBr are similar to those of $HgCl_2$, therefore it is possible that the chlorine atoms in the HgX_2 molecules of $HgCl_2$, have been replaced by Br atoms. Since the radius of the Br atom is larger than that of the Cl atom, the lattice is dilated in this case. The parameters of β - HgClBr are the same as those reported for β - $Hg(Cl, Br)_2$ and its x-ray powder patterns is similar to $HgCl_2$. This phase, therefore also possesses linear halogen - Hg - halogen molecules but the distribution of all Cl and Br atoms may be random. There are numerous halomercurates (II) with various cations. The stability of halomercurates (II) ions in aqueous solution is F << Cl << Br << I, therefore only some fluoromercurates (II) are known.

In iodocomplexes, the large iodine atoms seem to form only three and four co-ordinate complex with mercury (II). The sulphonium compounds $(Me_3S)^+HgI_3^-$ and $(Me_3S)_2HgI_4$ are apperently ionic [43]. Both CuI and AgI form remarkable complexes with Hg (II) iodide, which exist in high and low temperature form (α - and β -). The crystal structure of the yelllow, tetragonal Ag_2HgI_4 has cube close packed iodine atoms, with some of the tetrahedral holes filled by Ag^+ and Hg^{+2} atoms in a regular manner. Its red modification has cubic structure of zinc blende.

The isomorphous Cu_2HgI_4 shows analogous thermochromic properties.

The formation of Cu_2HgI_4 from HgI_2 and CuI in solid state is well known. It is expected that HgI_2 vapourises to react with CuI to give Cu_2HgI_4 via counter diffusion of Cu^+ and Hg^{+2} through Cu_2HgI_4. It is dark brown above 70^0c and scarlet below this temperature.

During the last decade, there has been a great emphasis to study the reactions of silver and copper halides with mercury halides in solid state [44,45]. The aim was to get a knowledge of behaviour of interaction between the compounds. The study has been further extended to the compounds of silver molybdate and tungstate [46, 47]. The peculiarity of these reactions are that they take place at room temperature or near room temperature. In all the studies, mercury (II) halides react via vapour phase and by ion diffusion. Mercury halides normally being molecular in nature, the reaction by ionic mechanism at the interface is quite interesting and needs further investigation. The present investigation has been primarily undertaken to understand the kinetics and mechanism of silver and copper halides with mixed mercury halides and to understand the role of mercury (II) during the course of reaction.

References

1. Massey, A., in "Comprehensive Inorganic Chemistry", ed. Bailer, J.C., Emeleus, H.J., Nyholm, R.S. and Trotman, A.F., Dickinson, Peramon, Oxford, vol. 3, P.1, (1973).

2. Wells, A.F. : "Structural Inorganic Chemistry", 5th edn., Clarendon, Oxford (1984).

3. Cotton, F.A. and Wilkinson, G. : "Advanced Inorganic Chemistry", Wiley Interscience, New York, 4th edn. (1980).

4. Huheey, J.E. : "Inorganic Chemistry : Principles of structure and Reactivity", 3rd edn. Harper International, Cambridge, (1983).

5. Greenwood, N. N., and Earnshaw A. : "Chemistry of the Elements", Pergamon, Oxford, (1984).

6. Hatfield, W.E. and Whyman, R. : Transition Met. Chem., 47, 5, (1969).

7. Spiro, T.G. (ed) : :Copper Protein", Wiley International, New York, (1981); Lontie, R. : Copper protein and Copper Enzymes", CRC Press, Boca Raton, FL, vol 1 - III, (1984).

8. H. Sigel (ed); "Metal Ions in Biological Systems", Dekker, New York, vol 1 -13, (1973-81).

9. Karlin, K.D. and Zubieta, J., (ed) : (a) "Copper Coordination Chemistry : Biochemical and Inorganic Perspectives", Adenine

Press, New York, (1983); (b) "Biological and Inorganic Copper Chemistry, Adenine Press, New York, (1986).

10. Wyckoff, R.W.G. and Posnjak, E : J. Am, Chem. Soc. 79, 1049 (1957).

11. Sidwick, N.V. : The Chemical elements and their properties (Oxford University Press), (1950).

12. Shetton, R.A.J. : Trans. Farad. Soc. 57, 2113 (1961).

13 Smithells, C.J. (editor) : Metals Reference Book 3rd edition (Butterworth, London) (1962).

14. Farha, F. and Iwamoto, R.T. : Inorg. Chem. 4, 484 (1965).

15. Kubota, M. and Johnstan, D.L. : J. Inorg. Nucl. Chem. 29, 719 (1967).

16. Peters, D.G. and Caldwall, R.L. : Inorg. Chem. 6, 1478 (1967).

17. Cutforth, B.D. and Gillespie, R.J. :Inorg. Synth. 19, 22 (1979).

18. Block B.P. : Inorganic Polymers, editors : Stone, F.G.A. and Grahman, W.Z.G. (Acedemic Press, New York). Chap. 8 (1962).

19. Wells, A.F. : Structural Inorganic Chemistry 3rd edition, (Oxford Univ. Press), (1962).

20. Baglio, J.A. et.al. : J. Inorg. Nucl. Chem. 32, 795 (1970).

21. Ahrland, S. and Togesson, B : Acta Chem. Scand. A 31, 615

(1977).

22. Jacobs, R.B. :Phys. Rev., 54, 325, 468 (1938).

23. Born, M. and Mayer, J.E. : J. Chem. Phys. 1, 643 (1933).

24. Huggins, M.L. and Mayer, J.. : J. CHem. Phys. 1, 643 (1933).

25. Huggins, M.L. : ibid, 5,143 (1937).

26. Huggins, M.L. : Phase transformation in Solids, Wiley, New York, p. 238 (1951).

27. Vanklooster, J.Chem. Edn. 17, 361 (1940).

28. Kubaschewski, O. and Evans, F.L.L. : "Mettalurgical Thermo chemistry", Pergamon, New York (1958).

29. Sidgwick, N.V., "Chemical Elements and their Compounds", Oxford Univ. Press, vol 1 p. 123 (1958).

30. Selected values of Thermodynamic Properties p. 667, National Bureau of standard (1952).

31. Jaffrey, G.A. and Vlasse, M. : Inorg. Chem., 6, 396 (1976).

32. Subramanium, V.H. and Narasimhan, P.T. J.Mol. Struct., 58, 193 (1980).

33. Segupta, S. and Giezendanner : J. Magn. Reson., 38, 553 (1980).

34. Veerweel, H.J. and Bijvoet, J.M. : Z. Kristallogr., 77, 122 (1931).

35. Pistorius, C.W.F.T. : Prog. Solid State Chem. 11, 1 (1976).

36. Adams, D.M. and Appleby, R. : J. Chem. Soc. Dalton Trans.,

1535 (1977).

37. Adams, D.M. and Appleby, R. : J. Chem. Soc. Dalton Trans., 1530 (1977).

38. Rastogi, R.P. and Dubey, B.L. :J. Am. Chem, Soc. 89, 200 (1967).

39. Rastogi, R.P. and Dubey, B.L. : J.Inorg. Nucl. Chem., 31, 1530, (1969).

40. Rastogi, R.P. and Dubey, B.L. and Agarwal, N.D. : J. inorg. Nucl. Chem., 37, 1167 (1975).

41. Givan, A. and Loewenschuss, A. : J. Chem. Phys. 72, 3809 (1980).

42. Mehdi, S. and Ansari, S.M. : J. Solid State Chem. 40, 122 (1981).

43. Fenn, R.H. : Acta Cryst., 20, 20, 24 (1966).

44. Ansari, S.M. :Ph.D. Thesis submitted to Aligarh Muslim Univertsity, "Studies on the interaction of Silver iodide and Mercury (II) Halides in Solid State" in (1976).

45. Ahmad, A. : Ph.D. Thesis submitted to Aligarh Muslim University "Studies on the interaction of copper (I) and Mercury (II) Halides in Solid State" in (1979).

46. Jain, Amita : Ph.D. Thesis submitted to Aligarh Muslim University, "Studies on the interaction of silver Tungstate

and Mercury (II) Halides In Silod State" in (1986).

47. Rafiuddin : Ph.D. Thesis submitted to Aligarh Muslim University, "Studies on the interaction of Silver Molybdate and Mercury (II) Halides in Solid State" in (1987).

Preparation of Copper (I) iodide, CuI.

Copper (I) iodide was prepared following the methods of Berthemot [1] and Guichard [2]. Two moles of KI (BDH, Analar Grade) in 150 ml double distilled water and one mole of cupric sulphate (BDH, Analar Grade) in 3 litres double distilled water were mixed. The mixture was boiled to remove the excess iodine. The resulting white CuI was washed and purified with double distilled water and alcohol respectively. The CuI was kept for few days in a thermostat maintained at 80-100°c to get rid of any moisture present. X-ray diffraction studies showed it to be single phase CuI, and its d values and the related intensities matched well to that of γ-CuI [3]. CuI being photosensitive, was kept in a dark bottle.

Preparation of Copper (I) Tetra Mercurate (II), Cu_2HgI_4.

Although Cu_2HgI_4 is known to be formed [4] in solid state by the interaction of CuI and HgI_2, this method was not followed for its preparation. It was prepared by simultaneous precipitation from solution containing stoichiometric amounts of reactants. This method yielded more satisfactory results than solid state product. Aqueous solutions containing mixtures of cupric nitrate (BDH, Analar Grade) with total metal ion concentration about 0.4M

was added to boiling solution of approximately 0.1M K_2HgI_4, which was earlier prepared by mixing stoichiometric solution of mercuric nitrate and potassium iodide in sufficient quantity to remove the iodine formed [5] and to decrease the loss of material remaining in solutions. If this was not done, results were found to be poor, the product consisting largely of Copper (I) iodide rather than Cu_2HgI_4.

Cu_2HgI_4 obtained as dark red mass was filtered and washed with potassium iodide solution and double distilled water, dried thereby over porous plate in a thermostat at about 100°c. Cu_2HgI_4 exists in two polymorphic forms, the low temperature β-Cu_2HgI_4 which is stable below 69°c, and the high temperature α-Cu_2HgI_4 which is stable above 69°c [6].

X-ray diffraction studies showed it to be low temperature single phase β-Cu_2HgI_4. The calculated d values match well with the ASTM powder diffraction file [7] and the intensities also match well. The d values and corresponding intensities are given in Table I.

TABLE I

X-ray diffraction of β-Cu_2HgI_4, taken by "Norelco, (philips 1010) Diffractometer using CuK_α radiation and Ni-filter, aplying 32 Kv at 12 mA.

d, in A°	I/I_o	d in A°	I/I_o
5.43	23	1.84	58
3.52	100	1.67	12
3.43	22	1.55	35
3.03	15	1.52	42
2.71	8	1.47	41
2.68	28	1.39	45
2.27	30	1.38	8
2.14	85(100)	1.32	22
2.01	25	1.24	40

Preparation of Silver Iodide, AgI

Silver iodide was prepared [8] by mixing in dark, hot aqueous solutions of $AgNO_3$ (E. Merck) and KI (BDH., A.R.) prepared in double distilled water. The precipitate was collected and washed

in dark with hot double distilled water and was dried in an air oven at 100°c for two days. Dried precipitate was powdered in a mortar and sieved for 300 mesh size particles. The x-ray analysis showed it to be of gamma form [9]. The observed d values and intensities are reported in Table II.

TABLE II

X-ray diffraction pattern for AgI, taken by Norelco Geiger counter diffractometer (PW 1010 Philips) using CuK_{α} radiation and Ni filter, applying 32 Kv at 12 mA.

d in A	I/I_o	d in A°	I/I_o
2.74	100	1.302	9
2.28	50	1.242	6
1.95	28	1.150	4
1.60	5	1.02	4
1.48	9	0.88	4

Preparation of Mercuric Chloro Bromide, (HgClBr)

HgClBr was prepared by Oppenheim's method [10]. Equimolar nixture of $HgBr_2$ (E. Merck) and $HgCl_2$ (E. Merck) in acetone were

mixed. On standing yellow shining crystals were obtained. These were filtered off and washed with double distilled water. X-ray analysis showed it to be single phase HgClBr.

Mercuric chlorobromide was also prepared by heating an equimolar mixture of $HgCl_2$ (B.D.H., A.R.) and $HgBr_2$ (Albright and Wilson, London) in solid state [11] at 90°c for 4 days. A white crystalline material was obtained. The product was analysed by x-ray and observed d values and co-ordinating intensities are reported in Table III.

TABLE III

X-ray diffraction data for β-HgClBr taken by Norelco Geiger counter x-ray diffractometer (PW 1010 Philips) using CuK_α radiation with Ni Filter, applying 32 Kv at 12 mA.

d in A°	I/I_o	d in A°	I/I_o
4.51	100	2.19	29
4.15	36	2.10	18
3.44	32	2.04	27
3.08	90	1.97	30
2.76	52	1.81	18
2.48	18	1.71	9

TABLE IV

X-ray diffraction patern for HgClI was taken by "Norelco" diffractometer (PW 1010 Philips) using CuK_{α} radiation and Ni filter, applying 32 Kv at 12 mA.

d in A°	I/I_o	d in A°	I/I_o
6.73	100	2.428	25
4.39	70	2.348	35
4.09	45	2.239	18
3.91	18	2.217	30
3.74	90	2.140	30
3.37	95	2.120	12
3.20	5	2.097	10
3.12	7	2.026	22
3.04	25	1.97	18
2.93	45	1.94	18
2.78	55	1.925	9
2.705	30	1.795	20
2.554	10	1.686	9

Preparation of Mercuric Chloro Iodide (HgClI)

Mercuric chloroiodide was prepared by heating an equimolar mixture of $HgCl_2$ (B.D.H., A.R.) and HgI_2 (B.D.H., A.R.) in solid state at 90°c for 4 days. A yellow crystalline material was obtained which decomposes below 40°c to reddish orange colour after sometime. This was studied by x-ray diffraction using Ni-filter, CuK_α radiation and a G.M. counter. The observed d values and corresponding intensities are reported in Table IV.

TABLE V

X-ray diffraction pattern for $HgBr_2$ using CuK_α radiation and Ni filter applying 32 Kv at 12 mA.

d in A°	I/I_o	d in A°	I/I_o
6.18	100	2.08	25
3.81	9	2.07	69
3.64	58	2.00	20
3.25	43	1.82	21
2.80	45	1.76	12
2.62	33	1.58	43
2.31	29	1.55	33
2.16	19	1.51	11

$HgBr_2$ (Albright and Wilson LTD. London), HgI_2 (E. Merck) and $HgCl_2$ (B.D.H., A.R.) were used without further purification. The purity was checked by x-ray diffraction analysis. The x-ray data were same as reported for $HgCl_2$ [12] and HgI_2 [13]. The data has been found different from the published one for $HgBr_2$ [14]. The observed d values and corresponding intensities are reported in Table V.

REFERENCES

1. Berthemot, J.B. : Jour. Pharm. 14, 614 (1830).

2. Guichard, M. : Compt. rend., 144, 1430 (1907).

3. ASTM, Powder Diffraction file, No. 6-0246.

4. Pinnock, A.J. : J. Soc. Chem. Ind. 38, 78 (1919).

5. Meyer, M. : J. Chem. Educ. 20, 145 (1943).

6. Ketelaar, Z. : Z. Krist. 87, 440 (1934).

7. ASTM, Powder Diffraction, file No. 18-0450.

8. Bradley, J.N. and Greene, P.D. : Trans Faraday. Soc., 63, 1023 (1967).

9. ASTM, x-ray Powder Diffraction, file No. 9-399.

10. Oppenheim, A. : Ber., 2, 571 (1869).

11. Mehdi, S. and Ansari, S.M. : J. Solid State Chem., 40, 22 (1981).

12. ASTM, Powder Diffraction, file No. 4-0335.

13. ASTM, Powder Diffraction, file No. 4-0456.

14. ASTM, Powder Diffraction, file No. 24-0753.

EXPERIMENTAL

Copper (I) Iodide and mercuric chlorobromide when mixed in an agate mortar, produce light red colour product which turns to dark brown colour at temperatures above 70°C.

Kinetic Measurements

The kinetics of the reaction in the solid state were studied by capillary method [1]. CuI and HgClBr were powdered separately in an agate mortar and sieved to above 300 mesh. The kinetics of the solid state reaction were studied by placing the HgClBr over CuI in a vertical pyrex glass tube of 0.5 cm uniform internal diameter and approximately 10 cm long. The weighed amounts of CuI and the glass tube were kept for half an hour in the incubator maintained at the desired temperature. Now this CuI was put into the glass tube and pressed by applying uniform pressure (approximately) with the help of brass rod of external diameter equalling the internal diameter of the glass tube. Now the weighed HgClBr was placed over CuI in the tube and again pressed by applying almost the same pressure. The glass tube was sealed by placing the glass rods from both sides. This whole exercise was carried out in the incubator maintained at $\pm$ 0.5°C. The progress of the reaction was followed by measuring the total

thickness of the product layer formed at the interface by a travelling microscope (least count 0.001cm) having a calibrated scale in the eyepiece. Three sets were prepared in the similar manner. The data were recorded simultaneously. The values in the Table I present the average of the three sets. To check the reproducibility of the experiment, the interaction between Copper (I) iodide and mercuric chlorobromide was run in triplicate and the results (Table II) of all three were found to be exactly the same. This shows that the averaging of the values of the three sets can be taken without affecting the result.

The kinetic data best fit the equation,

$$X^n = kt$$

where X is the thickness of the product layer formed (in cm) at time t (in hrs), and k and n are constants. The validity of this equation was tested by plotting logX versus logt, where straight lines were obtained (fig.3). The fitting was done using linear least squares curve fitting technique and the values of "k" and "n" were obtained by the best fit plot. The error in k, if any must be due to the error in the measured "X" values. Therefore, the best fit "n" value was substituted in equation $X^n = kt$ to obtain the various "k" values for different "X" and its corresponding t values to calculate the extent of precision.

The values of n and k at different temperatures for different set of reactions with their probable precision are reported in Table I. The values of n, in $X^n = kt$, does not vary significantly for a particular set of reaction at all temperatures showing it to be independent of temperature. This suggests that mechanism remains the same at all temperatures.

TABLE I

Dependence of parameters of equation $X^n = kt$ on temperature

Temperature ($^{\circ}C \pm 0.05$)	k (cm/hr)	Standard	Relative Standard Deviation	n
50	3.26×10^{-4}	1.241×10^{-5}	3.037×10^{-2}	2.27
60	3.592×10^{-4}	1.934×10^{-5}	4.480×10^{-2}	2.35
70	6.477×10^{-4}	5.519×10^{-5}	6.75×10^{-2}	2.48
80	1.006×10^{-3}	6.795×10^{-5}	4.159×10^{-2}	2.40
90	3.082×10^{-3}	1.500×10^{-4}	3.594×10^{-2}	2.30
100	1.884×10^{-2}	1.155×10^{-2}	4.38×10^{-2}	1.76
110	2.20×10^{-2}	1.355×10^{-3}	5.38×10^{-2}	2.48

TABLE II

Temperature 70°C

I set		II set		III set	
Time(hrs)	Thickness of product layer(cm)	Time(hrs)	Thickness of product layer(cm)	Time(hrs)	Thickness of product layer(cm)
0.5	0.040	0.5	0.040	0.5	0.040
1.0	0.055	1.0	0.055	1.0	0.055
1.5	0.060	1.5	0.060	1.5	0.060
2.0	0.065	2.0	0.065	2.0	0.065
2.5	0.072	2.5	0.072	2.5	0.072
3.0	0.080	3.0	0.080	3.0	0.080
3.5	0.082	3.5	0.083	3.5	0.083
4.0	0.090	4.0	0.090	4.0	0.090
4.5	0.095	4.5	0.095	4.5	0.095
5.0	0.100	5.0	0.100	5.0	0.100
5.5	0.105	5.5	0.105	5.5	0.105
6.0	0.110	6.0	0.110	6.0	0.110
6.5	0.115	6.5	0.115	6.5	0.115

Soon after the placement of the HgClBr powder over the CuI in the reaction tube a brown red boundary formed at the interface which turned brown above 70°C and this grew with time on CuI side. After sometime, a gap developed between the HgClBr and the brown colour product, while another layer of white colour product also appeared. On cooling to room temperature the dark brown product turned to scarlet red colour. Cu_2HgI_4 is dark brown above 70°C and scarlet below this temperature [2]. The kinetics were studied at different temperatures in a similar way. Later, when the reactants were placed in a tube with some gap, the product layers were similar as when they were in contact. This implied that HgClBr reacts with CuI via vapour phase.

Analysis of the product layer

Several reaction tubes having the red and white product layers were broken carefully and the different layers were collected separately. The products thus obtained were dissolved in concentrated nitric acid. In the white product layer, Cu^+, I^-, Cl^- and Br^- were confirmed by the spot tests [3]. X-ray diffraction pattern was identical with that of CuCl and γ-CuBr.

The spot test for the scarlet product layer showed the presence of Cu^+, Hg^{+2} and I^-. X-ray diffraction pattern showed it to be single phase β-Cu_2HgI_4.

X-ray studies

The reactants HgClBr and CuI (both above 300 mesh size) were mixed thoroughly in an agate mortar in different molar ratios and heated at 100°C for three days. The x-ray diffractograms of the reaction mixtures at room temperature were recorded by Norelco Geiger Counter X-ray Diffractometer (PW 1010 Philips) using CuK_{α} radiation and Ni-filter applying 32 Kv at 12 mA.

The compounds present were identified by calculating the d values and the corresponding intensities of the lines and comparing them with the standard values of the expected compounds. The compounds obtained in different molar mixtures are given in Table III.

Resistivity Measurements

HgClBr and CuI were thoroughly mixed with each other in the molar ratio 1 : 4 and immediately poured into a die and pressed into a disc by applying a pressure of 4000 pounds with the help of Carver Laboratory Press (Model C) Fred S. Carver INC, New Jeresy USA. This disc was then fixed between platinum electrodes and the change in resistance against time was noted at 80°C by LCR (Gen. Rad. 1659 digibridge) at frequency 10×10^3 Hz. Similar experiments were carried out with different molar mixtures. The

results are depicted in fig. 1.

TABLE III

Compounds present in different molar ratio mixtures of HgClBr and CuI.

Mixture	Molar Ratio of HgClBr : CuI	Compounds identified after heating the mixture at 100°C for 3 days and thereafter cooling to room temperature
I	1 : 4	Cu_2HgI_4, CuCl and CuBr
II	1 : 3	Cu_2HgI_4, CuCl, CuBr and HgI_2
III	1 : 2	Cu_2HgI_4, CuCl, CuBr and HgI_2
IV	1 : 1	CuCl, CuBr, HgI_2, $HgCl_2$ and HgBrI
V	2 : 1	Cu_2HgI_4, CuCl, CuBr and HgI_2

Reflectance Spectra

The reflectance measurements for the different molar mixtures of the reactants, heated at 100°C for three days, was made at room temperature with PYE UNICAM PU 8800 UV/VIS Spectrophotometer

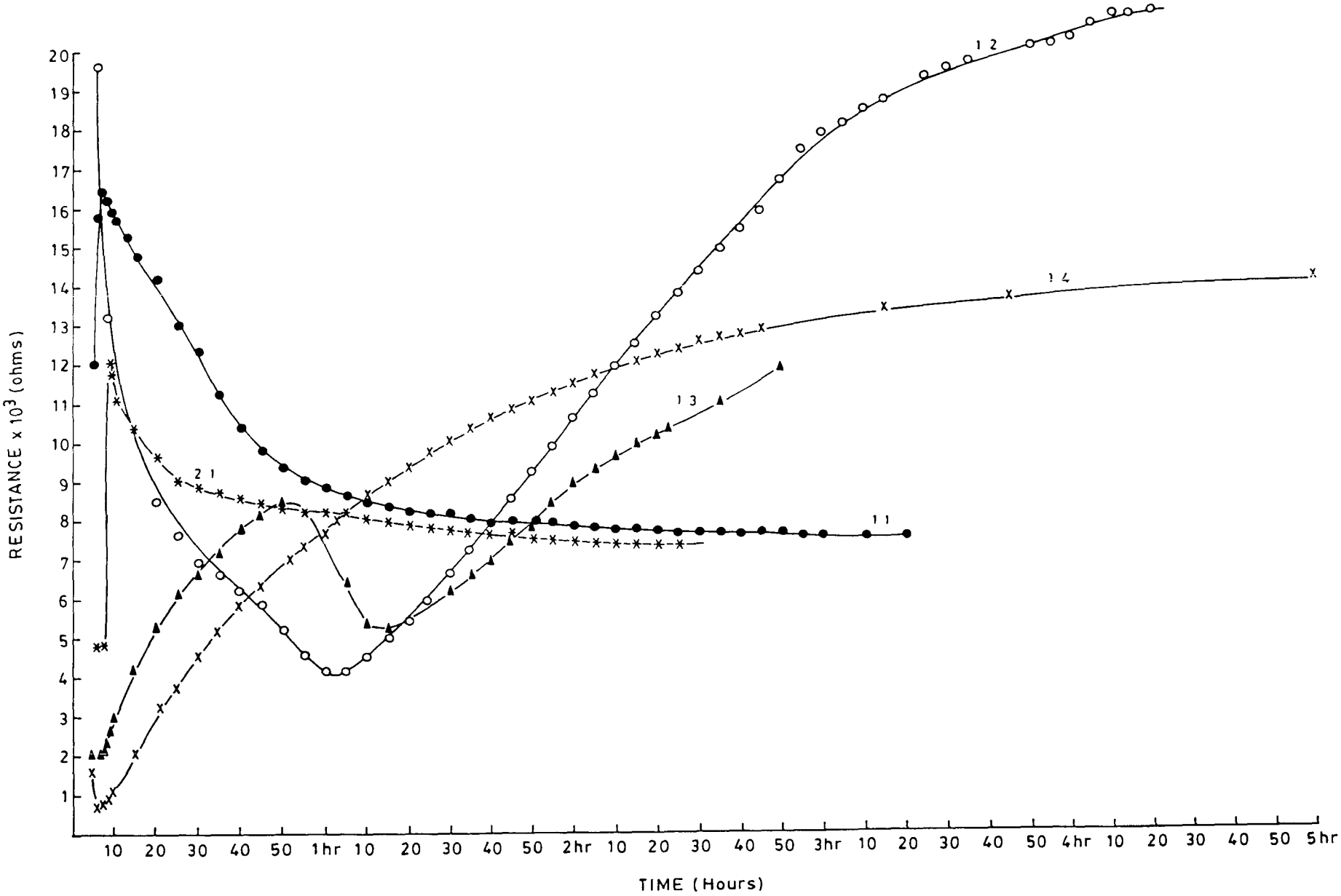

FIG 1. RESISTIVITY CHANGE AS A FUNCTION OF TIME FOR HgClBr AND CuI REACTION IN DIFFERENT MOLAR RATIOS AT 80°C.

(Philips), using white standard as a reference material. The results are depicted in fig. 2.

Results and Discussion

The x-ray diffraction analysis (Table III) of 1 : 4 molar mixtures of HgClBr and CuI heated at 100 °C for 3 days and then cooled to room temperature, indicated the presence of CuCl, CuBr and β-Cu_2HgI_4. This suggests that the reaction can be represented as :

$$HgClBr + 4CuI \longrightarrow CuCl + CuBr + Cu_2HgI_4 \quad \ldots (1)$$

However, in addition to CuCl, CuBr and Cu_2HgI_4, HgI_2 was also detected in samples analysed just after hours of heating. This was further confirmed by placing a smaller amount of CuI over a larger amount of HgClBr and allowing the reaction to go on till the whole of CuI was consumed. At the end of the reaction capillary, the presence of HgI_2 on CuI side was confirmed by chemical analysis and x-ray diffraction analysis. This evinces beyond doubt that the reaction takes place in more than one step via the formation of HgI_2.

Electrical resistivity measurements (fig. 1) for 1 : 4 molar mixture of HgClBr and CuI show a sharp decrease followed by a

continuous rise in the resistivity leading to a constant value. The presence of a minima in the resistance time curve in the initial stages clearly suggests that the reaction represented by equation (1) passes through the formation of some intermediate product. This intermediate is immediately consumed giving a new material of high electrical resistivity. Since CuI is known to react fast [4] with HgI_2 to produce Cu_2HgI_4, which has a very low resistance, it is therefore, presumed that in the first step of this reaction, HgI_2 is formed fast through simple exchange mechanism :

$$HgClBr + 2CuI \text{ -----> } CuCl + CuBr + HgI_2 \qquad \ldots (1\text{-a})$$

The HgI_2 so formed is immediately consumed by the unreacted CuI present in the reaction mixture to form low resistivity Cu_2HgI_4.

$$HgI_2 + 2CuI \text{ ------> } Cu_2HgI_4 \qquad \ldots (1\text{-b})$$

The fall in resistivity in the initial stages is due to the formation of Cu_2HgI_4 which is having a high conductivity and also due to the fact that step (1-b) is reported to be taking place very fast [5]. The overall reaction taking place can, therefore, be represented as :

$$HgClBr + 2CuI \longrightarrow CuCl + CuBr + HgI_2$$

$$HgI_2 + 2CuI \longrightarrow Cu_2HgI_4$$

$$HgClBr + 4CuI \longrightarrow Cu_2HgI_4 + CuCl + CuBr$$

TABLE IV

X-ray measurements for the reaction mixture HgClBr + 4CuI

d in A°	I/I_o	d in A°	I/I_o
4.162	12	2.26 +	20
3.58 +	37	2.19 +	35
3.52 +	100	2.14 +	60
3.38 +	20	2.03 + x	25
3.32 x	32	1.85 +	25
2.79 + *	22	1.83 +	32
2.77 + *	30	1.79 + x	10
2.64 + *	22	1.64 + *	17
2.31 +	12	1.44 + x	17

\+ lines of β-Cu_2HgI_4 [12]

* lines of CuCl [7]

x lines of γ-CuBr [6]

This explains only the initial fall in resistance but not the increase there after. The x-ray diffraction pattern of this mixture is shown in Table IV.

The x-ray diffraction analysis of the 1:3 molar mixture of HgClBr and CuI showed the presence of CuCl, CuBr, Cu_2HgI_4 and HgI_2.

The reaction was supposed to take the entire course observed in 1:4 molar mixture but the electrical resistivity measurement showed that the resistivity first increased, followed by a decrease and again a rise. This indicates that the reaction sequence in 1:3 molar mixture is entirely different than the one observed for 1:4 molar mixture. On the basis of resistivity measurements and the x-ray analysis, the sequence of reaction in 1:3 molar mixture is proposed as follows :

$$HgClBr + 2CuI \longrightarrow CuCl + CuBr + HgI_2 \quad \ldots (2a)$$

$$HgI_2 + 2CuI \longrightarrow Cu_2HgI_4 \quad \ldots (2b)$$

$$HgClBr + Cu_2HgI_4 \longrightarrow CuBr + CuCl + 2HgI_2 \quad \ldots (2c)$$

$$HgI_2 + 2CuI \longrightarrow Cu_2HgI_4 \quad \ldots (2d)$$

$$2HgClBr + 6CuI \longrightarrow 2CuCl + 2CuBr + Cu_2HgI_4 + HgI_2 \quad \ldots (2)$$

Step (2a) is the simple exchange reaction as in the 1:4 molar

mixture, there is momentary increase in the resistivity pertaining to the formation of HgI_2, thereafter a continuous decrease in the resistivity is due to the formation of low resistance Cu_2HgI_4 by the reaction of CuI and HgI_2 formed in the step (2a). The step (2c) produces more resisting HgI_2 which is being formed by the reaction of Cu_2HgI_4 formed in step (2b), with the excess HgClBr present in the mixture. This step was separately confirmed by reacting Cu_2HgI_4 and HgClBr in a capillary tube. Various layers obtained were collected separately and analysed chemically and by x-ray for HgI_2, CuCl and CuBr. The formation of HgI_2 in this step explains the rise in resistivity. However, the HgI_2 formed, is being consumed by CuI to produce Cu_2HgI_4, which gives rise to the decrease in the resistivity. However, the formation of HgI_2 in step (2c) is slow, so it gives rise to the resistivity in the resistivity curve (fig.1). The d-values of γ-CuBr and CuCl do not match well with the standard d-values reported in the ASTM files [6, 7]. There seems some distortion which is due to the formation of a solid solution between CuBr and CuCl. The x-ray diffraction pattern of this mixture is shown in Table V.

TABLE V

X-ray measurements for the reaction mixture HgClBr + 3CuI

d in A°	I/I$_o$	d in A°	I/I$_o$
5.46 +	18	2.19 +	39.47
4.12	47	2.145 ∔ +	55.26
3.58	57	2.01 ∔ x +	18
3.49 + x ∔	100	1.87 + ∔ +	13
3.3 +	26	1.80 ∔	18
3.32 * x	42	1.83 +	31
3.07 +	23	1.711 + ∔ x	13
3.01 ∔ +	31	1.42 + ∔ x	10
2.76 + ∔ *	28	1.38 + ∔ x *	13
2.63 ∔	21	1.387 + x *	15

\+ lines of β- Cu_2HgI_4 [12]

* lines of CuCl [7]

x lines of γ- CuBr [6]

∔ lines of HgI_2 [13]

The x-ray diffraction analysis of 1 : 2 molar mixture of HgClBr and CuI showed the presence of CuBr, CuCl, Cu_2HgI_4 and

HgI_2 and $HgCl_2$. The electrical resistivity measurements indicate that the reaction is multi-step. In the initial stage, the resistivity rises due to the formation of non conducting product. Thereafter, it continuously decreases till it is almost constant. On the basis of this behaviour, the following mechanism is proposed to take place in 1 : 2 molar mixture :

$$HgClBr + 2CuI \longrightarrow CuCl + CuBr + HgI_2 \quad \ldots (3a)$$

$$HgI_2 + 2CuI \xrightarrow{\text{(fast)}} Cu_2HgI_4 \quad \ldots (3b)$$

$$HgClBr + Cu_2HgI_4 \longrightarrow CuBr + CuCl + 2HgI_2 \quad \ldots (3c)$$

$$2HgClBr + HgI_2 \longrightarrow 2HgClI + HgBr_2 \quad \ldots (3d)$$

$$HgBr_2 + 4CuI \longrightarrow 2CuBr + Cu_2HgI_4 \quad \ldots (3e)$$

$$4HgClBr + 8CuI \longrightarrow 4CuBr + 2CuCl + Cu_2HgI_4 + HgI_2 + HgCl_2 \quad \ldots (3)$$

Steps (3a) and (3b) are in accordance with the reaction as were in the case of 1:4 and 1:3 molar mixtures. Steps (3c) and (3d) produce HgI_2, $HgBr_2$ and HgClI which have high resistivity and this accounts for the increase in the resistivity. Step (3e) results in the formation of Cu_2HgI_4. That accounts for the fall in the resistivity. The reactivity of CuI and $HgBr_2$ has already been reported [7]. Since HgClI is not very stable [8, 9], it

TABLE VI

X-ray measurements for the reaction mixture HgClBr + 2CuI

d in A°	I/I$_o$	d in A°	I/I$_o$
6.83	40	2.13 + ∔ ♢	28
3.95	20	2.06 + x ∔ ♢	24
3.79	80	2.01 + * x ∔ ♢	20
3.44 + ∔	100	1.99 * ∔ ♢	24
3.27 x	40	1.95 * ∔ ♢	20
2.98 x ∔ ♢	30	1.91 * ∔ ♢	12
2.84 * x ∔	72	1.83 + * ∔ ♢	16
2.59 + ∔	16	1.81 + ♢	40
2.34 ♢	32	1.74 + x ∔ ♢	24
2.28 + ♢	20	1.73 x ∔ ♢	20
2.24 + ♢	28	1.60 + * ∔ ♢	16
2.23 + ♢	24	1.49 + x ∔ ♢	12
2.19 + ∔ ♢	16		

\+ lines of β- Cu_2HgI_4 [12] ; ∔ lines of HgI_2 [13]

* lines of CuCl [7]

♢ lines of $HgCl_2$ [15]

x lines of γ- CuBr [6]

decomposes into $HgCl_2$ and HgI_2. The x-ray diffraction pattern of this mixture is shown in Table VI.

The products identified by x-ray analysis of 1:1 molar mixture of HgClBr and CuI are CuCl, CuBr, HgClI (HgI_2 + $HgCl_2$) and HgBrI. The resistivity measurements show that the reaction is a two step one. In the first step, the resistivity rises due to the formation of Cu_2HgI_4, then excess of HgClBr combines with Cu_2HgI_4 formed in the first step, giving rise to HgClI and HgBrI which have comparatively higher resistivity. However, HgClI is not very stable at room temperature, it soon decomposes into $HgCl_2$ and HgI_2 which are identified in the x-ray analysis. This suggests, the following mechanism :

$$HgClBr + 2CuI \longrightarrow CuCl + CuBr + HgI_2$$

$$HgI_2 + 2CuI \longrightarrow Cu_2HgI_4$$

$$HgClBr + Cu_2HgI_4 \longrightarrow 2CuI + HgClI + HgBrI$$

$$2HgClBr + 2CuI \longrightarrow CuCl + CuBr + HgClI + HgBrI$$

The x-ray diffraction pattern of this mixture is shown in Table VII.

Results of x-ray analysis (Table III) and electrical resistivity measurements (fig. 1) with 2 : 1 molar mixture of

TABLE VII

X-ray measurements for the reaction mixture HgClBr + CuI

d in A°	I/I$_o$	d in A°	I/I$_o$
3.77 ò	20	2.09 x + ò +	13
3.41 +	100	2.05 x + ò +	10
3.22 x +	44	2.06 x + ò +	20
3.17 * + +	13	1.97 x + ò +	27
2.95 x ò +	27	1.84 + ò +	20
2.78 x + ò +	13	1.78 x + ò +	24
2.74 * + ò +	24	1.76 x + ò +	7
2.71 * + +	20	1.69 x + ò +	17
2.65 ò	24	1.69 x + ò +	89
2.60 ò	13	1.68 x + ò +	20
2.35 ò +	13	1.61 * + ò +	48
2.27 ò +	20	1.60 x + ò +	79
2.21 +	31	1.58 + ò +	17
2.16 + ò +	13	1.58 + ò +	13
2.13 + ò +	27	1.54 + ò +	10

* lines of CuCl [7] ; ò lines of HgBrI [14]

x lines of γ-CuBr [6] ; + lines of $HgCl_2$ [15]

+ lines of HgI_2 [13]

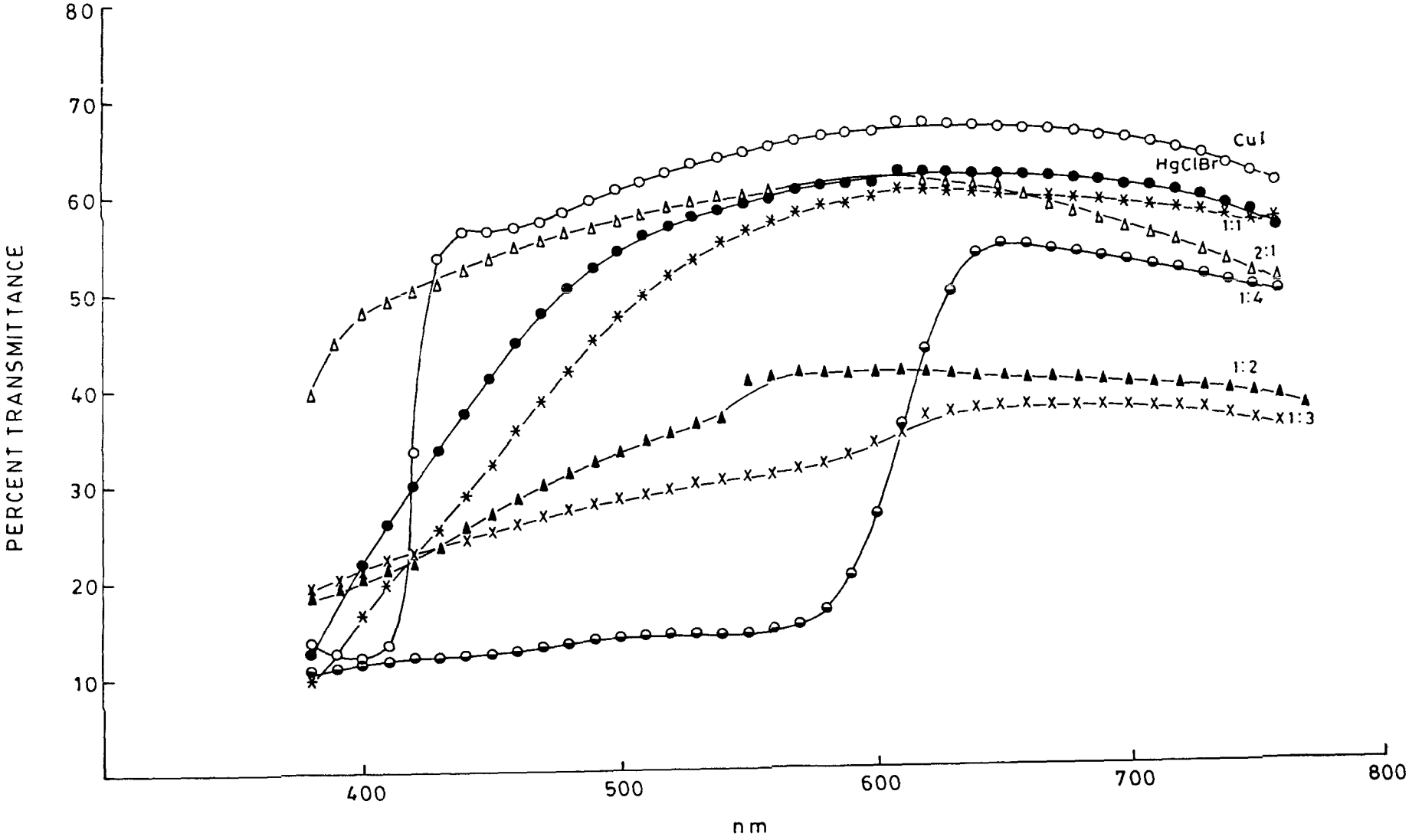

FIG. 2. REFLECTANCE SPECTRA FOR THE REACTION BETWEEN HgClBr AND CuI IN DIFFERENT MOLAR RATIOS.

HgClBr and CuI suggest that the reaction in this case follow the same path as for 1 : 1 molar mixture at 80°C. The x-ray diffraction pattern of this mixture is shown in Table VIII.

However, the reaction may be taking place at room temperature but it is too slow to be followed at room temperature.

The reflectance studies (fig.2) clearly indicate that the products in 1:4, 1:3 and 1:2 molar mixtures of HgClBr and CuI are not similar therefore, the mechanisms of these reaction may also not be following the same course as has already been discussed above. The sequence of reaction for 1:1 and 2:1 molar mixtures should be the same because the end products as reflected by the reflectance studies are looking to be the same. In all the cases, the percent transmittance do differ from the percent transmittance of the reactants HgClBr and CuI.

Mechanism of lateral diffusion:

Soon after placing HgClBr over CuI in the reaction capillary, at 50 °C, red coloured layer developed at the interface. The product layer grew with time towards the CuI side. A gap developed between the white layer and HgClBr. When the experiment was repeated with an air gap of varying dimensions between the

TABLE VIII

X-ray measurement for the reaction mixture 2HgClBr + CuI

d in A°	I/I_o	d in A°	I/I_o
6.31 +	100	2.12 +	40
4.21 +	22	2.05 x + ò	29
3.684 +	88	2.03 x + ò	22
3.29 x +	68	1.96 * + ò	22
2.84 * x +	44	1.88 * + ò	11
2.66 *	40	1.84 * + ò	18
2.34 ò	37	1.76 x + ò	14
2.31 ò	18	1.7 x + ò	18
2.27 ò	14	1.47 * x +	14

* lines of CuCl [7]

x lines of γ-CuBr [6]

\+ lines of HgI_2 [13]

ò lines of HgBrI [14]

two reactants, the reaction proceeded in similar way giving the same kinds of layers on CuI side as was the case when the reactants were in contact. The dimension of the air gap did not

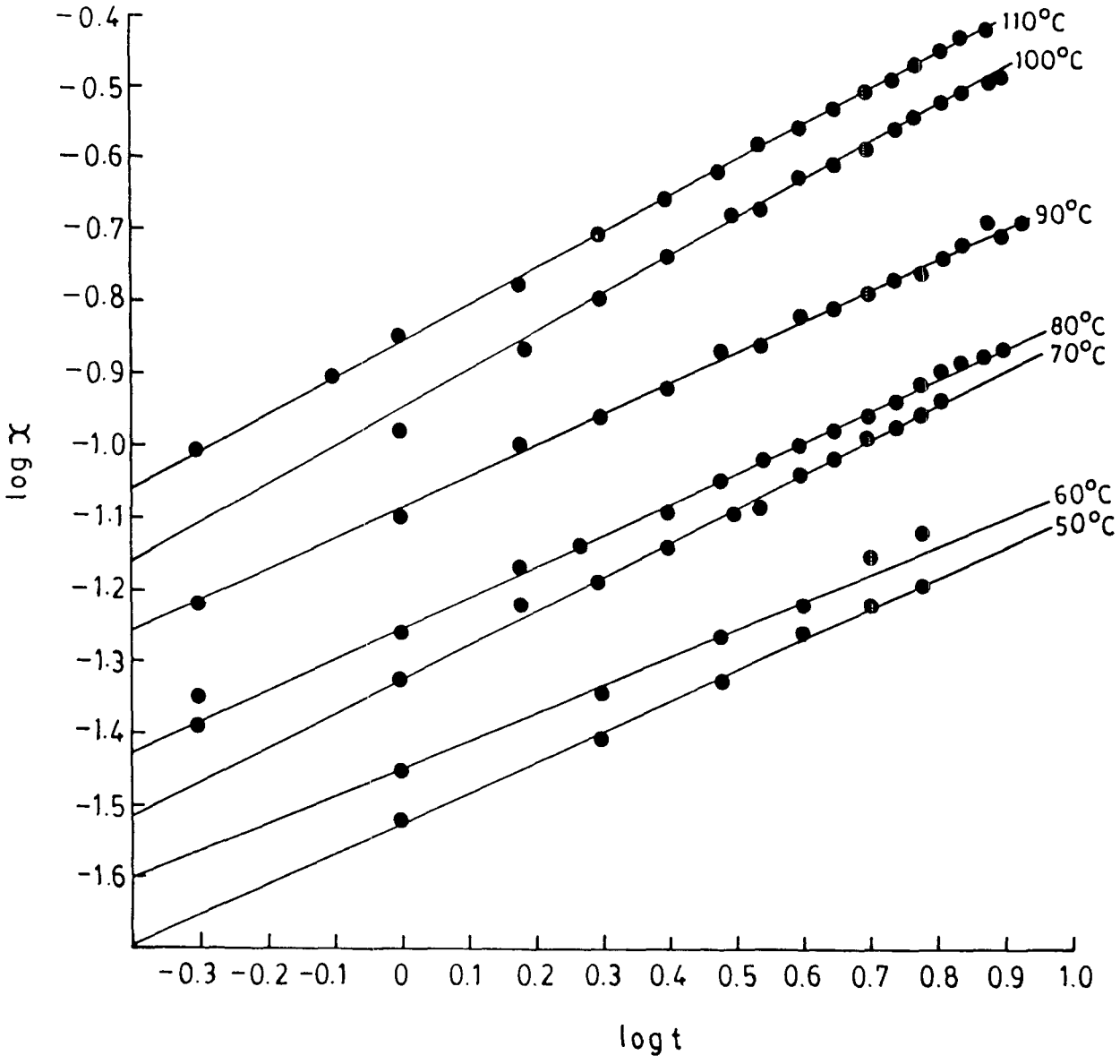

FIG. 3. KINETIC DATA FOR LATERAL DIFFUSION AND TEST FOR EQUATION $X^n = kT$ FOR THE REACTION BETWEEN HgClBr AND CuI.

affect the sequence of the layers. This shows that the mobile component is HgClBr. HgClBr molecules react with the CuI to form coloured Cu_2HgI_4. X-ray and chemical analysis of the different layers thus formed showed the following sequence of products in the reaction capillary.

CuI ¦ HgI_2, Cu_2HgI_4, CuBr, CuCl ¦ HgClBr

The rate of growth of product layers decreased with time. Initially, the process is fast and reaction controlled. As the thickness of the product layers became significant, HgClBr took greater time to diffuse through the product layers. The process now becomes diffusion controlled and the rate of the reaction thus falls regularly with the growth of the product layers. The lateral diffusion data best fit the rate equation (fig. 3).

$$X^n = kt \qquad \ldots (1)$$

where X is the total thickness (in cm) of the product layers at time t(in hrs), n and k are constants. The rate constant, k follows the Arrhenius equation

$$k = A \exp(-E/RT) \qquad \ldots (2)$$

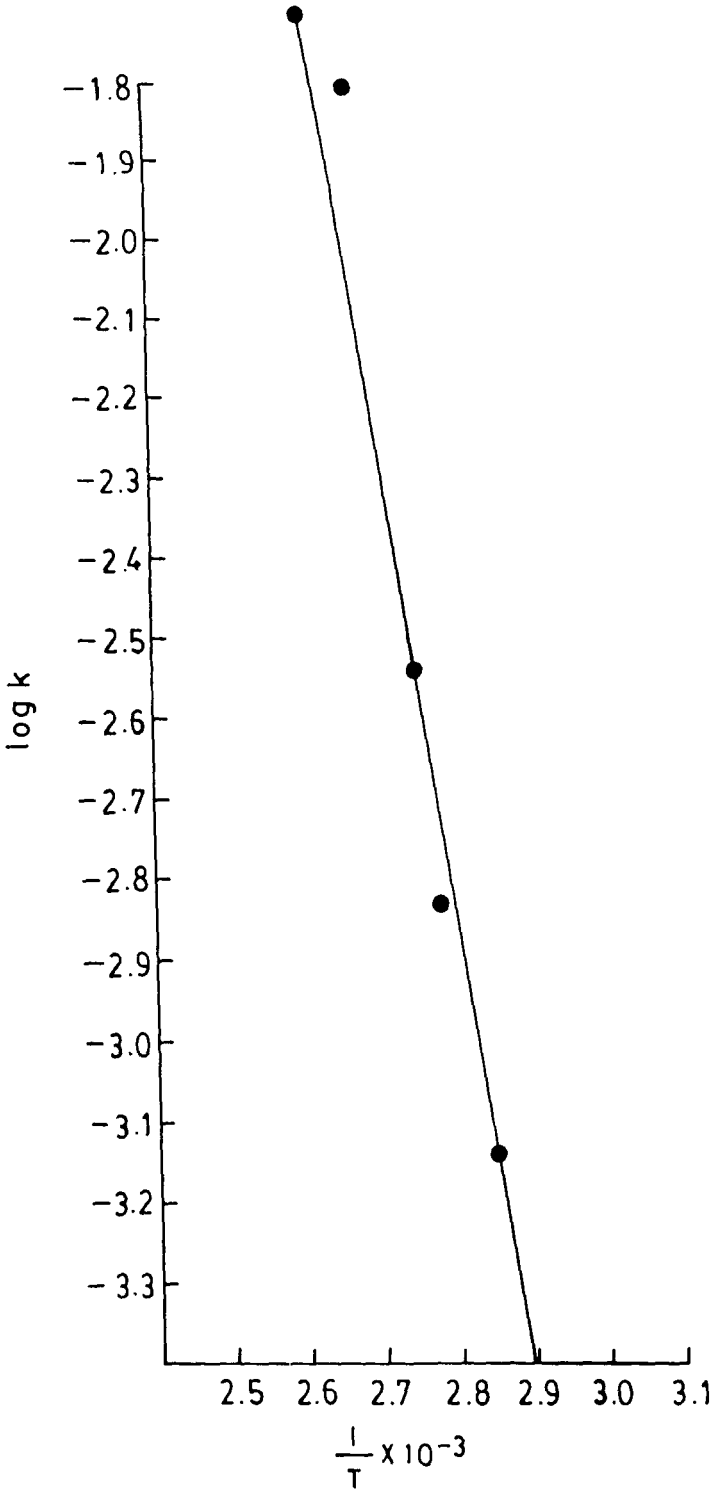

FIG.4. DEPENDENCE OF k ON TEMPERATURE FOR THE REACTION BETWEEN HgClBr AND CuI.

affect the sequence of the layers. This shows that the mobile component is HgClBr. HgClBr molecules react with the CuI to form coloured Cu_2HgI_4. X-ray and chemical analysis of the different layers thus formed showed the following sequence of products in the reaction capillary.

CuI | HgI_2, Cu_2HgI_4, CuBr, CuCl | HgClBr

The rate of growth of product layers decreased with time. Initially, the process is fast and reaction controlled. As the thickness of the product layers became significant, HgClBr took greater time to diffuse through the product layers. The process now becomes diffusion controlled and the rate of the reaction thus falls regularly with the growth of the product layers. The lateral diffusion data best fit the rate equation (fig. 3).

$$X^n = kt \qquad \ldots (1)$$

where X is the total thickness (in cm) of the product layers at time t(in hrs), n and k are constants. The rate constant, k follows the Arrhenius equation

$$k = A \exp(-E/RT) \qquad \ldots (2)$$

The activation energy evaluated from the log k versus 1/T plot (fig. 4) made by least square fit method was found to be 43.3 kJ/mol . The reaction rate constant measured with an initial air gap between the reactants decreased with the increase in the length of the air gap. The energy of activation suggests that the reaction is diffusion controlled taking place via vapour phase diffusion [10].

References

1. Rastogi, R.P. and Dubey, B.L. : J. Am. Chem. Soc. 89, 200 (1967).

2. Kelelaar, Z. : Z. Krist. 87, 440 (1934).

3. Fiegel, F. and Ager, V. : Spots Tests in Inorganic Analysis (Elsevier Publishing Company) 1972, pp. 203, 145 and 147.

4. Pinnock, A.T. : J. Soc. Chem. Ind. 38, 78, (1919).

5. Wagner, C. and Koch, E. : Z. Physik. Chem. 1334, 1167 (1975).

6. ASTM Powder Diffraction File No. 6-0292.

7. ASTM Powder Diffraction File No. 6-0344.

8. Beg, M.A. and Ahmad, A. : Bull. Chem. Soc. Jpn. 55(3), 5660 (1982).

9. Rastogi, R.P. et. al. : J. Inorg. Nucl. Chem., 37, 1167 (1975).

10. ASTM Powder Diffraction File No. 4-0454.

11. Rastogi, R.P. et al. : J. Sci. Indust. Res. 37, 622 (1978).

12. ASTM Powder Diffraction File No. 18-0450.

13. ASTM Powder Diffraction File No. 21-1157.

14. ASTM Powder Diffraction File No. 30-835.

15. ASTM Powder Diffraction File No. 4-033.

EXPERIMENTAL

Silver iodide and mercuric chlorobromide do not react at low temperature in the capillary tube but when they were mixed in an agate mortar, produced yellow colour.

Kinetic Measurements

The kinetics of the reaction in the solid state were studied by placing mercuric chlorobromide over silver iodide (both above 300 mesh size) in a vertical pyrex glass tube as described in the preceeding chapter.

Soon after the placement of the HgClBr powder over AgI in the tube, a red boundary formed at the interface and this grew with time on the AgI side. After sometime, a yellow product layer started to develop in between HgClBr and the red product, and a gap developed between HgClBr and the yellow product. The rate of the reaction was followed by measuring the total thickness of the red and yellow layers. The rate constants for different sets are reported in Table I. The probable precision was calculated as described in the earlier chapter.

Analysis of the product layer

A reaction tube having two distinct layers of the product was broken and the two product layers were carefully collected

TABLE I

Dependence of Parameters of equation $x^n = kt$ on temperature

Temperature ($^{o}C \pm 0.05$)	k (cm/hr)	Standard Deviation	Relative Standard Deviation	n
50	7.533×10^{-4}	3.505×10^{-4}	3.460×10^{-2}	2.00
60	1.036×10^{-3}	3.065×10^{-4}	2.186×10^{-2}	2.04
70	4.386×10^{-3}	1.349×10^{-3}	1.715×10^{-1}	1.701
80	4.720×10^{-3}	2.170×10^{-4}	3.326×10^{-2}	1.947
100	1.150×10^{-2}	5.512×10^{-4}	3.383×10^{-2}	1.82
105	1.679×10^{-2}	6.126×10^{-4}	3.004×10^{-2}	1.93
110	2.088×10^{-2}	8.943×10^{-4}	3.367×10^{-2}	1.89

separately. The products thus obtained were dissolved separately in concentrated Nitric acid. In the yellow product layer Ag^{+}, Cl^{-} and Br^{-} were detected by spot tests. X-ray diffraction pattern was identical with that of AgCl and AgBr.

The spot test for the red layer showed the presence of Ag^{+}, Hg^{+2} and I^{-} and the x-ray pattern of the material indicated it to be β- Ag_2HgI_4.

X-ray studies

The reactants, silver iodide and mercuric bromochloride, in different molar ratios were mixed thoroughly in an agate mortar and heated at 100°c for three days. X-ray diffraction patterns of all reaction mixtures were taken at room temperature by a Norelco Geiger Counter X-ray Diffractometer using CuK_{α} radiation with a Ni-filter, applying 32 Kv at 12 mA current. The compounds were identified by calculating the d values of the lines and corresponding intensities of the lines and comparing them with the standard values of the expected compounds. The compounds obtained in different molar mixtures are given in Table II.

Resistivity Measurements

Resistivity measurement for the mixture 1 : 4, 1 : 3, 1 : 2, 1 : 1 and 1 : 2 of HgClBr and AgI were done as described earlier and the results are depicted in fig. 1.

Reflectance Spectra

The reflectance measurements of 1 : 4, 1 : 3, 1 : 2, 1 : 1 and 2 : 1 molar ratio mixture of HgClBr and AgI was made in the similar fashion as described earlier. The results are depicted in fig. 2.

TABLE II

Compounds present in different molar ratio mixtures of HgClBr and AgI

Mixture	Molar ratio of HgClBr : AgI	Compounds identified after heating the mixture at 100°C for 3 days and thereafter cooling to room temperature
I	1 : 4	Ag_2HgI_4, AgCl and AgBr
II	1 : 3	Ag_2HgI_4, AgCl, AgBr and HgI_2
III	1 : 2	AgCl, AgBr and HgI_2
IV	1 : 1	AgCl, AgBr, $HgCl_2$, HgI_2 and HgBrI
V	2 :1	AgCl, AgBr, HgClI, HgBrI and HgClBr

RESULTS AND DISCUSSION

For a comprehensive understanding of the process, the following aspects are to be considered

(a) Mechanism of chemical interaction and

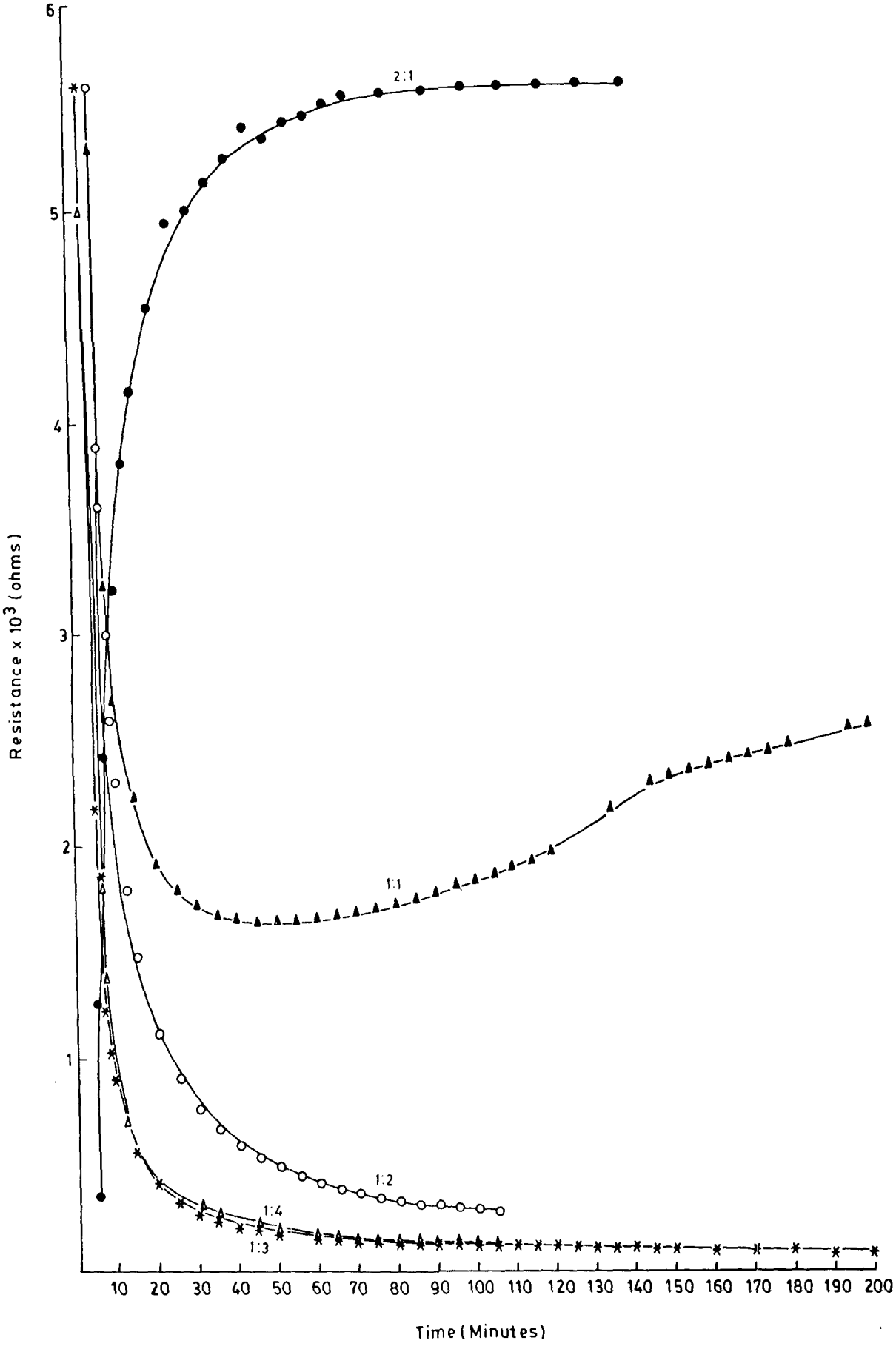

FIG.1. RESISTIVITY CHANGE AS A FUNCTION OF TIME FOR THE REACTION BETWEEN HgClBr AND AgI IN DIFFERENT MOLAR RATIOS.

(b) Mechanism of lateral diffusion when the reactants were kept in contact, and when they were separated by an air gap.

Mechanism of chemical interaction

The x-ray diffraction measurements (table III to VII) reveal that HgClBr and AgI react in solid state in the molar ratio 1 : 4.

$$HgClBr + 4AgI \longrightarrow Ag_2HgI_4 + AgCl + AgBr \quad \ldots (1)$$

It was observed that as soon as the reactants were mixed in this molar ratio at room temperature, red colour appeared which gradually transformed to yellow colour. This process was slow at room temperature, but the process became fast when this mixture was kept at 55°c. The red colour is perhaps due to the formation of HgI_2 that appeared as an intermediate and reacted immediately with AgI to produce the adduct Ag_2HgI_4. (Ag_2HgI_4 is yellow below 50.7°C (β - form) and red above this temperature (α-form) [1]).

$$HgClBr + 2AgI \longrightarrow AgCl + AgBr + HgI_2 \quad \ldots (1a)$$

$$2AgI + HgI_2 \longrightarrow Ag_2HgI_4 \quad \ldots (1b)$$

But the resistivity curve (fig.1) has only one inflection. There is no evidence of HgI_2 in the x-ray patterns of the stoichiometric mixtures as well. The first step is simple

exchange reaction, which are usually fast [2]. But as soon as HgI_2 is produced it is being consumed by the AgI present in the mixture. The formation of Ag_2HgI_4 from AgI and HgI_2 is known to be very fast [3] even at low temperatures. This explains why the resistivity measurement does not provide any evidence for step (1a). Nevertheless the evidence of the formation of HgI_2 is obtained when the reaction is carried out in the glass tube,

TABLE III

X-ray diffraction pattern for the reaction HgClBr + 4AgI

d in A°	I/I_o
3.63 *	100
2.69 +	45
2.75 +	15
2.22 *	60
2.02 + x	25
1.90 + x *	35

\+ lines of AgCl [3] ; * lines of Ag_2HgI_4 [5]

x lines of AgBr [4]

which was kept at 80°c for quite a long time till all of the AgI was consumed. In the end of the glass tube on AgI side, a red layer was observed which was identified to be HgI_2.

The x-ray diffraction pattern for this molar mixture is given in Table III.

The x-ray pattern of 1 : 3 molar ratio of HgClBr and AgI revealed that the products were Ag_2HgI_4, AgCl, AgBr and HgI_2. In view of this, the stoichiometric reaction may be represented as follows :

$$2HgClBr + 6AgI \longrightarrow Ag_2HgI_4 + 2\,AgCl + 2AgBr + HgI_2 \quad \ldots (2)$$

The resistivity measurements simply suggest that chemical interaction in 1:3 molar mixture might be following the same pattern as that of 1:4 molar mixture . The presence of HgI_2 in the x-ray pattern confirmed that the reaction is going through the formation of HgI_2. Since the amount of AgI in this case is smaller as compared to that in 1:4 molar mixture; HgI_2 produced in the first step is not consumed in the second step. Some of HgI_2 remained unreacted.

The x-ray diffraction pattern for this molar mixture is given in Table IV.

TABLE IV

X-ray diffraction pattern for the reaction HgClBr + 3AgI

d in A	I/I_o
4.435	15
4.35	15
4.09 +	18
3.66 * +	100
3.48 x *	18
2.85 x * +	57
2.80 x * +	12
2.735 + +	15
2.22 *	60
2.02 + x +	33
1.89 + x * +	30

\+ lines of AgCl [4]

x lines of AgBr [5]

* lines of β-Ag_2HgI_4 [6]

\+ lines of HgI_2 [7]

X-ray analysis of 1:2 molar mixture of HgClBr and AgI showed the presence of AgCl, AgBr and HgI_2. The resistivity measurements indicate that the chemical interaction should be in the similar fashion as that of the interaction with 1:4 or 1:3 molar mixtures. The only difference being in the concentration of HgI_2.

However, no lines of Ag_2HgI_4 were detected in the x-ray pattern. This is due to the fact that Ag_2HgI_4 might have reacted with the excess amount of the HgClBr in the mixture. In view of this, following mechanism for 1:2 molar mixture is proposed.

$$HgClBr + 2AgI \text{ -----> } AgCl + AgBr + HgI_2 \quad \ldots (3a)$$

$$HgI_2 + 2AgI \text{ ------> } Ag_2HgI_4 \quad \text{(fast)} \quad \ldots (3b)$$

$$HgClBr + Ag_2HgI_4 \text{ ----> } AgBr + AgCl + 2HgI_2 \quad \ldots (3c)$$

$$2HgClBr + 4AgI \text{ ------> } 2AgBr + 2AgCl + 2HgI_2$$

Step (3c) was separately confirmed.

X-ray analysis of 1 : 1 mixture showed the presence of AgCl, AgBr, $HgCl_2$, and HgI_2 and HgBrI Table II. The resistivity measurements indicate that the resistance decreases in the initial stages, and then it continuously increase to almost a

TABLE V

X-ray diffraction pattern for the reaction HgClBr + 2AgI

d in A°	I/I_o	d in A°	I/I_o
6.75	34	3.78	26
6.42	30	3.70	21
6.23 ÷	30	3.58 ÷	17
5.92	30	3.42	21
5.71	34	3.30 + x	17
5.54	30	3.10 + x	42
5.35	26	2.97 x ÷	17
5.06	26	2.94 x ÷	17
4.84	21	2.85 + x	100
4.45	26	2.47 ÷	13
4.35	26	2.20 ÷	26
4.07 ÷	28	2.09 x ÷	34
3.99	43	2.01 x ÷	36

\+ lines of AgCl [4]

x lines of AgBr [5]

÷ lines of HgI_2 [7]

constant. Hence, the reaction is contemplated to take place in two steps. As is the case in all the preceeding molar mixtures, the first stage is the formation of HgI_2 which is immediately consumed by AgI to form Ag_2HgI_4 which is well indicated by the initial decrease in resistivity (Ag_2HgI_4 being more conducting).

$$HgClBr + 2AgI \longrightarrow AgCl + AgBr + HgI_2 \quad \ldots (4a)$$

$$HgI_2 + 2AgI \longrightarrow Ag_2HgI_4 \quad \ldots (4b)$$

Now, the Ag_2HgI_4 formed in step (4b) combines with the excess of HgClBr present in the reaction mixture.

$$HgClBr + Ag_2HgI_4 \longrightarrow HgClI + HgBrI + 2AgI \quad \ldots (4c)$$

The rise in resistivity is due to the predominance of step (4c). Hence the overall reaction can be represented as under

$$HgClBr + 2AgI \longrightarrow AgCl + AgBr + HgI_2$$

$$HgI_2 + 2AgI \longrightarrow Ag_2HgI_4$$

$$HgClBr + Ag_2HgI_4 \longrightarrow HgClI + HgBrI + 2AgI$$

$$2HgClBr + 2AgI \longrightarrow AgCl + AgBr + HgClI + HgBrI$$

The x-ray diffraction pattern for this molar mixture is given in Table VI.

The x-ray pattern of 2:1 molar ratio mixture of HgClBr and AgI show the presence of AgCl, AgBr, HgClI, HgBrI and HgClBr

Table II. The resistivity measurements (fig.1) indicate that this is a two step reaction. The resistance increases and thereafter it attains a constant value. However as it happened in all other molar ratios, the reaction may be going through the formation of Ag_2HgI_4 which is a conducting material. According to this, the sequence of the reaction should be represented as :

TABLE VI

X-ray diffraction pattern for the reaction HgClBr + AgI

d in A°	I/I_o	d in A°	I/I_o
6.58 ò	64	2.9 x * ò	35
5.88	35	2.82 x	100
5.54	35	2.74 + ŧ * ò	35
3.74 ò	71	2.35 * ò	28
3.36 x ŧ ò	49	2.19 x ŧ ò	21
3.26 + ŧ *	21	1.99 x ŧ ò	60

\+ lines of AgCl [4] ; * lines of $HgCl_2$ [8]

x lines of AgBr [5] ; ò lines of HgBrI [9]

ŧ lines of HgI_2 [7]

$$HgClBr + 2AgI \longrightarrow AgCl + AgBr + HgI_2 \quad \ldots (5a)$$

$$HgI_2 + 2AgI \longrightarrow Ag_2HgI_4 \quad \ldots (5b)$$

However, the x-ray lines of Ag_2HgI_4 were not present in the x-ray diffraction pattern, indicating that Ag_2HgI_4 thus formed must be consumed immediately producing some non-conducting materials. This is indicated by the rise in the resitivity value, and when reaction was complete, it attained a constant value. Ag_2HgI_4 may be consumed by reacting with HgClBr present in excess in the mixture.

$$HgClBr + Ag_2HgI_4 \longrightarrow HgClI + HgBrI + 2AgI \quad \ldots (5c)$$

HgClI being unstable at room temperature, decomposed to HgI_2 and $HgCl_2$. Hence, the whole reaction sequence can be represented as :

$$HgClBr + 2AgI \longrightarrow AgCl + AgBr + HgI_2 \quad \ldots (5a)$$

$$HgI_2 + 2AgI \longrightarrow Ag_2HgI_4 \quad \ldots (5b)$$

$$HgClBr + Ag_2HgI_4 \longrightarrow HgClI + HgBrI + 2AgI \quad \ldots (5c)$$

$$2HgClBr + 2AgI \longrightarrow AgCl + AgBr + HgClI + HgBrI \quad \ldots (5)$$

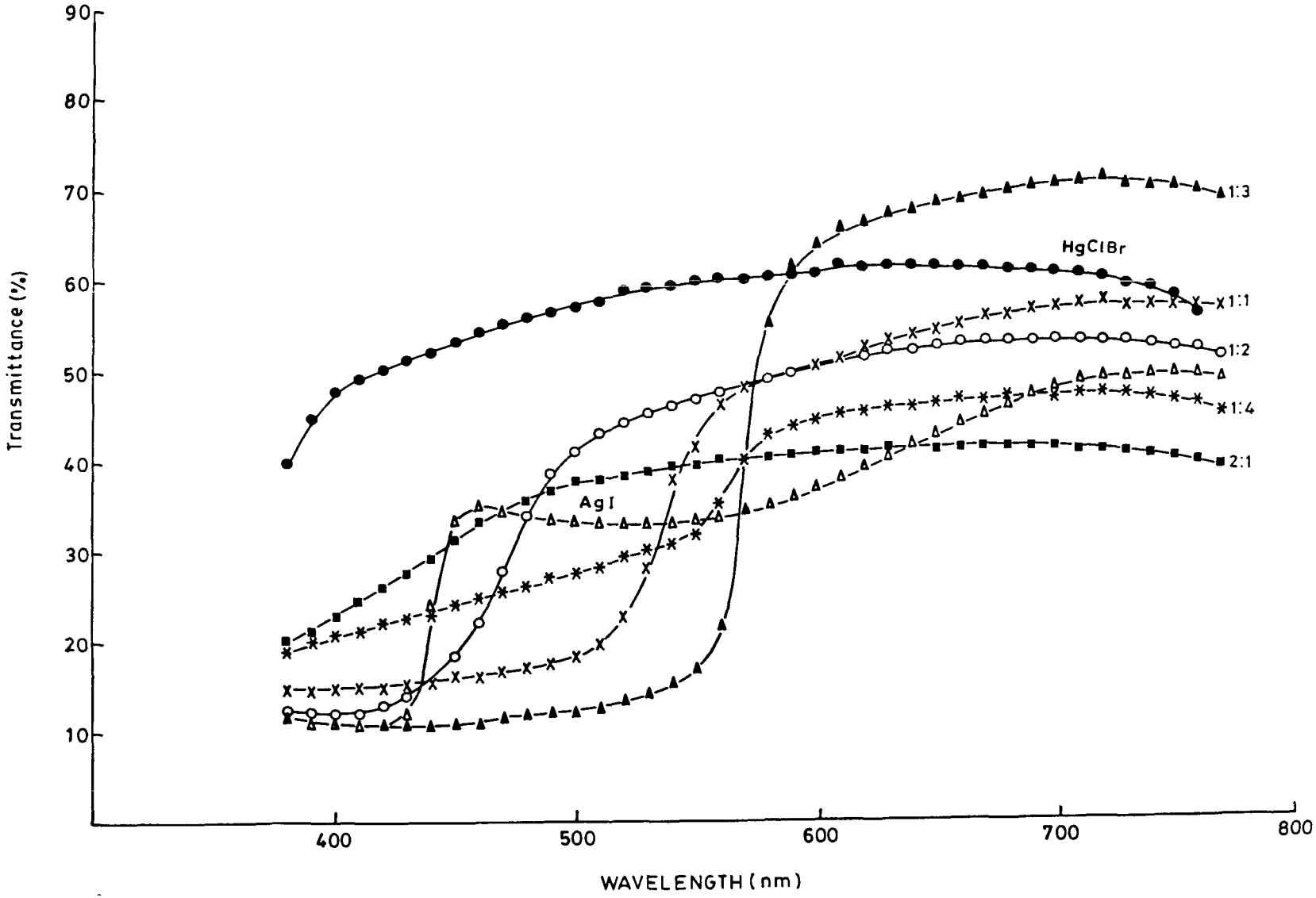

FIG.2. REFLECTANCE SPECTRA FOR THE REACTION BETWEEN HgClBr AND AgI IN DIFFERENT MOLAR RATIOS

The lines of HgClBr were also obtained, which only suggests that the reaction follows the same path as that of 1:1 molar mixture. The difference in resistivity curve is probably due to the presence of excess HgClBr in 1:2 molar ratio. The x-ray diffraction data for this molar mixture is given in Table VII.

The reflectance studies (fig.2) also suggests that product formed in 1:4, 1:3, and 1:2 molar mixtures of HgClBr and AgI must be similar, while in 1:1 and 1:2 molar mixtures, the percent transmittance show that the products are somewhat different in these cases.

Mechanism of Lateral Diffusion

Soon after placing HgClBr over AgI in the reaction capillary, at 50 ^{o}C, red coloured layer developed at the interface. The red product layer grew with time towards the AgI side, which later separated into red and yellow layers. A gap developed between the yellow layer and HgClBr. When the experiment was repeated with an air gap of varying dimensions between the two reactants, the reaction proceeded similarly giving the same kinds of layers on AgI side as was the case when the reactants were in contact. The dimension of the air gap did not affect the sequence of the layers. This shows that the mobile component is HgClBr.

TABLE VII

X-ray diffraction pattern for the reaction 2HgClBr + AgI

d in A°	I/I₀	d in A°	I/I₀
6.31	100	2.68 +	30
4.53 *	40	2.66 +	40
3.67 + *	100	2.64 +	30
3.45 + *	30	2.46 + ò *	30
3.39 x + ò	20	2.33 + ò	40
3.29 ŧ + *	70	2.24 + *	20
3.23 ŧ + *	30	2.12 + ò *	25
3.14 + *	40	2.1 + ò *	20
3.09 + ò *	70	2.05 x + ò	55
2.87 x ò	30	1.99 ŧ x ò *	70
2.85 x	60	1.97 ŧ x + ò	30
2.8 x	100	1.86 x ò *	30
2.77 ŧ + ò *	50		

ŧ lines of AgCl [4] ; ò lines of HgBrI [9]

x lines of AgBr [5] ; + lines of HgClI [10]

* lines of HgClBr [11]

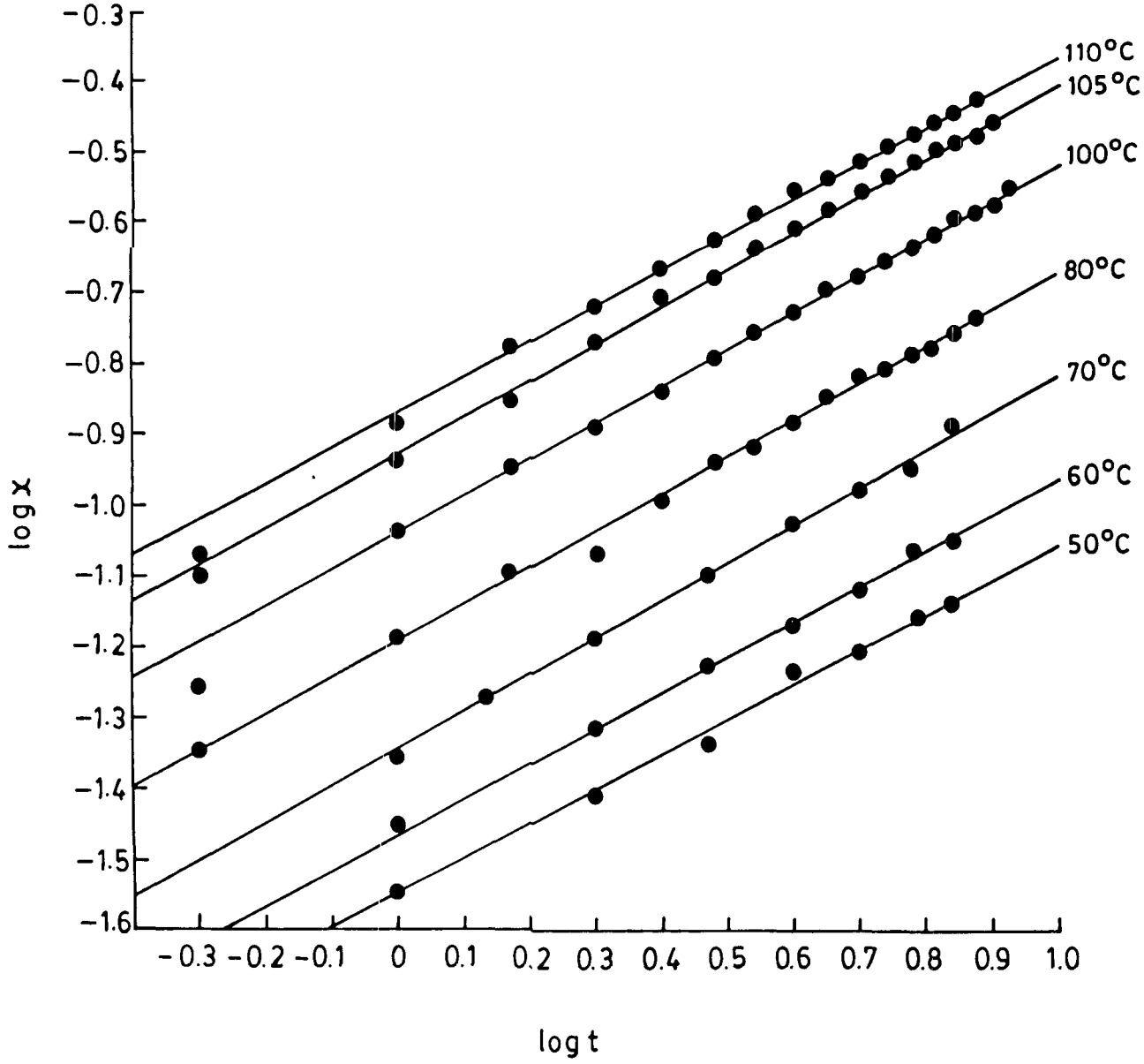

FIG.3. KINETIC DATA FOR LATERAL DIFFUSION AND TEST FOR EQUATION $X^n = k\,t$ FOR HgClBr — AgI REACTION.

X-ray and chemical analysis of the different layers, thus formed, showed the following sequence of products in the reaction capillary.

AgI	Ag_2HgI_4, red	AgBr, AgCl yellow	HgClBr

The rate of growth of product layers decreased with time. Initially, the process is fast and reaction controlled. As the thickness of the product layers became significant, HgClBr took greater time to diffuse through the product layers. The process now becomes diffusion controlled and the rate of the reaction thus falls regularly with the growth of the product layers. The lateral diffusion data best fit the rate equation (fig. 3).

$$X^n = kt \qquad \ldots (1)$$

where X is the total thickness (in cm) of the product layers at time t(in hrs), and k and n are constants. The rate constant, k follows the Arrhenius equation

$$k = A \exp(-E/RT) \qquad \ldots (2)$$

The activation energy evaluated from the log k versus 1/T plot (fig. 4) made by least square fit method was found to be 57.353kJ/mol . The reaction rate constant measured with an initial air gap between the reactants decreased with the increase

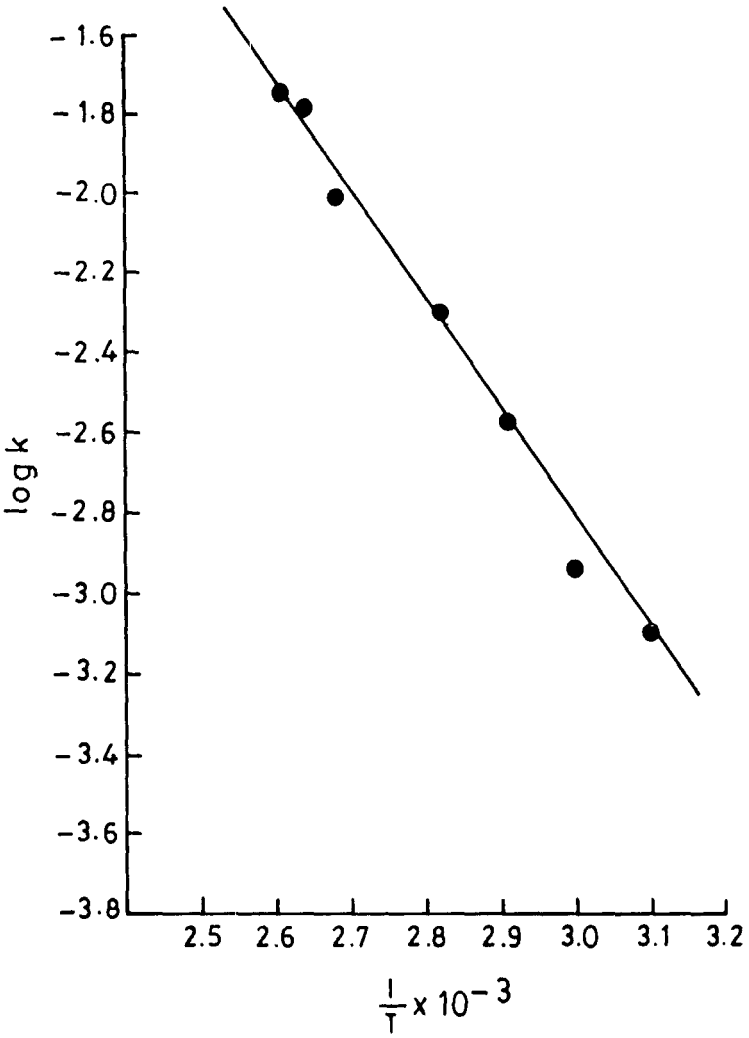

FIG.4. DEPENDENCE OF k ON TEMPERATURE FOR THE REACTION BETWEEN HgClBr AND AgI.

in the length of the air gap. The energy of activation suggests that the reaction is diffusion controlled taking place via vapour phase diffusion.

References

1. Crdenic, D. : Quart. Rev. 19, 303 (1965)

2. Link, H.L. and Wood, L.J. : J. Am. Chem. Soc. 62, 766 (1940).

3. Koch, E. and Wagner, C. : Z physik. Chem. B 34, 317 (1936).

4. ASTM, powder diffraction file No. 6-0480.

5. ASTM, powder diffraction file No. 6-0438.

6. ASTM, powder diffraction file No. 6-0480.

7. ASTM, powder diffraction file No. 21-1157.

8. ASTM, powder diffraction file No. 4-033.

9. ASTM, powder diffraction file No. 30-835.

10. ASTM, powder diffraction file No. 30-836.

11. Mehdi, S. and Ansari, S.M. : J. Solid State Chem. 40, 122 (1981).

EXPERIMENTAL

Copper (I) iodide and mercuric chloroiodide when mixed in an agate mortar, gave red coloured product which turns to dark brown at temperatures above 70°C.

Kinetic Measurements

The kinetics of the reaction were studied by placing HgClI over CuI (both above 300 mesh) in a vertical pyrex glass tube as described in the earlier chapter.

As soon as HgClI powder was placed over CuI in the tube, a scarlet colour boundary appeared at the interface which turned dark brown above 70°C and grew with time on the CuI side. After sometime, a white product started to develope between HgClI and the scarlet product, and a gap developed between HgClI and the white product. The dark brown product turned scarlet on cooling below 70°C (Cu_2HgI_4 is scarlet below 70°C and dark brown above this temperature). The brown and white layers grew simultaneously. The rate of the reaction was followed by measuring the total thickness of the brown and white layers. The rate constants for different sets are tabulated in Table I. The probable precision was calculated as done in the earlier chapters.

TABLE I

Dependence of parameters of equation $X^n = kt$ on temperature for HgClI - CuI reaction

Temperature ($^{o}C \pm 0.5$)	k (cm/hr)	Standard Deviation	Relative Standard Deviation	n
50	8.986×10^{-4}	3.427×10^{-5}	2.47×10^{-2}	1.82
60	1.055×10^{-3}	8.25×10^{-5}	5.95×10^{-2}	1.94
70	2.078×10^{-3}	3.207×10^{-4}	9.41×10^{-2}	1.97
80	3.583×10^{-3}	1.789×10^{-4}	2.97×10^{-2}	1.96
90	5.924×10^{-3}	3.49×10^{-4}	4.618×10^{-2}	1.98
100	1.196×10^{-2}	5.705×10^{-4}	3.78×10^{-2}	1.89
110	2.152×10^{-2}	2.38×10^{-3}	5.85×10^{-2}	1.89

Analysis of the product layer

Several reaction tubes having thick distinct scarlet and white product layers were broken carefully, and the layers were separated. The amounts thus obtained were dissolved in concentrated nitric acid separately. In the white product layer, Cu^{+}, Cl^{-} and I^{-} were confirmed and in the scarlet layer, Cu^{+}, Hg^{+2} and I^{-} were confirmed by spot tests [1]. X-ray diffraction

pattern showed white layer to be single phase γ- CuCl [2] and scarlet layer to be single phase β- Cu_2HgI_4 [3].

X-ray Studies

The reactants, HgClI and CuI in different molar ratios were mixed thoroughly in a mortar and heated at 100°C in an air thermostat for three days. X-ray diffraction patterns of all reaction mixtures were taken at the room temperature by a Norelco Geiger Counter X-ray Diffractometer by CuK_α radiation with a Ni-filter, applying 32 Kv at 12 mA current. The compounds were identified by calculating the d values of the lines and corresponding intensities of the lines and comparing them with the standard values of the expected compounds. The compounds obtained in different mixtures are given in Table II.

Resistivity Measurements

Resistivity measurements for the different molar mixtures of HgClI and CuI were done as earlier and results are depicted in fig. 1.

TABLE II

Compounds present in different molar ratio mixtures of HgClI and CuI

Mixture	Molar ratio of HgClI : CuI	Compounds identified on heating the mixture at 100°C for 3 days and thereafter cooling to room temperature
I	1 : 4	CuCl and β- Cu_2HgI_4
II	1 : 3	CuCl and β- Cu_2HgI_4
III	1 : 2	CuCl, β-$CuHgI_4$ and HgI_2
IV	1 : 1	β- Cu_2gI_4, CuCl, and HgI_2
V	2 : 1	β- Cu_2HgI_4, CuCl, HgI_2 and $HgCl_2$

Reflectance Spectra

The reflectance measurements for the different molar mixtures of the reactants, heated at 100°C for 3 days, was made as described earlier. The result is shown in fig. 2.

Results and Discussion

In order to understand the reaction between HgClI and CuI,

two aspects must be considered : namely, mechanism of chemical interaction when the reactants are intimately mixed in different molar ratios; and mechanism of lateral diffusion when the experiments are carried out in a capillary under isothermal conditions.

Mechanism of chemical interaction

X-ray pattern of reaction carried out with different molar ratios (table III to VII) suggest that reaction takes place in 1:3 molar ratio, unlike the reactions of HgClBr and CuI or HgClBr and AgI in which case the stoichiometry is 1:4.

In 1:3 molar ratio, the x-ray analysis indicates the presence of CuCl and β-Cu_2HgI_4. This suggest that the reaction can be represented as under :

$$HgClI + 3CuI \longrightarrow Cu_2HgI_4 + CuCl \qquad \ldots (1)$$

However, at higher temperatures, the reaction mass turned from red to chocolate coloured, showing the transition taking place in one of the products. Cu_2HgI_4 is red below 70°C (β -form) and chocolate above this temperature (α-form) [4]. Even at higher temperatures, a red colour was observed to be present. This could not be Cu_2HgI_4. To confirm this, experiments in capillary were

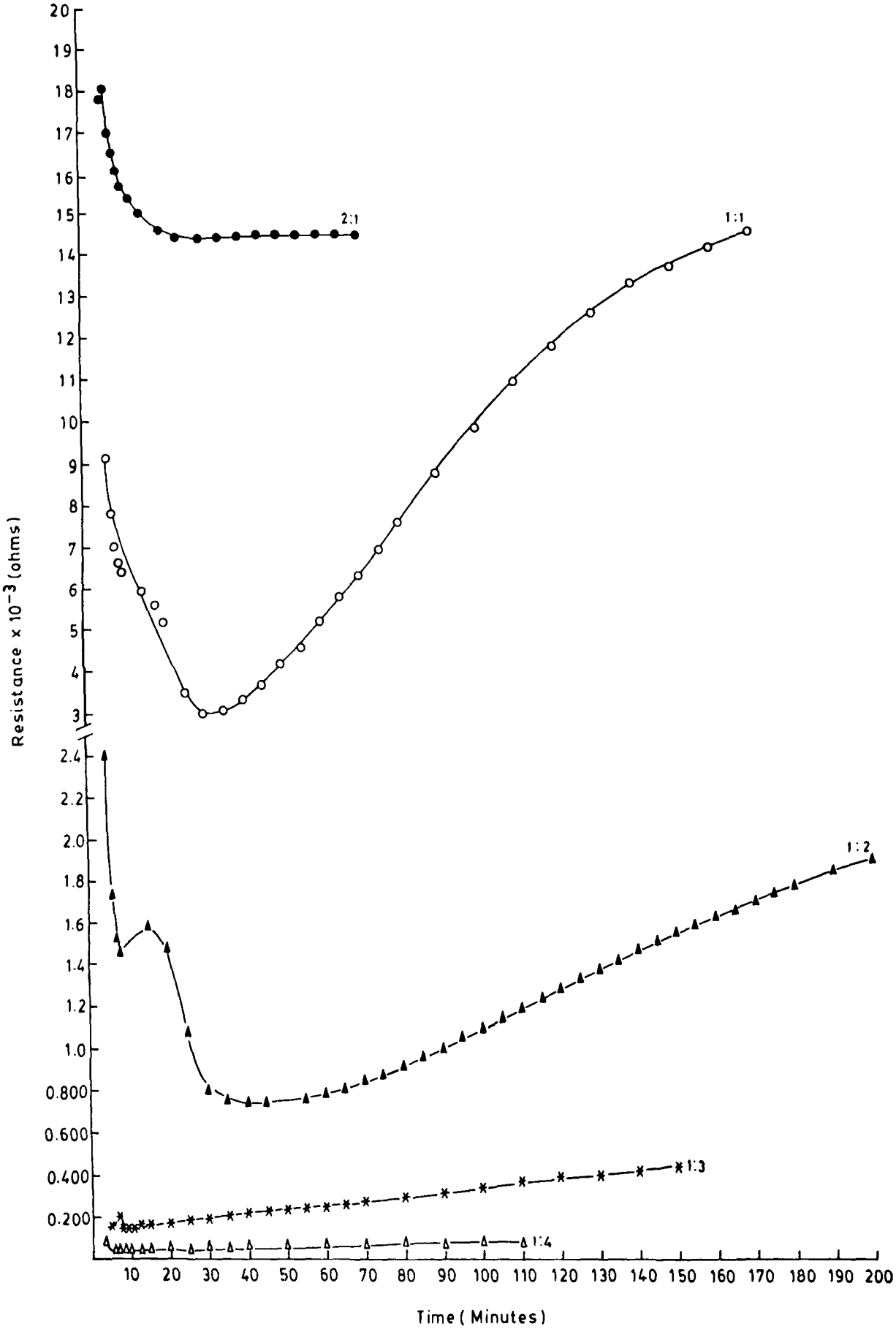

FIG.1. RESISTIVITY CHANGE AS A FUNCTION OF TIME FOR THE REACTION BETWEEN HgCl I AND CuI IN DIFFERENT MOLAR RATIOS.

carried out with excess of CuI. When all of the HgClI was consumed, a red layer was observed to be present. This layer was chemically analysed as HgI_2. X-ray patterns of this layer also showed it to be HgI_2. Hence, it is concluded that the reaction proceeds through the formation of HgI_2. The resistivity measurements (fig.1) suggest that the reaction is a one step reaction. But the presence of HgI_2 in the capillary experiment clearly indicates that it is being formed during the course of reaction. Therefore, the reaction takes place in two-steps, one of which may be quite fast to be detected during the resistivity measurements. In view of these, the following mechanism is proposed :

$$HgClI + CuI \text{ ------> } CuCl + HgI_2 \quad \ldots (1a)$$

$$HgI_2 + 2CuI \text{ ------> } Cu_2HgI_4 \quad \ldots (1b)$$

$$HgClI + 3CuI \text{ -----> } CuCl + Cu_2HgI_4$$

The step (1b) has already been reported to be taking place very fast [5].

TABLE III

X-ray measurements for the reaction mixture HgClI + 3CuI

d in A^{o}	I/I_o
3.64 +	43
3.50 +	100
2.25 +	87
1.84 + *	100

\+ lines of β-Cu_2HgI_4 [8]

* lines of CuCl [9]

The same course of interaction is being followed in the 1:4 molar mixtures of HgClI and CuI. The only difference is the presence of CuI in excess. The resistivity curve (fig.1) is also the same as that of 1:3 molar mixture.

The x-ray analysis of 1:2 molar mixture of HgClI and CuI showed the presence of Cu_2HgI_4, CuCl and HgI_2 in the reaction mixture at room temperature. The resistance curve (fig.1) indicates that the reaction is a multistep one. The resistance decreases fast in the initial stages, shows a slight increase for a little time, then again it falls down and thereafter it rises

TABLE IV

X-ray measurements for the reaction mixture HgClI + 4CuI

d in Å°	I/I_o	d in Å°	I/I_o
6.97	30	2.15 + x ò	76
5.98	53	2.01 + x ò	46
3.66 +	46	1.79 * x ò	30
3.50 + x	100	1.61 * x ò	38
2.23 + x ò	30		

\+ lines of β-Cu_2HgI_4 [8]

* lines of CuCl [9]

x lines of HgI_2 [10]

ò lines of $HgCl_2$ [11]

to a constant value. It is therefore concluded, that in the initial stages, a conducting product is formed, followed by a non-conducting material. On the basis of this observation,

the following mechanism is proposed :

$$HgClI + CuI \text{ ------} > CuCl + HgI_2 \quad \ldots (2a)$$

$$HgI_2 + 2CuI \text{ ------} > Cu_2HgI_4 \quad \ldots (2b)$$

$$HgClI + Cu_2HgI_4 \text{ -----} > CuI + CuCl + 2HgI_2 \quad \ldots (2c)$$

$$HgI_2 + 2CuI \text{ ------} > Cu_2HgI_4 \quad \ldots (2d)$$

$$2HgClI + 4CuI \text{ -----} > Cu_2HgI_4 + CuCl + HgI_2$$

The continous rise in resistivity is due to the unreacted HgI_2 formed in step (2c). The change in resistance in the reaction is due to the individual steps, but when the reaction is complete, the effect of HgI_2 to the resistance predominates. Hence, the rise in the final stage of the reaction.

The x-ray pattern of 1:1 molar mixture showed the presence of β-Cu_2HgI_4, CuCl and HgI_2. The resistivity measurements (fig.1) suggest it to be a two step reaction. The resistance decreases in the initial stages, and thereafter it is continuously increasing. Therefore, the following mechanism can be suggested :

$HgClI + CuI \text{ ------} > CuCl + HgI_2$ ... (3a)

$HgI_2 + 2CuI \text{ -------} > Cu_2HgI_4$ ... (3b)

$HgClI + Cu_2HgI_4 \text{ -----} > CuCl + CuI + 2HgI_2$ ... (3c)

$2HgClI + 2CuI \text{ -----} > 2CuCl + HgI_2$

TABLE V

X-ray measurements for the reaction mixture HgClI + 2CuI

d in A°	I/I_o
5.57	30
4.15 x	40
4.23	40
3.50 x +	100
3.12 *	60
2.71 *	30
2.15 x +	80

* lines of CuCl [9]

+ lines of β-Cu_2HgI_4 [8]

x lines of HgI_2 [10]

However, there are presence of lines β-Cu_2HgI_4 in x-ray pattern of 1:1 molar mixture. This may be due to the fact that the step (3c) is quite slow, and the reaction through step (3c) might not be going to completion.

TABLE VI

X-ray measurements for the reaction mixture HgClI + CuI

d in A°	I/I_o	d in A°	I/I_o
4.11 x	64	2.01 * + x	35
3.73 x	61	1.80 * + x	33
3.56 + x	100	1.78 + x	33
2.99 *	49	1.76 * + x	54
2.75 * + x	66	1.54 + x	41
2.28 + x	49	1.49 * +	33
2.18 + x	100	1.41 * x	

* lines of CuCl [9]

x lines of HgI_2 [10]

\+ lines of β-Cu_2HgI_4 [8]

In the 2:1 molar ratio mixture, the x-ray pattern showed the presence of β-Cu_2HgI_4, CuCl, HgI_2 and $HgCl_2$. From the resistivity

measurements (fig.1), it appears that the reaction is taking the similar course as in the case of 1:1 molar ratio reaction. The extra lines of $HgCl_2$ is due to the presence of the excess of HgClI. Since the x-ray pattern were taken at room temperature, HgClI being not very stable at room temperature [6,7] may have decomposed to HgI_2 and $HgCl_2$.

TABLE VII

X-ray measurements for the reaction mixture 2HgClI + CuI

d in A°	I/I_o	d in A°	I/I_o
4.25 x ò	28	2.15 + x	71
4.13 x ò	42	1.84 * + x	28
3.70	42	1.66 * + x	28
3.56 + x ò	100	1.52 + x ò	28
2.76 * + x ò	71	1.49 + x	57
2.59 + x	57	1.45 + ò	28
2.19 + x	100		

* lines of CuCl [9]

x lines of HgI_2 [10]

\+ lines of β-Cu_2HgI_4 [8]

ò lines of $HgCl_2$ [11]

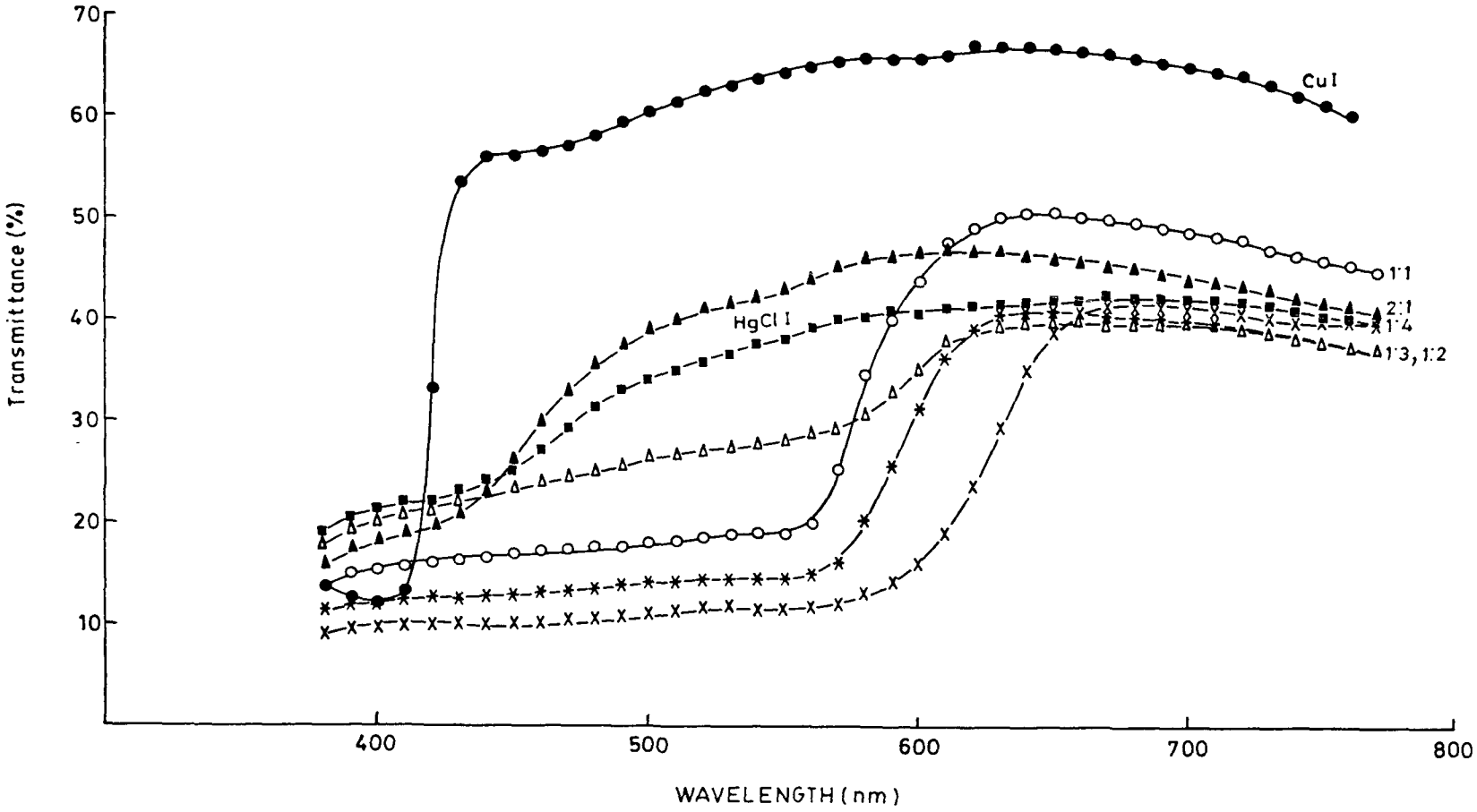

FIG. 2. REFLECTANCE SPECTRA FOR THE REACTION BETWEEN HgCl I AND CuI IN DIFFERENT MOLAR RATIOS.

Reflectance studies show that the same products are obtained when HgClI and ~~AgI~~ CuI are mixed in 1:4 and 1:3 molar ratios and same products when mixed in 1:1 and 1:2 ratios. Although the mechanism followed by 1:1 and 2:1 molar mixtures is the same, the difference in the reflectance spectra of the latter is due to the unreacted HgClI which decomposes into HgI_2 and $HgCl_2$.

Mechanism of Lateral Diffusion

Soon after placing HgClI over CuI in the reaction capillary at 50°C, scarlet coloured layer developed at the interface. The product layer grew with time towards the CuI side. A gap developed between the white layer and HgClI. When the experiment was repeated with an air gap of varying dimensions between the two reactants, the reaction proceeded in similar way giving the same kinds of layers on CuI side as was the case when the reactants were in contact. The dimensions of the air gap did not affect the sequence of the layers. This shows that the mobile component is HgClI. HgClI molecules react with CuI to form coloured Cu_2HgI_4. X-ray and chemical analysis of the different layers thus formed showed the following sequence of products in the reaction capillary.

CuI ¦ HgI_2, Cu_2HgI_4, CuCl, ¦ HgClI

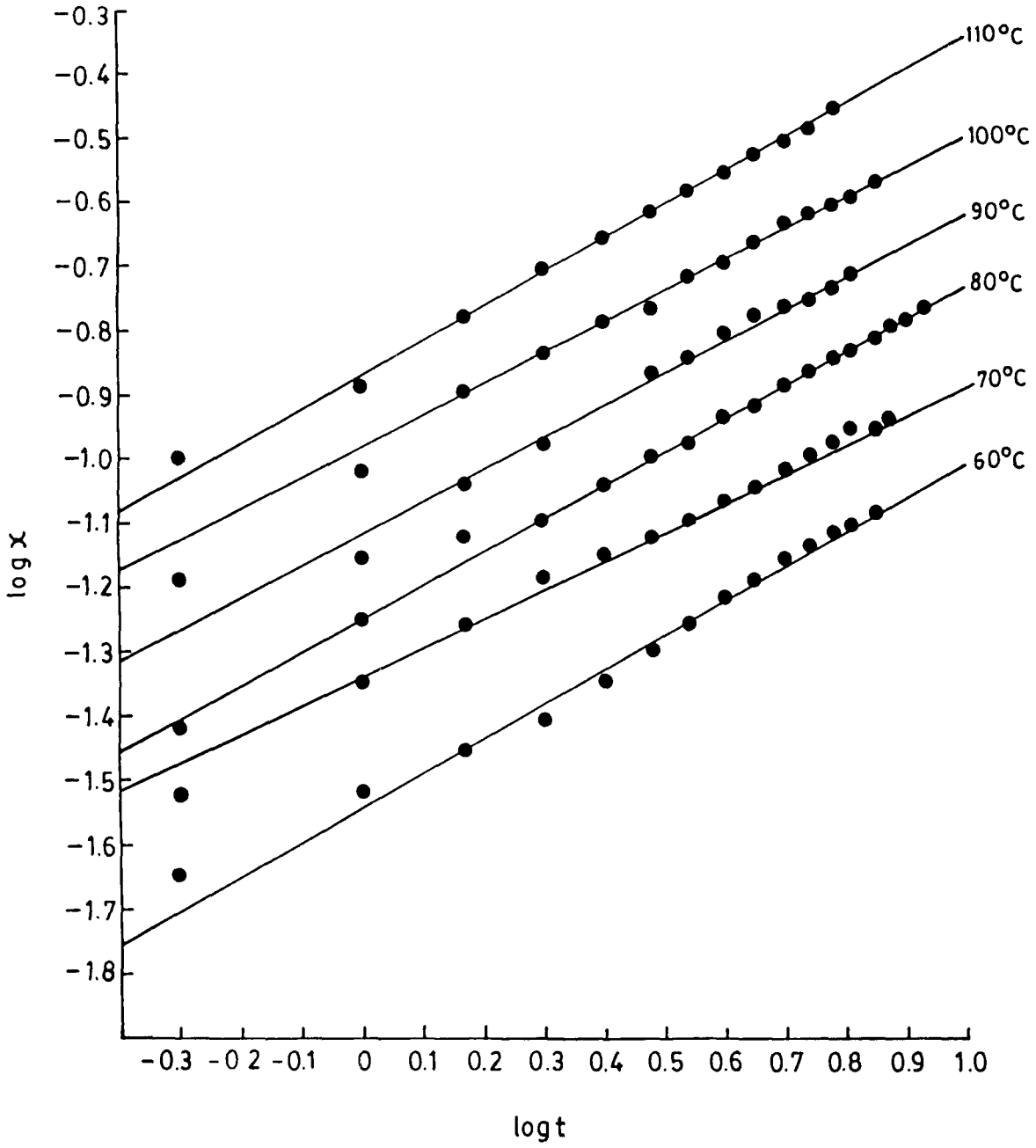

FIG.3. KINETIC DATA FOR LATERAL DIFFUSION AND TEST FOR EQUATION $X^n = kt$ FOR THE REACTION BETWEEN HgCl I AND CuI.

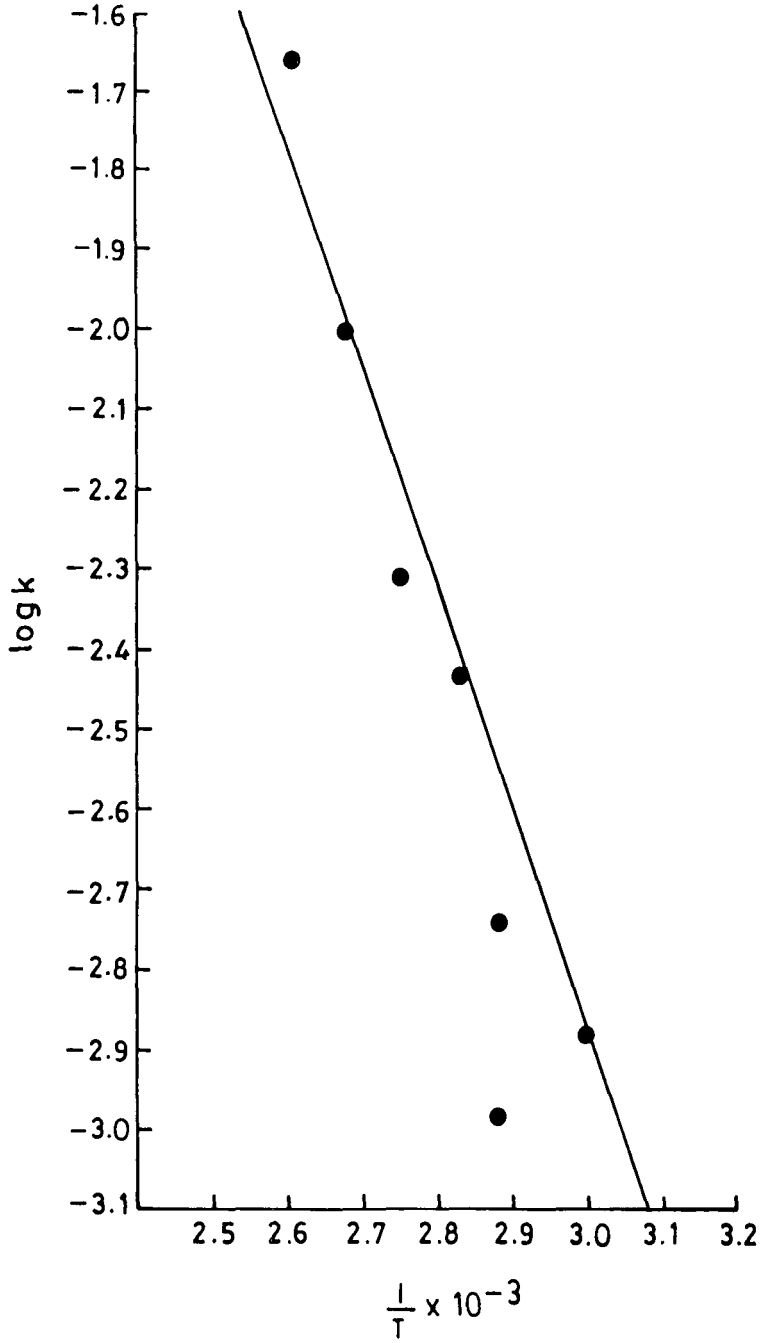

FIG.4. DEPENDENCE OF k ON TEMPERATURE FOR THE REACTION BETWEEN HgCl I AND CuI.

The rate of growth of product layers decreased with time. Initially, the process is fast and reaction controlled. As the thickness of the product layers became significant, HgClI took greater time to diffuse through the product layers. The process now becomes diffusion controlled and the rate of the reaction thus falls regularly with the growth of the product layers. The lateral diffusion data best fit the rate equation (Fig. 3)

$$X^n = kt$$

where X is the total thickness (in cm)of the product layers at time t(in hrs) and k and n are constants. k follows the Arrhenius equation

$$k = A \exp(-E/RT)$$

The activation energy evaluated from the log k versus 1/T plot (fig. 4) made by least square fit method was found to be 56.43kJ/mol . The reaction rate constant measured with an initial air gap between the reactants decreased with an increase in the length of the air gap. The energy of activation suggests that the reaction is diffusion controlled taking place via vapour phase diffusion [12].

References

1. Fiegel, F. and Anger, V. : Spot tests in Inorganic Analysis (Elsevier Publishing Company) pp. 203, 145 and 147 (1972).

2. ASTM Diffraction Data File No. 6-0292.

3. ASTM Diffraction Data File No. 18-0450.

4. Kelelaar, Z. : Z. Krist. 87, 440 (1934).

5. Wagner,C. and Koch, E. : Z. Physik. Chem. B 34, 317 (1936).

6. Rastogi, R.P. et. al. : J. Inorg. Nucl. Chem., 37, 1167 (1975).

7. ASTM Powder Diffraction File No. 4-0454.

8. ASTM Powder Diffraction File No. 18-0450.

9. ASTM Powder Diffraction FILE No. 6-0344.

10. ASTM Powder Diffraction File No. 21-1157.

11. ASTM powder Diffraction File No. 4-033.

12. Rastogi, R.P. et.al. : J. Soc. Indust. Res. 37, 1167 (1975).

EXPERIMENTAL

When silver (I) iodide and mercuric chloroiodide were mixed in an agate mortar, at room temperature (30°C) gave red colour which gradually turned yellow.

Kinetic Measurements

The kinetics of the reaction were studied by placing HgClI over AgI (both above 300 mesh) in a vertical pyrex glass tube as described earlier.

As soon as HgClI Powder was placed over AgI in the tube, a red colour boundary appeared at the interface which grew with time on the CuI side. After sometime a yellow product started to develop between HgClI and the red product, and a gap developed between HgClI and the yellow product. The red and yellow layers grew simultaneously. The rate of the reaction was followed by measuring the total thickness of the red and yellow layers. The rate constants for different sets are reported in Table I. The probable precision was calculated as described in the earlier chapters.

Analysis of the product layer

A reaction tube having thick distinct red and yellow product layers were broken carefully, and the layers were separated. The

amounts thus obtained were dissolved in concentrated nitric acid separately.

In the yellow product layer Ag^+ and Cl^- were detected by spot tests. X-ray diffraction pattern was identical with that of AgCl.

The spot test for the red layer showed the presence of Ag^+, Hg^{+2} and I^- and the x-ray pattern of the material indicated it to be β- Ag_2HgI_4.

TABLE I

Dependence of parameters of equation $X^n = kt$ on temperature for HgClI - AgI reaction.

Temperature ($^\circ C \pm 0.05$)	k (cm/hr)	standard Deviation	Relative Standard Deviation	n
50	8.07×10^{-4}	5.42×10^{-4}	3.51×10^{-2}	2.23
60	9.86×10^{-4}	1.178×10^{-4}	7.532×10^{-2}	2.36
70	3.55×10^{-3}	6.812×10^{-5}	1.667×10^{-2}	2.019
80	2.39×10^{-3}	1.774×10^{-4}	4.39×10^{-2}	2.433
90	1.157×10^{-2}	4.76×10^{-4}	3.66×10^{-2}	1.856
100	1.435×10^{-2}	8.75×10^{-4}	3.979×10^{-2}	1.925
110	2.111×10^{-2}	1.496×10^{-3}	5.28×10^{-2}	1.94

X-ray studies

The reactant HgClI and AgI in different molar ratios were mixed thoroughly in an agate mortar and heated at 100°C for three days. X-ray diffraction pattern of all the reaction mixtures were taken at room temperature by a Norelco Geiger counter x-ray Diffractometer by CuK_{α} radiation with a Ni-filter, applying 32 Kv at 12 mA current. The compounds were identified by calculating the d values of the lines and the corresponding intensities of the lines and comparing them with the standard values of the expected compounds. The compounds obtained in different mixtures are given in Table II.

Resistivity Measurements

Resistivity measurements for the mixture 1:3, 1:2, 1:1 and 2:1 of HgClI and AgI were done as described earlier and the results are depicted in Fig. 1.

Reflectance Spectra

The reflectance measurements of 1:3, 1:2, 1:1 and 2:1 molar ratio mixture of HgClI and AgI was made in the similar fashion as described earlier. The results are depicted in Fig. 2.

TABLE II

Compounds present in different molar ratio mixtures of HgClI and AgI

Mixture	Molar Ratio of HgClI : AgI	Compounds identified after heating the mixture at 100°C for 3 days and thereafter cooling to room temperature
I	1 : 3	AgCl and Ag_2HgI_4
II	1 : 2	AgCl, $HgCl_2$, HgI_2 and Ag_2HgI_2
III	1 : 1	AgCl, $HgCl_2$, HgI_2 and Ag_2HgI_4
IV	2 : 1	AgCl, $HgCl_2$, HgI_2 and Ag_2HgI_4

Results and Discussion

For a comprehensive understanding of the process, the following aspects are to be considered :

(a) Mechanism of chemical interaction and

(b) Mechanism of lateral diffusion when the reactants were kept in contact, and when they were separated by an air gap.

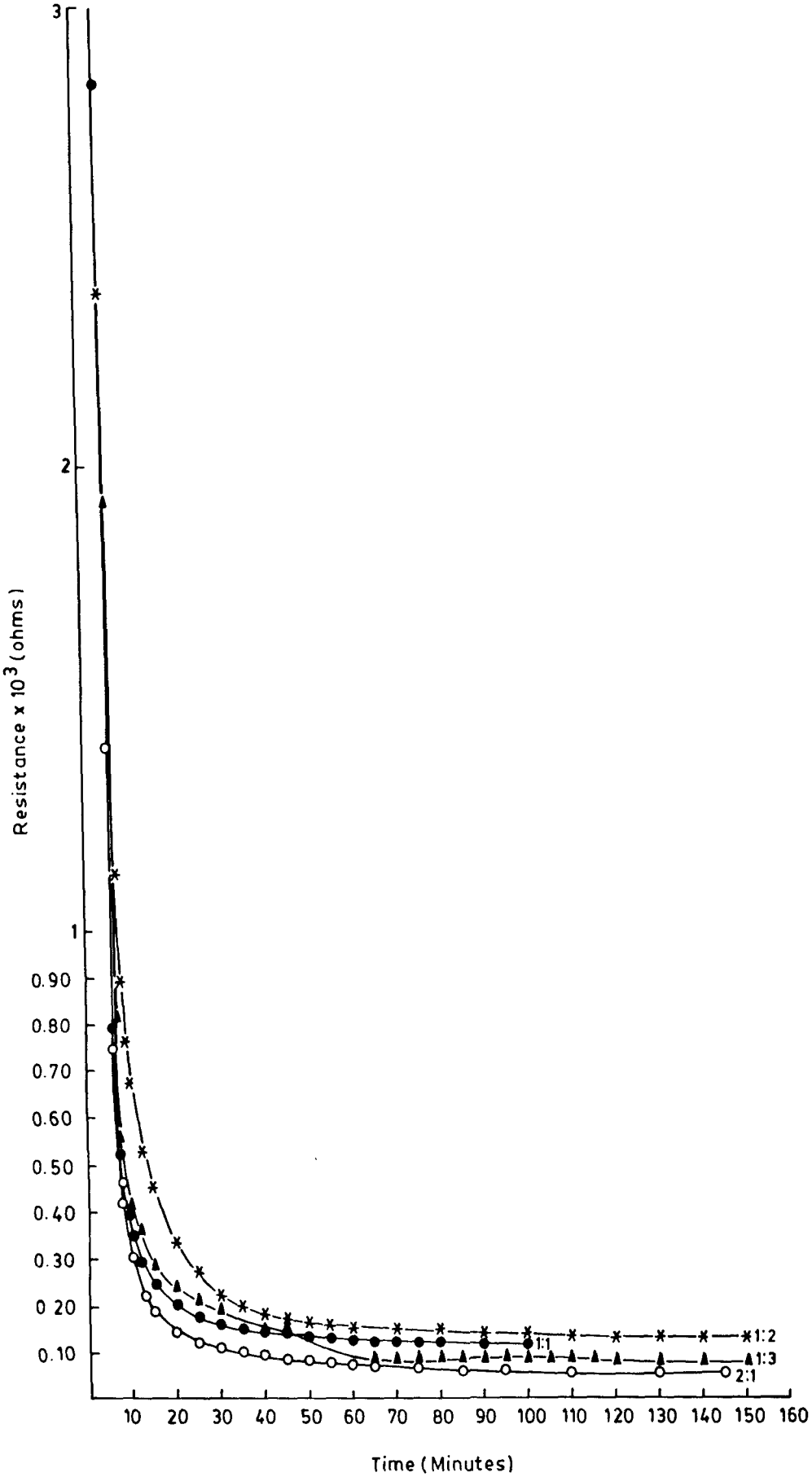

FIG.1. RESISTIVITY CHANGE AS A FUNCTION OF TIME FOR THE REACTION BETWEEN HgCl I AND AgI IN DIFFERENT MOLAR RATIOS .

Mechanism of chemical interaction

It is evident from Table II that HgClI and AgI react by the same mechanism in different molar mixtures.

1:3 molar mixture of HgClI and AgI, maintained at 100°C for 3 days after mixing, showed the presence of AgCl and β-Ag_2HgI_4 (Table II).

$$HgClI + 3AgI \longrightarrow AgCl + Ag_2HgI_4 \quad \ldots (1)$$

The resistivity measurements (fig.1) made with 1:3 molar mixture of HgClI and AgI gave no evidence for any substep of the reaction (1). The abrupt decrease in the resistance with time shows that this reaction is very fast even at room temperature. However, it was observed that as soon as the reactants were mixed at room temperature, a red coloured product was formed that gradually turned yellow. The red colour is perhaps due to the formation of HgI_2 which immediately reacted with AgI to give the addition product Ag_2HgI_4. (Ag_2HgI_4 is yellow below 50.7° (β-form) and red above this temperature (α-form) [1]).

$$HgClI + AgI \longrightarrow AgCl + HgI_2 \quad \ldots (1a)$$

$$HgI_2 + 2AgI \longrightarrow Ag_2HgI_4 \quad \ldots (1b)$$

The resistivity diagram (fig.1) shows only one inflection. Further, there is no evidence of HgI_2 in the x-ray pattern of 1:3

molar ratio of HgClI and AgI. Instantaneous appearance of red colour suggests that Step (1a) is very fast. step (1b) is known to be fast [2] even at low temperature. Therefore, HgI_2 formed in step (1a) simultaneously reacts with AgI present in the reaction mixture to give Ag_2HgI_4. This explains why there is no evidence for step (1a).The x-ray diffraction pattern for this mixture is shown in Table III.

TABLE III

X-ray diffraction pattern for the reaction HgClI + 3AgI

d in A°	I/I_o	d in A°	I/I_o
5.5	13	2.33 x	28
4.05	12	2.22 x	71
3.76	50	2.07 x	12
3.63 x	100	1.98 +	19
2.92 x	10	1.90 +	35
2.80 + x	19	1.68 +	5
2.56 x	9	1.53 +	5
2.44 x	9	1.47 +	5

\+ lines of AgCl [3]

x lines of β-Ag_2HgI_4 [4]

TABLE IV

X-ray diffraction pattern for the reaction HgClI + 2AgI

d in A°	I/I₀	d in A°	I/I₀
6.5	6	2.33 x ò	16
4.05 + ò	6	2.26 x ò	16
4.01 +	12	1.99 + x + ò	16
3.81	32	1.91 + x + ò	35
3.65 x + ò	100	1.75 x + ò	6
3.12 + x + ò	16	1.45 x + ò	9
2.81 + x	16		

\+ lines of AgCl [3]

x lines of Ag_2HgI_4 [4]

\+ lines of HgI_2 [5]

ò lines of $HgCl_2$ [6]

The x-ray pattern, at room temperature of 1:2, 1:1 and 2:1 molar mixtures of HgClI and AgI carried out by mixing and heating for 3 days (table IV to VI) showed the presence of AgCl, Ag_2HgI_4, HgI_2 and $HgCl_2$ in all the three mixtures. The resistivity curves (fig.1) for these molar mixtures were similar to the one obtained

for 1:3 molar ratio. This clearly indicates that the reaction with mixtures in above molar ratios follow the same mechanism as that for 1:3 molar mixture. The presence of $HgCl_2$ and HgI_2 in the mixture is due to the presence of excess HgClI that do not take part in the reaction. Since HgClI is not very stable at room

TABLE V

X-ray diffraction pattern for the reaction HgClI + AgI

d in A°	I/I_o	d in A°	I/I_o
4.19 ŧ ὸ	49	2.78 + ŧ ὸ	92
3.98	100	2.25 x ὸ	71
3.59 x ŧ ὸ	42	2.11 x ŧ	71
3.23 + x	62	1.97 + x ŧ ὸ	42
3.12 ὸ	100	1.73 x ŧ ὸ	14
2.88 x	42	1.67 + x ŧ	14

\+ lines of AgCl [3]

x lines of Ag_2HgI_4 [4]

ŧ lines of HgI_2 [5]

ὸ lines of $HgCl_2$ [6]

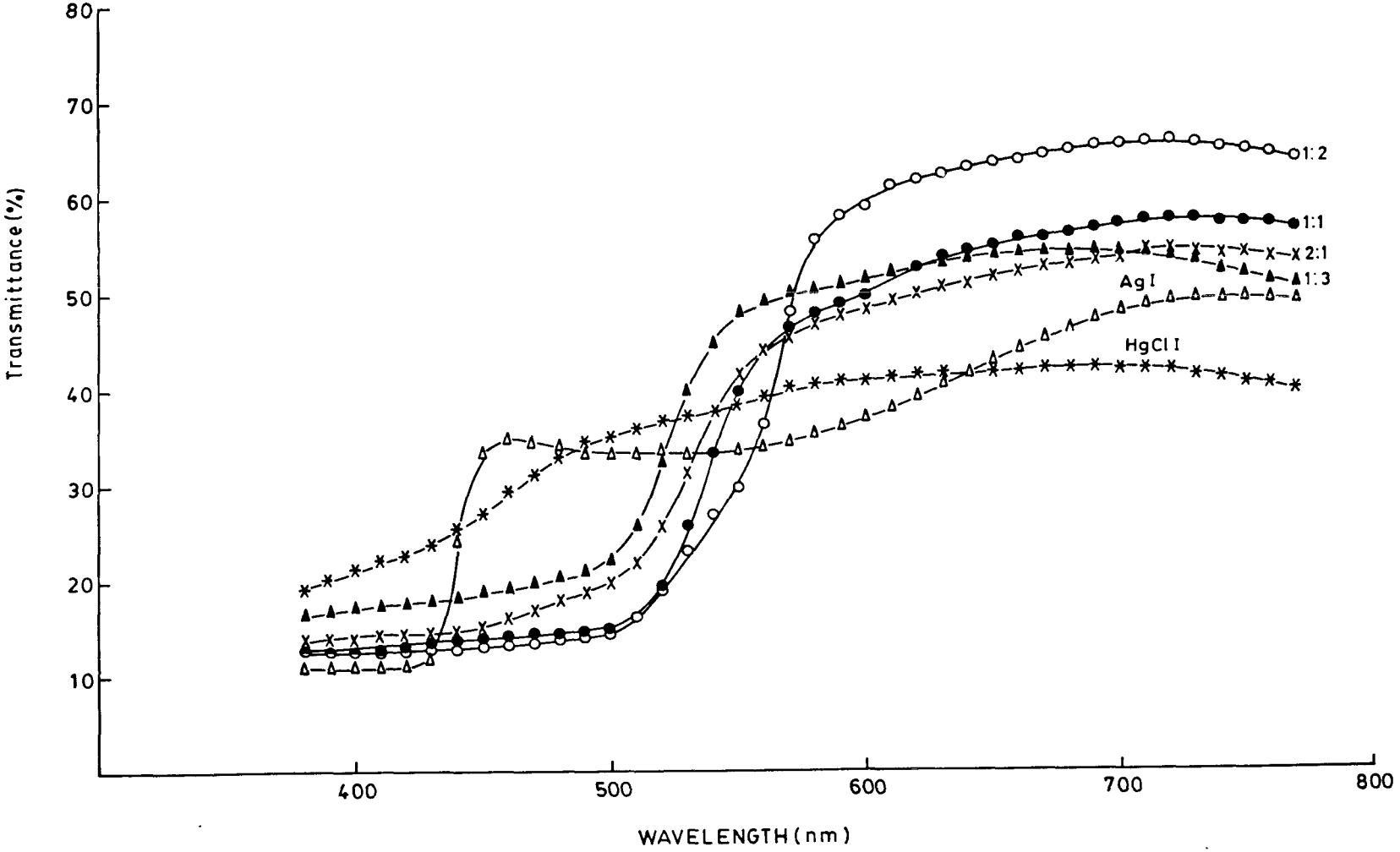

FIG. 2. REFLECTANCE SPECTRA FOR THE REACTION BETWEEN HgCl I AND AgI IN DIFFERENT MOLAR RATIOS.

temperature, it decomposes into its component HgI_2 and $HgCl_2$.

The reflectance studies (fig.2) also point to the fact, that, the same products are obtained when HgClI and AgI reacts in different molar ratios.

TABLE VI

X-ray diffraction pattern for the reaction 2HgClI + AgI

d in A°	I/I_o	d in A°	I/I_o
4.18 ŧ	57	2.77 + ŧ	21
4.01	92	2.187 x ŧ	71
3.25 + x	57	2.104 x ŧ	64
3.105 ŧ	100	2.015 + ŧ	28
3.055 ŧ	57	1.97 + x ŧ	35
2.86 x	35	1.93 + x ŧ	21

\+ lines of AgCl [3]

x lines of Ag_2HgI_4 [4]

ŧ lines of HgI_2 [5]

ð lines of $HgCl_2$ [6]

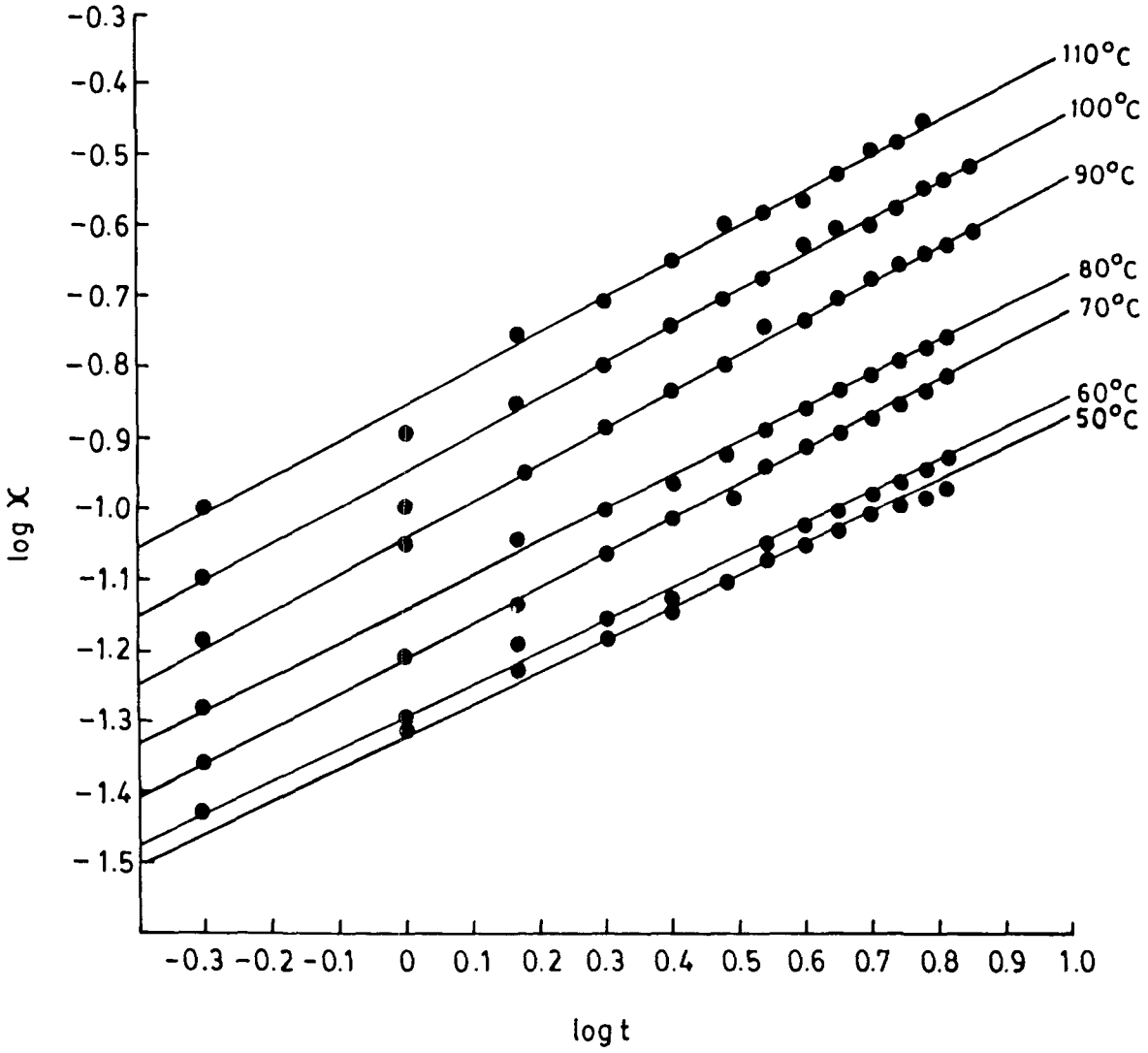

FIG.3. KINETIC DATA FOR LATERAL DIFFUSION AND TEST FOR EQUATION $X^n = kt$ FOR THE REACTION BEWEEN HgCl I AND AgI.

Thr x-ray paterns of the 1:3 molar mixture also reveals that d-values of AgCl and Ag_2HgI_4 are not as exact as indicated by their ASTM - Diffraction files [2,3]. The d values of AgCl has increased to a little extent, whereas that of Ag_2HgI_4 has decreased to about the same extent. This gives an idea that there is formation of solid solution AgCl - Ag_2HgI_4.

Mechanism of lateral diffusion

Soon after placing HgClI over AgI in the reaction capillary, at 50°C, red coloured layer developed at the interface. The product layer grew with time towards the silver iodide side, which later separated into red and yellow layers. A gap developed between the yellow layer and HgClI. When the experiment was repeated with an air gap of varying dimensions between the same kinds of layers on AgI side as was the case when the reactants were in contact. The dimensions of the air gap did not affect the sequence of the layers. This shows that the mobile component is HgClI. X-ray and chemical analysis of the different layers thus formed showed the following sequence of products in the reaction capillary.

AgI ¦ Ag_2HgI_4, AgCl, HgI_2 + $HgCl_2$ ¦ HgClI

The rate of growth of product layers decreased with time.

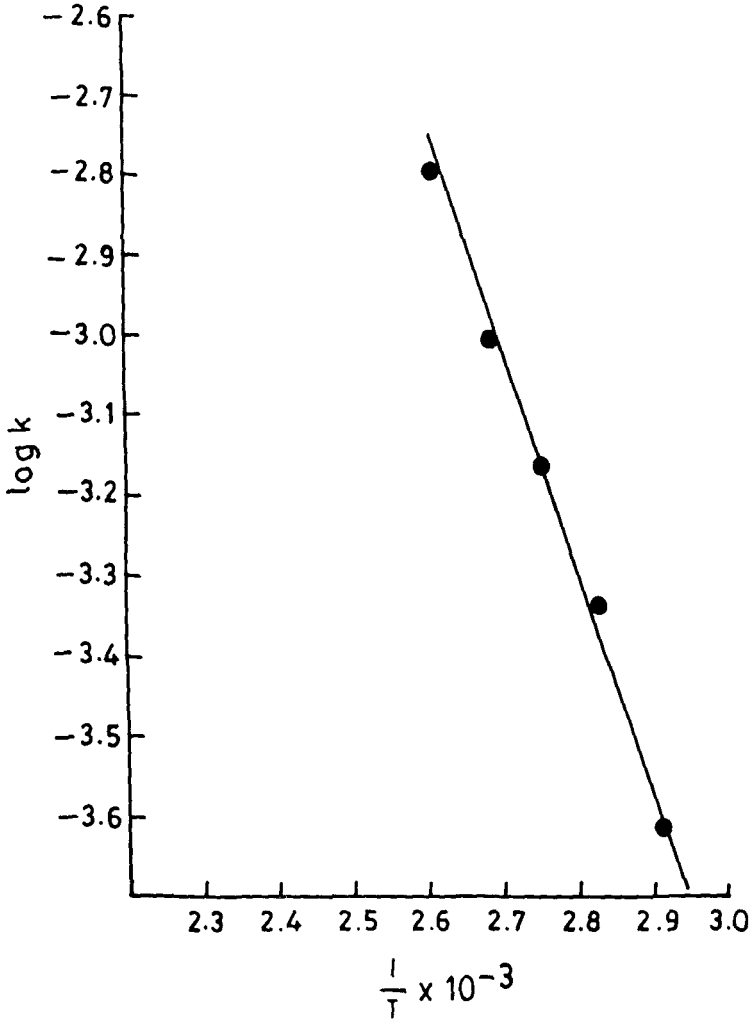

FIG.4. DEPENDENCE OF k ON TEMPERATURE FOR THE REACTION BETWEEN HgCl$_2$ AND Cu_2HgI_4.

Initially, the process is fast and reaction controlled. As the thickness of the product layers became significant, HgClI took greater time to diffuse through the product layers. The process now becomes diffusion controlled and the rate of the reaction thus falls regularly with the growth of the product layers. The lateral diffusion data best fit the rate equation (fig. 3).

$$X^n = kt \qquad \ldots (1)$$

where X is the total thickness (in cm)of the product layers at time t(in hrs), and k and n are constants. The rate constant, k follows the Arrhenius equation :

$$k = A \exp(-E/RT) \qquad \ldots (2)$$

The activation energy evaluated from the log k versus 1/T plot (fig.4) made by least square fit method was found to be 111.84 kJ/mol . The reaction rate constant measured with an initial air gap between the reactants decreased with the increase in the length of the air gap. The energy of activation suggests that the reaction is diffusion controlled taking place via vapour phase diffusion [6].

References

1. Crdenic, D. : Qurt. Rev. 19, 303 (1965).

2. Koch, E. and Wagner, C. : Z.Physic. Chem. B 34, 317 (1936).

3. ASTM, powder diffraction file No. 6-0480.

4. ASTM, powder diffraction file No. 6-0480.

5. ASTM, powder diffraction file No. 21-1157.

6. ASTM, powder diffraction file No. 4-033.

7. Rastogi, R.P. et. al. : J. Soc. Indust. Res. 37, 622 (1978).

EXPERIMENTAL

When HgClI and Cu_2HgI_4 were mixed at room temperature, a red colour product appeared which did not change its colour at higher temperature.

Kinetic Measurements

The kinetics of the reaction in the solid state were studied by placing HgClI over Cu_2HgI_4 (both above 300 mesh size) in a vertical pyrex glass tube as described earlier.

Soon after the placement of the HgClI powder over Cu_2HgI_4 in the tube, a red boundary formed at the interface and this grew with time on the Cu_2HgI_4 side. After sometime, a white product developed between HgClI and the red product and a gap appeared between the white product and HgClI. The rate of the reaction was followed by measuring the total thickness of the product layers. The rate constants for different sets are reported in Table I.

Analysis of the product layer

A reaction tube having distinct product layers was broken carefully and the products collected separately. The products thus obtained were dissolved separately in concentrated nitric acid.

TABLE I

Dependence of parameters of equation $x^n = kt$ on temperature

temperature (°C ± 0.5)	k (cm/hr)	Standard Deviation	Relative Standard Deviation	n
70	2.515×10^{-4}	5.95×10^{-6}	1.908×10^{-2}	1.57
80	5.16×10^{-4}	1.20×10^{-5}	1.77×10^{-2}	1.52
90	6.30×10^{-4}	1.85×10^{-5}	2.47×10^{-2}	1.59
100	1.11×10^{-3}	2.46×10^{-5}	1.76×10^{-2}	1.59
110	1.24×10^{-3}	2.58×10^{-5}	1.45×10^{-2}	1.69

In the white product layer, Cu^+, I^- and Cl^- were confirmed by the spot tests [1]. X-ray diffraction pattern was identical with that of CuCl.

The spot tests for the red product layer showed the presence of Hg^{2+} and I^-. X-ray diffraction pattern was identical with that of HgI_2.

X-ray studies

The reactant HgClI and Cu_2HgI_4 were mixed thoroughly in different molar ratios in an agate mortar and heated at 100°C for 3 days. X-ray diffraction patterns of all the reaction mixtures

were taken at room temperature by a Norelco Geiger Counter X-ray Diffractometer by CuK_{α} radiation with a Ni-filter, applying 32 Kv at 12 mA current. The compounds were identified by calculating the d values of the lines and corresponding intensities of the lines and comparing them with the standard values of the expected compounds. The compounds obtained in different mixtures are given in Table II.

TABLE II

Compounds present in different molar mixtures of HgClI and Cu_2HgI_4

Mixture	Molar ratio of HgClI : Cu_2HgI_4	Compounds identified after heating the mixture at 100°C for 3 days and thereafter cooling to room temparatura
I	1 : 3	CuCl, CuI, HgI_2 and β-Cu_2HgI_4
II	1 : 2	CuCl, CuI and HgI_2
III	1 : 1	CuCl, HgI_2 and β-Cu_2HgI_4
IV	2 : 1	CuCl and HgI_2
V	3 : 1	CuCl and HgI_2

Resistivity Measurements

Resistivity measurements for the mixture 1:3, 1:2, 1:1, 2:1 and 3:1 of HgClI and Cu_2HgI_4 were done as described earlier and the results are depicted in fig. 1.

Reflectance Spectra

The reflectance measurements of 1:3, 1:2, 1:1, 2:1 and 3:1 molar ratio mixture of HgClI and Cu_2HgI_4 was made in the same way as described earlier. The results are shown in fig. 2.

RESULTS and DISCUSSION

For a comprehensive understanding of the process, the following aspects are to be considered :

(a) Mechanism of chemical interaction and

(b) Mechanism of lateral diffusion when the reactants are kept in contact, and when they are separated by an air gap.

Mechanism of chemical interaction

The x-ray diffraction studies (table III to VII) showthat the reaction of HgClI and Cu_2HgI_4 take place differently when they are mixed in different molar ratios.

1:2 molar mixture of HgClI and Cu_2HgI_4, mixed and heated to

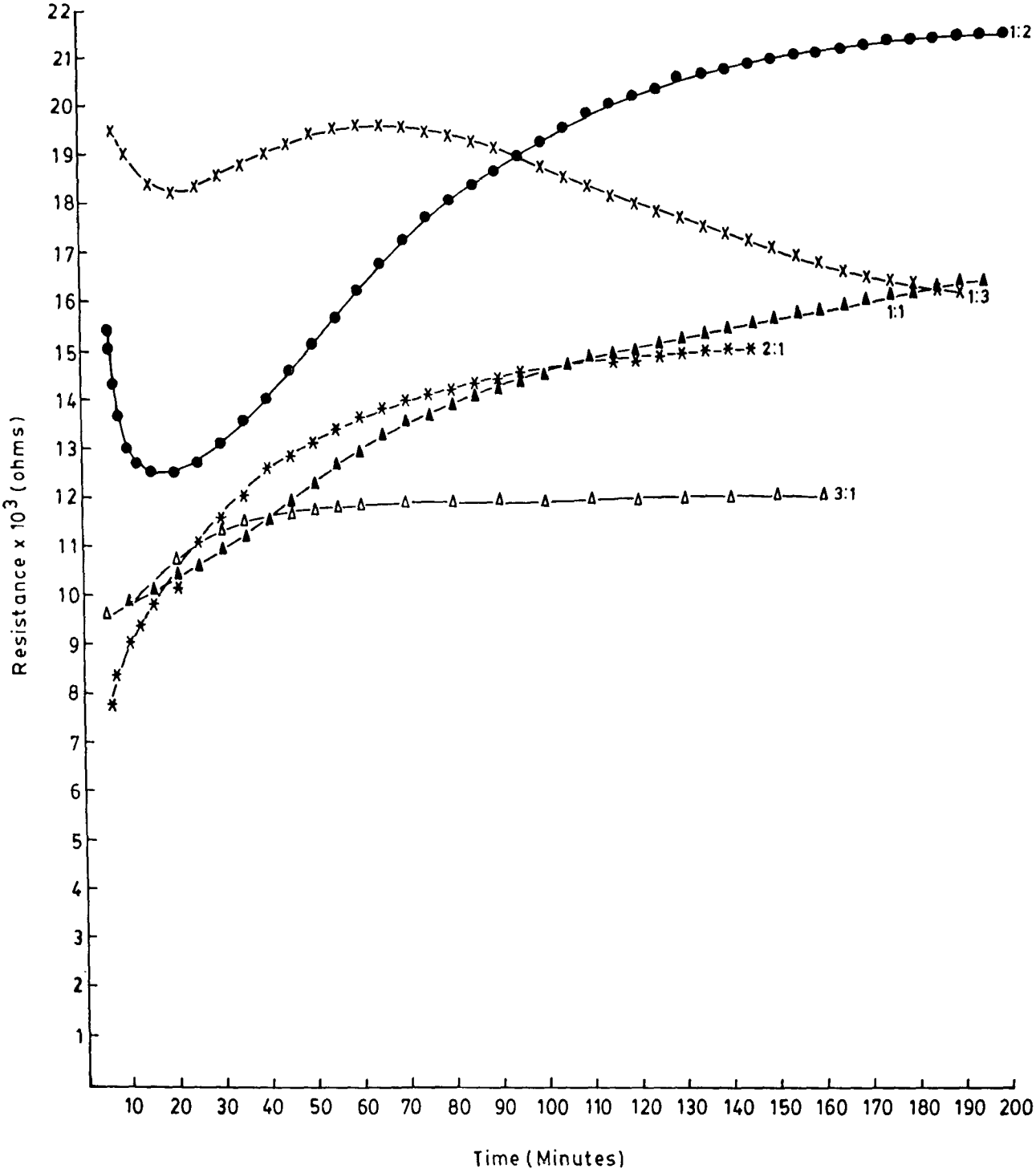

FIG. 1. RESISTIVITY CHANGE AS A FUNCTION OF TIME FOR THE REACTION BETWEEN HgCl I AND Cu_2HgI_4 IN DIFFERENT MOLAR RATIOS.

100°C for about three days showed the presence of CuCl, CuI and HgI_2 (table III).

$$HgClI + 2Cu_2HgI_4 \text{ -----> } 3CuI + CuCl + 3HgI_2 \quad \ldots (1)$$

The resistivity measurements (fig.1) show it to be a multi-step reaction. The resistivity first decreases, showing the foemation of a conducting material and thereafter continously rises. The first step is therefore proposed as:

$$HgClI + Cu_2HgI_4 \text{ -----> } CuI + CuCl + 2HgI_2 \quad \ldots (1a)$$

The fall in resistance is due to the formation of CuI and CuCl which have lower resistance as compared to those of reactants [2].Now there are two possibilities, thereafter, HgI_2 undergoes an exchange reaction with CuCl

$$2CuCl + HgI_2 \text{ ------> } CuI + HgCl_2 \quad \ldots (1b)$$

and HgI_2 combines with CuI giving the more conducting Cu_2HgI_4

$$2CuI + HgI_2 \text{ -------> } Cu_2HgI_4 \quad \ldots (1c)$$

However, the fact that exchange reactions are often fast [3], coupled with our observation of rise in resistivity after initial fall indicates that the step (1b) predominantly affects the rise in resistivity. Hence, the second step may be represented by

(1b). However, as (1c) is known to occur, one cannot neglect the step (1c) altogether, although the resistivity measurements do not support this. As $HgCl_2$ is known to react [4] with Cu_2HgI_4, $HgCl_2$ formed in the step (1b) must be simultaneously being consumed through (1d) and therefore does not show up in the x-ray analysis of the end products.

$$Cu_2HgI_4 + HgCl_2 \text{ ------> } 2CuCl + 2HgI_2 \quad \ldots \quad (1d)$$

Hence, the mechanism of 1:2 molar mixture can be represented as :

$$HgClI + Cu_2HgI_4 \text{ -----> } CuI + CuCl + 2HgI_2$$

$$2CuCl + HgI_2 \text{ ------> } 2CuI + HgCl_2$$

$$Cu_2HgI_4 + HgCl_2 \text{ -----> } 2CuCl + 2HgI_2$$

$$HgClI + 2Cu_2HgI_4 \text{ ------> } CuCl + 3CuI + 3HgI_2$$

The x-ray analysis of 1:3 molar mixture of HgClI and Cu_2HgI_4 showed the presence of CuI, CuCl, HgI_2 and β-Cu_2HgI_4.

The resistivity measurement (fig.1) suggests that the reaction is a multi-step one. The resistance first decreases, then after showing a slight increase it finally falls

TABLE III

X-ray measurementd for the reaction HgClI + $2Cu_2HgI_4$

d in A°	I/I$_o$
5.47	8
4.17 ò	16
3.53 x ò	100
3.40 x	13
3.01 x ò	7
2.65 +	7
2.16 x ò	49
1.85 + x ò	18

+ lines of CuCl [5]

x lines of CuI [6]

ò lines of HgI_2 [7]

continuously to a constant value. The presence of Cu_2HgI_4 in the product analysis of this molar mixture is probably an indirect proof that the mechanism proposed above is being followed, because Cu_2HgI_4 is present in greater amount in the mixture than is required for the proposed mechanism of 1:2 molar ratio and

hence is responsible for the final fall in resistance. This Cu_2HgI_4, left unreacted, is also shown up in the x-ray analysis of the end products.

TABLE IV

X-ray measurements for the reaction mixture HgClI + $3Cu_2HgI_4$

d in A°	I/I_o
5.422 +	13
4.14 ð	13
3.52 x ð +	100
3.39 x +	18
2.78 + ð +	9
2.66 + +	11
2.16 x ð +	65
1.84 + x ð +	23

+ lines of CuCl [5]

x lines of CuI [6]

ð lines of HgI_2 [7]

+ lines of Cu_2HgI_4 [8]

The reaction with molar ratios 1:1, 2:1 and 3:1 in HgClI and Cu_2HgI_4 mixture seems to follow the similar mechanism, because the resistivity curves of all the three mixtures has the same pattern.

The reaction appears to occur in 2:1 molar mixture. In this molar mixture x-ray analysis indicated the presence of CuCl and HgI_2 (table II). The resistivity measurements (fig.1) show a regular increase in the resistance till it attains a constancy. Hence there may be more than one step involved. The course of reaction must be different from the one that has been discussed for 1:3 or 1:2 molar mixtures of the same reaction, as in those cases the resistance decreased initially whereas in 1:1, 2:1 and 3:1 molar mixture, there is no indication of any decrease in resistance value. Therefore, the first step must be entirely different from that of 1:3 or 1:2 molar mixtures. This step must correspond to the formation of non-conducting product. Therefore, the first step is likely to be as follows:

$$2HgClI + Cu_2HgI_4 \text{ -----> } 2CuI + HgCl_2 + 2HgI_2 \quad \ldots (2a)$$

Now, CuI combines immediately with HgI_2 to form Cu_2HgI_4.

$$2CuI + HgI_2 \text{ ------> } Cu_2HgI_4 \quad \ldots (2b)$$

Cu_2HgI_4 formed in step(2b) combines with $HgCl_2$ formed in step(2a).

$$Cu_2HgI_4 + HgCl_2 \text{ ------} > 2CuCl + 2HgI_2 \quad \ldots (2c)$$

Step (2c) has separately been confirmed. Although Cu_2HgI_4 is a conducting material, so the resistance of this must show a decrease in the resistivity curve. But, step (2b) as already reported in earlier chapters takes place very fast; therefore, this may not be indicated in the resistivity curve, as it is immediately consumed by $HgCl_2$ to produce HgI_2. The overall reaction may be represented as :

$$2HgClI + Cu_2HgI_4 \text{ -----} > 2CuCl + 3HgI_2$$

In the similar molar mixture of HgClI and Cu_2HgI_4, x-ray analysis indicated the presence of CuCl, HgI_2 and Cu_2HgI_4. The resistivity (fig.1) and the reflectance studies (fig.2) show that it follows the same mechanism as that of 2:1 molar mixture. Here Cu_2HgI_4 remains unreacted as it is present in excess as demanded by the stoichiometry of the reaction according to the proposed mechanism. Hence, it shows up in the x-ray anlysis of the end products.

TABLE V

X-ray measurements for the reaction $2HgClI + Cu_2HgI_4$

d in A°	I/I_o
6.28 ò	7
4.11 ò	65
3.57 ò	80
3.14 + ò	19
3.01 ò	34
2.85	11
2.77 +	42
2.63 ò	11
2.19 ò	100
1.92 + ò	30
1.86 + ò	34

+ lines of CuCl [5]

ò lines of HgI_2 [6]

TABLE VI

X-ray measurements for the reaction HgClI + Cu_2HgI_4

d in A°	I/I₀
6.23 ò	30
4.13 ò	75
3.59 ò +	90
3.53 ò +	100
3.01 ò +	30
2.77 + ò +	25
2.63 + +	25
2.19 ò +	65
2.16 ò +	55

\+ lines of CuCl [5]

ò lines of HgI_2 [7]

\+ lines of Cu_2HgI_4 [8]

X-ray analysis of 3:1 molar mixture of HgClI and Cu_2HgI_4 showed the presence of CuCl, $HgCl_2$ and HgI_2. From the resistivity (fig.1) and reflectance (fig.2) measurements, we conclude, that the

reaction is following the mechanism proposed for 2:1 molar mixture.

TABLE VII

X-ray measurements for the reaction $3HgClI + Cu_2HgI_4$

d in A°	I/I_o
6.23 ὸ	45
4.11 ὸ *	86
3.59 ὸ *	100
3.12 + ὸ *	27
3.00 ὸ *	49
2.76 + ὸ *	45
2.18 ὸ *	95
2.05 ὸ *	9
1.92 + ὸ *	22
1.85 + ὸ *	22

+ lines of CuCl [5]

ὸ lines of HgI_2 [7]

* lines of $HgCl_2$ [9]

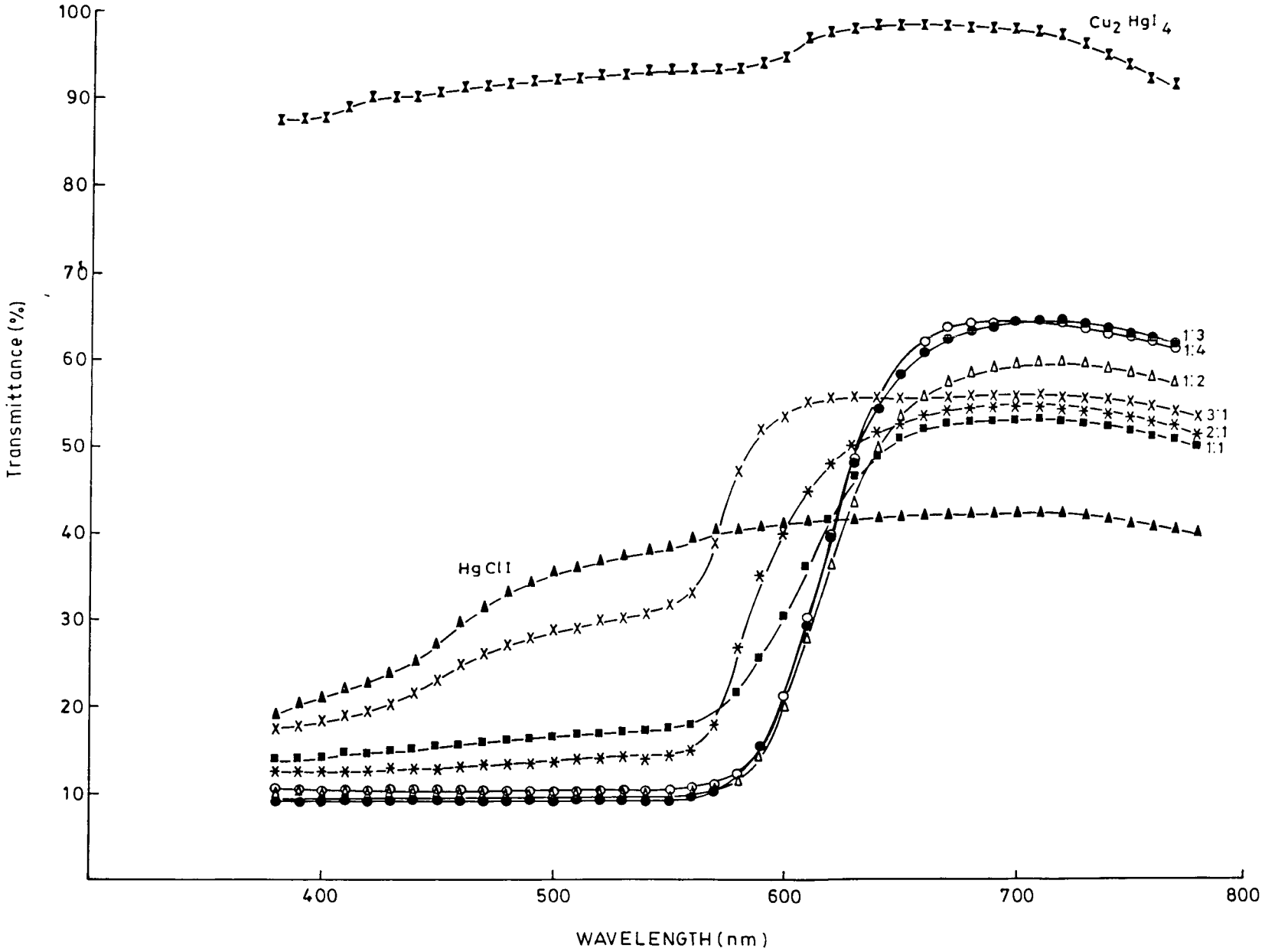

FIG. 2. REFLECTANCE SPECTRA FOR THE REACTION BETWEEN HgCl I AND Cu_2HgI_4 IN DIFFERENT MOLAR RATIOS.

It seems from the discussion that when Cu_2HgI_4 is in excess, one type of mechanism is followed in which case the Stoichiometry of the reaction is 1:2 of HgClI and Cu_2HgI_4. When HgClI is in excess, stoichiometry of the reaction is 2:1 of HgClI and Cu_2HgI_4.

The reflectance studies (fig.2) also show that the products in the molar ratios 1:3, 1:2 and 1:1, 1:2, 1:3 of HgClI and Cu_2HgI_4 are similar in the former, and is different but similar in the latter.

Mechanism of lateral diffusion

Soon after placing HgClI over Cu_2HgI_4 in the reaction capillary, at 50°C, a red coloured layer developed at the interface. The product layer grew with time towards the Cu_2HgI_4 side, which later separated into red and white layers. A gap developed between the white layer and HgClI. When the experiment was repeated with an air gap of varying dimensions between the two reactants, the reaction proceeded in similar way giving the same kinds of layers on Cu_2HgI_4 side as was the case when the reactants were in contact. The dimension of the air gap did not affect the sequence of the layers. This shows that the mobile component is HgClI. HgClI molecules react with the Cu_2HgI_4

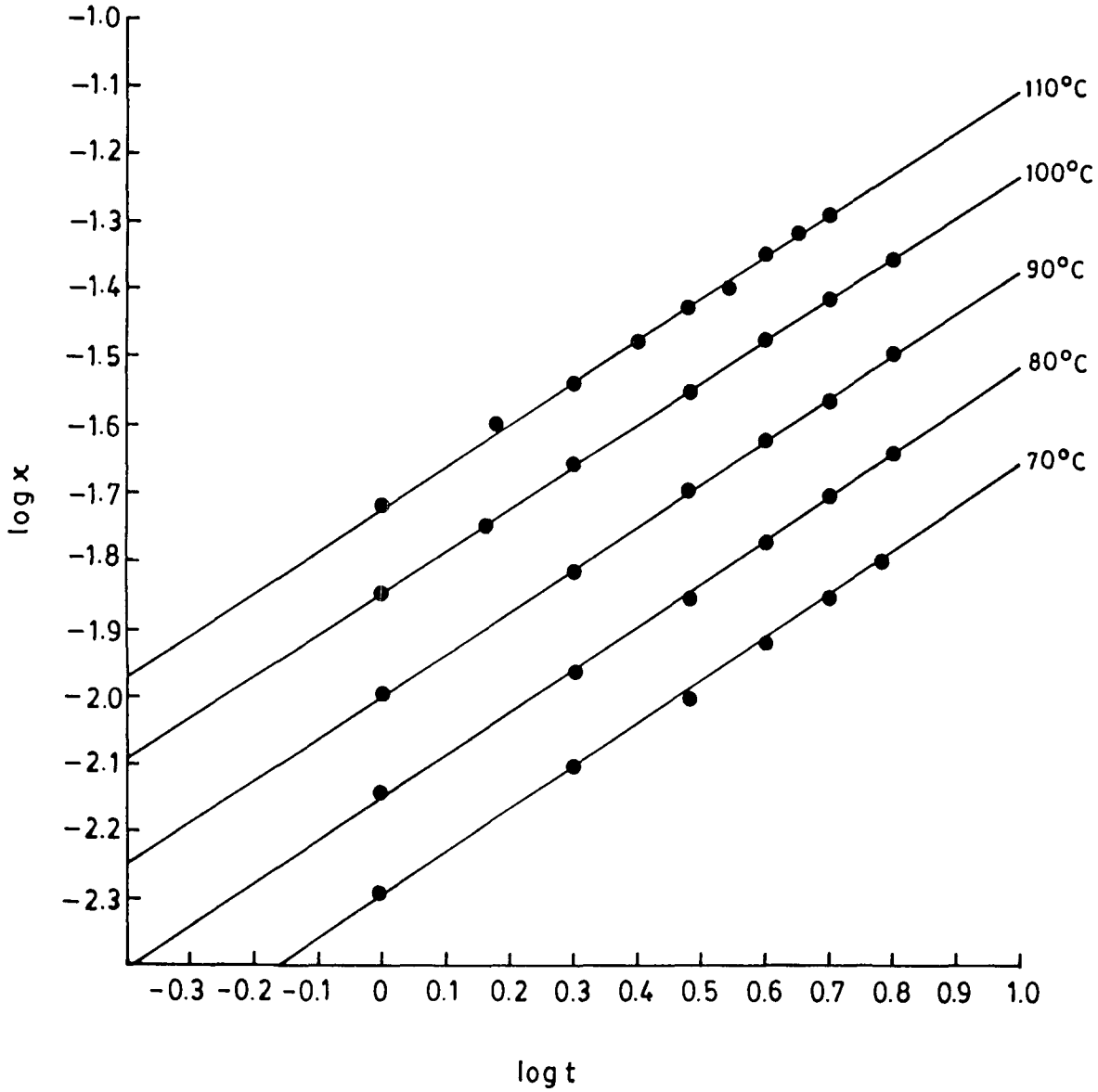

FIG.3. KINETIC DATA FOR LATERAL DIFFUSION AND TEST FOR EQUATION $X^n = kt$ FOR HgCII — Cu_2HgI_4 REACTION.

It seems from the discussion that when Cu_2HgI_4 is in excess, one type of mechanism is followed in which case the Stoichiometry of the reaction is 1:2 of HgClI and Cu_2HgI_4. When HgClI is in excess, stoichiometry of the reaction is 2:1 of HgClI and Cu_2HgI_4.

The reflectance studies (fig.2) also show that the products in the molar ratios 1:3, 1:2 and 1:1, 1:2, 1:3 of HgClI and Cu_2HgI_4 are similar in the former, and is different but similar in the latter.

Mechanism of lateral diffusion

Soon after placing HgClI over Cu_2HgI_4 in the reaction capillary, at 50°C, a red coloured layer developed at the interface. The product layer grew with time towards the Cu_2HgI_4 side, which later separated into red and white layers. A gap developed between the white layer and HgClI. When the experiment was repeated with an air gap of varying dimensions between the two reactants, the reaction proceeded in similar way giving the same kinds of layers on Cu_2HgI_4 side as was the case when the reactants were in contact. The dimension of the air gap did not affect the sequence of the layers. This shows that the mobile component is HgClI. HgClI molecules react with the Cu_2HgI_4

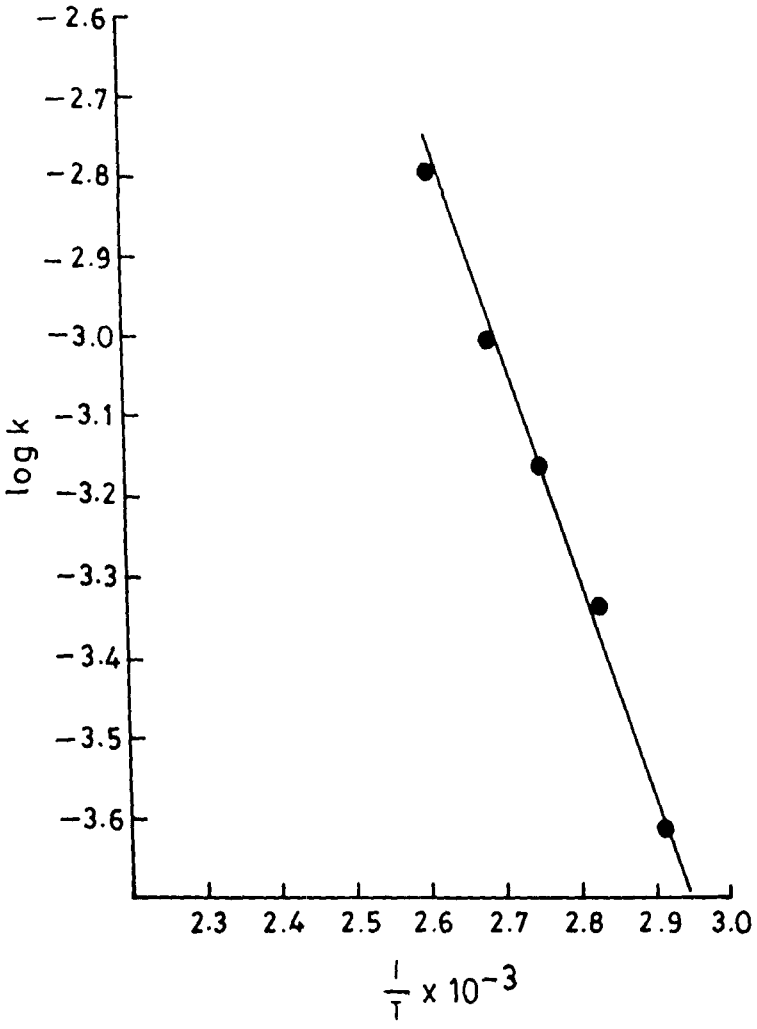

FIG.4. DEPENDENCE OF k ON TEMPERATURE FOR THE REACTION BETWEEN HgCl I AND Cu_2HgI_4.

molecules to form coloured HgI_2. X-ray and chemical analysis of the different layers thus formed showed the following sequence of products in the reaction capillary.

$$Cu_2HgI_4 \;\vdots\; HgI_2,\ CuCl \;\vdots\; HgClI$$

The rate of growth of product layers decreased with time. Initially, the process is fast and reaction controlled. As the thickness of the product layers became significant, HgClI took greater time to diffuse through the product layers. The process now becomes diffusion controlled and the rate of the reaction thus falls regularly with the growth of the product layers. The lateral diffusion data best fit the rate equation (fig. 3)

$$X^n = kt \qquad \ldots (1)$$

where X is the total thickness (in cm) of the product layers at time t (in hrs) and k and n are constants k follows the Arrhenius equation

$$k = A \exp(-E/RT) \qquad \ldots (2)$$

The activation energy evaluated from the log k versus 1/T plot (fig.4) made by least square fit method was found to be 43.382 kJ/mole. The reaction rate constant measured with an initial air gap between the reactants decreased with an increase

in the length of the air gap. The energy of activation suggests that the reaction is diffusion controlled taking place via vapour phase diffusion.

References

1. Fiegel, F. and Ager. : Spot tests in Inorganic Analysis (Elsevier Publishing Company) pp. 203, 145 and 147 (1972).
2. Mellor, J.W. : "A Comprehensive Treatise on Inorganic and Theoretical Chemistry, Vol III, 203, Longmans Canada Ltd, (1961).
3. Link, H.L. and Wood, L.J. : J. Am. Chem. Soc. 62, 766 (1940).
4. Ahmad, A. : Ph. D. Thesis submitted to Aligarh Muslim University, "Studies on the interaction of Copper (I) and Mercury (II) Halides in Solid State", p. 129 (1979).
5. ASTM powder Diffraction, file No. 6-0344.
6. ASTM powder Diffraction, file No. 6-0246.
7. ASTM powder Diffraction, file No. 21-1157.
8. ASTM powder Diffraction, file No. 18-0450.
9. ASTM powder Diffraction, file No. 4-033.

Solid State Reaction Between CuI and HgClBr : Role of electrical resistivity in determining the mechanism of the reaction.

SABA BEG and AFAQ AHMAD *

Department of Chemistry

Aligarh Muslim University, Aligarh-202002 (INDIA)

ABSTRACT : The reaction between CuI and HgClBr in Solid State has been studied by resisvitity measurements, reflectance studies, X-ray diffraction analysis and Chemical analyses. The reaction occurs differently in different molar ratios. The Kinetics and mechanism of the reaction has been studied by visual technique. The reaction follows the usual parabolic rate law, $X^n = Kt$. The k's show the Arrehenius dependence. The energy of activation calculated, by the least square fitting , to be 43.30 KJ/mol, suggesting that the reaction is diffusion controlled taking place via vapor phase diffusion of HgClBr.

Introduction :

Solid state reactions are of practical interest specially in the preparation of spinels, ceramics, catalysts and pharmaceutical materials (1-3). From time to time, studies have been made to understand mechanism and reactivity of such reactions. In Solid state reactions breaking and reforming of chemical bonds in the solid is essentially a geometrical reshffling of lattice elements.

In previous papers (4-8), a comprehensive picture of the initial surface reaction followed by diffusion of reactants through the product layer has been obtained including informations about the mode of diffusion. In order to have more information about the mechanism of reaction between copper halides & mixed mercury halides additional data are required. In the present paper, we have studied the reaction between CuI and HgClBr to understand the reactivity of copper (I) Iodide towards HgClBr .

Experimental

$HgBr_2$, (E.Merck), $HgCl_2$, $CuSO_4$, KI were of BDH quality and were used as such. CuI was prepared following the technique reported earlier (4). HgClBr was prepared by the method reported by Ansari & Mehdi (9).

Electrical conductivity measurements were made on compressed samples using a teflon conductivity cell. Powdered CuI and HgClBr

(each above 200 mesh size), in different molar ratios, were thoroughly mixed, poured into a die and pressed into disks, about 0.2×10^{-2} m thick and 0.31×10^{-4} m^2 in surface area by applying 15Kpa pressure with the help of a hydraulic press (Carver Laboratory Press, Model C, Fred S. Carver Inc , USA). The resistance measurements were made at $80^{o}C$ by keeping the compressed disks between platinum electrodes using LCR conductivity bridge (Gen Rad Model 1659 USA). The results are plotted against time for various molar mixtures (fig.1). The kinetics of the reaction between CuI & HgClBr were studied using the visual technique described elsewhere (io). Weighed amounts of HgClBr was placed over weighed CuI in glass capillary of uniform bore. The reaction capillary was placed in an air thermostat maintained to $\pm 1^{o}C$. The progress of the reaction was followed by measuring the total thick ness of the product layers formed at the interface by a callibrated travelling microscope. Each experiment were run in triplicate simultaneously, and the agreement between the corresponding values of different sets was within the experimental error limits. The average values were used for calculating the rate constants given in Table I.

The X-ray diffractograms of powdered CuI and HgClBr mixed in different molar ratios were recorded by Norelco Geiger X-ray diffroctometer (PW 1010 Philips) using CuKa radiation & Ni-filter applying 32 KV at 12mA by the following method. The reactants in different molar ratios were mixed in an agate mortar, and kept in the air thermostat for over 3 days to ensure complete reaction. The

diffractograms of these mixtures were then recorded at room temperature. Compounds present in different mixtures were identified by calculating their d-values and comparing them with the standard d-values of the expected compounds from ASTM cards. Compounds identified in different mixtures of the reactions are given in table II.

Reflectance Study :

Reflactance spectra were recorded for samples with molar mixtures 4:1, 3:1, 2:1, 1:1 & 1:2 of CuI & HgClBr by UV-spectrophotometer attached with reflectance attachment in KBR. The results are shown in the fig-4.

Results and Discussion :

The X-ray diffraction analysis (Table -III) of 4:1 molar mixtures of CuI and HgClBr heated at 100°C for 3 days and then cooled to room temperature, indicated the presence of CuCl, CuBr and $-Cu_2HgI_4$. This suggests that the reaction can be represented as :

$$4\ CuI + HgClBr \longrightarrow CuCl + CuCl + CuBr + Cu_2HgI_4 \qquad (1)$$

However, in addition to CuCl, CuBr & Cu_2HgI_4, HgI_2 was also detected in samples analysed just after hours of heating by placing a smaller amount of CuI over a larger amount of HgClBr and allowing the reaction to go on till the whole of CuI was consumed. At the end of the reaction capillary, the presence of HgI_2 on CuI side was confirmed by chemical analysis and x-ray diffractogram. This evinces beyond doubt that the reaction takes place in more than one step via the formation of HgI_2.

Electrical resistivity measurements (fig-1) for 4:1 molar mixture of CuI and HgClBr show a sharp decrease, in follwed by continous vise in the resistivity leading to a constant value. The presence of a minima in the resistance time curve in the initial stages clearly suggsts that the reaction represented by equation (1) pases through the formation of some intermediate product. This intermediate is immediately consumed giving a material of high electrical resistivity. Since CuI is known to raect fast (4) with HgI_2 to produce Cu_2HgI_4 , which has very low resistance, it is therefore, presumed that in the first step HgI_2 is formed fast through simple exchange mechanism,

$$2CuI + HgClBr \longrightarrow CuCl + CuBr + HgI_2.$$

The HgI_2 so formed is immediately consumed by the unreacted CuI present in the reaction mixture to form low resistivity Cu_2HgI_4.

$$2CuI + HgI_2 \longrightarrow Cu_2HgI_4$$

The overall reaction taking place can, therefore, be represented as:

$$2CuI + HgClBr \longrightarrow CuI + CuBr + HgI_2$$

$$2CuI + HgI_2 \longrightarrow Cu_2HgI_4$$

$$4CuI + HgClBr \longrightarrow \overline{Cu_2HgI_4} + \overline{CuCl + CuBr}$$

This explains only the initial fall in resistance but not the increase thereafter.

The X-ray diffraction analysis of the 3:1 molar mixture of CuI and HgClBr showed the presence of CuCl, CuBr, Cu_2HgI_4 and HgI_2.

The rraction was supposed to take the enitre course observed with 4:1 molar mixture but the electrical resistivity measurements showed that the resistivity first increased, followed by a decrease and again a rise. This indicates that the reaction sequence in 3:1 molar mixture is entirely resistivity measurements & the x-ray analysis, the sequence of reaction in 3:1 molar mixture is proposed as follows:

$$2CuI + HgClBr \longrightarrow CuCl + CuBr + HgI_2 \quad (2a)$$

$$2CuI + HgI_2 \longrightarrow Cu_2HgI_4 \quad (2b)$$

$$Cu_2HgI_4 + HgClBr \longrightarrow CuBr + CuCl + 2HgI_2 \quad (2c)$$

$$2CuI + HgI_2 \longrightarrow Cu_2HgI_4 \quad (2d)$$

$$6CuI + 2HgClBr \longrightarrow 2CuCl + 2CuBr + Cu_2HgI_4 + HgI_2 \quad (2)$$

Step (2a) is tne simple exchange reaction, as in the 4:1 molar mixture, there is momentary decrease in the resistivity pertaining to the formation of H_gI_2, thereafter a continuous decrease in resistivity is due to the formation of low resistance Cu_2HgI_4 by the reactionof CuI & H_gI_2 formed in the step (2a) . The step (2c) produces more resisting H_gI_2 which is being formed by the reaction of $Cu_2H_gI_4$ formed instep (2b) with unreacted H_gClBr. This step was separately confirmed by reacting $Cu_2H_gI_4$ and H_gClBr in a capillary tube. Various layers obtained were collected separately and analysed chemically and by X-ray for H_gI_2 & CuBr. The formation of H_gI_2 in this step explains the fall in resistivity. However, the H_gI_2 formed , is being consumed by CuI to produce Cu_2HgI_4, which gives rise to the decrease in the vesistivity. The d-values of CuBr and CuCl do not match well with the standard d-values reported in the ASTM Files (11). There seems some distortin which is due to the formation of a solid solution between CuBr & CuCl. The X-ray diffraction analysis of 2:1 molar mixture of CuI and H_gClBr showed the presence of cuBr, CuCl, $Cu_2H_gI_4$ and H_gI_2. The electrical resisturity measurements indicate that the reaction is multi-step. In the initial stage the resistivity rises due to the formation of ($Cu_2H_gI_4$) , then it decreases due to the formation of conducting product/s. Thereafter, it continuously decreases till it is atmost constant.

On the basis of this behaviour, the following mechanism is proposed to take place in 2:1 mixture.

$$2CuI + HgClBr \longrightarrow CuCl + CuBr + HgI_2 \quad (3a)$$

$$2CuI + Cu_2HgI_4 \longrightarrow Cu_2HgI_4 \quad (3b)$$

$$Cu_2HgI_4 + HgClBr \longrightarrow CuBr + CuCl + 2HgI_2 \quad (3c)$$

$$HgI_2 + 2HgClBr \longrightarrow 2HgClI + HgBr_2 \quad (3d)$$

$$4CuI + HgBr \longrightarrow 2CuBr + Cu_2HgI_4 \quad (3e)$$

$$3CuI + HgClBr \longrightarrow 4CuBr + 2CuCl + Cu_2HgI_4 + HgI_2 \quad (3)$$

Steps (3a) and (3b) are in accordance with the reaction as were in the case of 4:1 molar mixtures. Steps (3c)& (3d) produce HgI_2, $HgBr$ and $HgClI$ which have high resistivity and their accounts for the increase in the resistivity. Step (3e) results in the formation of Cu_2HgI_4 that accounts for the fall in the resistivity. The reactivity of CuI & $HgBr_2$ has already been reported (5). Since $HgClI$ is not very stable it decomposes into $HgCl_2$ & HgI_2. The products inentified by X-ray analysis in 1:1 molar mixture of CuI and $HgClBr$ are CuCl, CuBr, $HgClI$ (HgI_2+HgCl_2) and $HgBrI$. The resistivity measurements shows that the reaction is a two step one. In the first step, the resistivity falls due to the formation of Cu_2HgI_4, then excess of $HgClBr$ combines with Cu_2HgI_4 formed in the first step, giving rise to $HgClI$ and $HgBrI$ which have comparatively higher resistivity. However, $HgClI$

is not very stable at room temperature, it soon decomposes into H_gCl_2 which are identified in the X-ray analysis. These suggest the following mechanism.

$$2CuI + H_gClBr \longrightarrow CuCl + CuBr + H_gI_2$$

$$2CuI + H_gI_2 \longrightarrow Cu_2H_gI_4$$

$$Cu_2H_gI_4 + H_gClBr \longrightarrow 2CuI + H_gClI + HIBrI$$

$$2CuI + H_gClBr \longrightarrow CuCl + CuBr + H_gCl_2 + H_gBrI$$

Results of X-ray analysis (Table II) and electrical resistivity measurements (fig-1) with 1:2 molar mixture of CuI & H_gClBr auggest that the reaction in this case as well, follow the same path as for 1:1 molar mixture at 80^oC.

However, the raction may be taking place at room temperature but it is too slow to be followed at room temperatures .

Mechanism of lateral diffusion :

Soon after placing H_gClBr over CuI in the reaction capillary, at 50^oC a chocklate coloured layer developed at the interface. The product layer grew with time towards the CuI Side, which later separated into white and light yellow layers, gap developed between the white layer and H_gClBr. When the experiment was repeated with an air gap of varying dimensions between the two reactants, the reaction proceeded

in similar way giving the same kinds of layers on CuI side as was the case when the reactants were in contact. The dimensions of the air gap did not affect the sequence of the layers. This shows that the mobile component is H_gClBr. H_gClBr molecules react with CuI to produce CuCl, CuBr and H_gI_2 . The latter then reacts with the CuI to form coloured $Cu_2H_gI_4$. X-rays and chemical analysis of the different layers formed showed the following sequence of products in the reaction capillary.

$$CuI/Cu_2H_gI_4,\ CuBrCuCl,\ H_gI_2\ /\ H_gClBr$$

The rate of growth of product layers decreased with time. Initially, the process is fast and reaction controlled. As the thickness of the product layers became significant the H_gClBr took greater time to diffuse through the product layers. The process now becomes diffusion controlled and the rate of the reaction thus falls regularly with the growth of the product layers. The lateral diffusion data best fit the parabolic rate equation (fig-3)

$$X^2 = Kt \qquad \text{(1)}$$

Where X is the total thickness of the product layers at time t, and K the parabolic rate constant. The rate constant, K, follows the Arrehenus equation.

$$k = A \exp(-E/RT) \qquad \text{(2)}$$

The activation energy evaluated from the log K versus 1/T plot (fig.3) made by least square fit method was found to be 43.30kJ. The reaction constant measured with an initial air gap between the reactants decreased with the increase in length of the air gap. The energy of activation suggests that the reaction is diffusion controlled taking place via vapor phase diffusion (3).

Acknowlegement: Dr. Safia Mehdi, Scientist, IICT, Hyderabad for the help in X-ray diffraction studies.

TABLE - 1

Temperature ($^{o}C \pm 0.5$)	k (cm/hr)	Standard Deviation	Relative Standard deviation	n
50	3.26×10^{-4}	1.241×10^{-5}	3.037×10^{-2}	2.27
60	3.592×10^{-4}	1.934×10^{-5}	4.480×10^{-2}	2.35
70	6.477×10^{-4}	5.519×10^{-5}	6.75×10^{-2}	2.48
80	1.006×10^{-3}	6.795×10^{-5}	4.159×10^{-2}	2.40
90	3.082×10^{-3}	1.500×10^{-4}	3.594×10^{-2}	2.30
100	1.884×10^{-2}	1.155×10^{-3}	4.38×10^{-2}	1.76
110	2.20×10^{-2}	1.355×10^{-3}	5.28×10^{-2}	2.48

T A B L E - II

Compounds identified by X_ray analysis by heating the mixture to 100°C for over 3 days and then cooling to room temp.

Molar ratio of CuI : HgClBr	Compounds Present
4 : 1	Cu_2HgI_4 , CuCl , CuBr
3 : 1	Cu_2HgI_4 , CuCl, CuBr, HgI_2
2 : 1	Cu_2HgI_4 , CuCl, CuBr, HgI_2
1 : 1	CuCl , CuBr , HgI_2 + $HgCl_2$, HgBrI
1 : 2	Cu_2HgI_4 , CuCl , CuBr , HgI_2

References:

1. J.A. Hedvall, J. Chem. Educ, 30 , 638 (1953).
2. W.D. Kingery, Introduction to ceramics (John Wiley, New Yark).67, (1960).
3. R.P. Rastogi, J. Scient. Indus. Res. 29, 177 (1970)
4. M.A. Beg and A. Ahmad, Bull, Chem. Soc. Jpn, 55, 297 (1982).
5. M.A. Beg and A.Ahmad, Bull. Chem. Soc. Jpn, 55, 3607 (1982).
6. M.A. Beg, Rafiuddin and A. Ahmad, J-Solid State, Chem, 80 , 94 (1989)
7. M.A. Beg and S.M. Ansari, J. Solid State Chem. 18 , 1 (1976)
8. M.A. Beg and S.M. Ansari, J. Solid State Chem. 23 409 (1978)
9. S.M. Ansari & Safia Mehdi, J.Solid State Chem. 40, 22 (1981)
10. R.P. Rastogi and B.L. Dubey , J. Am. Chem. Soc. 89 , 200 (1967)
11. ASTM files Nos. 6-0292, 6-0344.